UNIVERSITÀ DI SIENA 1240

The Field Cages of the new Time Projection Chambers (TPCs) for the T2K Upgraded Near Detector:

production, characterization, electric field performance and advanced track reconstruction

Candidate: Matteo Feltre

Supervisor: Prof. Gianmaria Collazuol

Co-supervisor: Prof. Pier Simone Marrocchesi

Overview

1. **Introduction to Neutrino Physics**
2. **T2K Experiment**
3. High-Angle Time Projection Chamber
4. Field Cage production and characterization
5. Study on Field Cage 0 insulation issue
6. Study on Electric field of Field Cages
7. Track Reconstruction algorithm with Machine Learning

Brief History of Neutrino Physics

Neutrinos are **neutral fermions** belonging to the **lepton** families

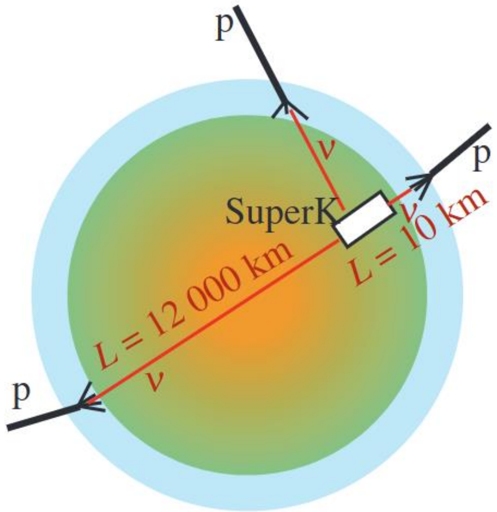

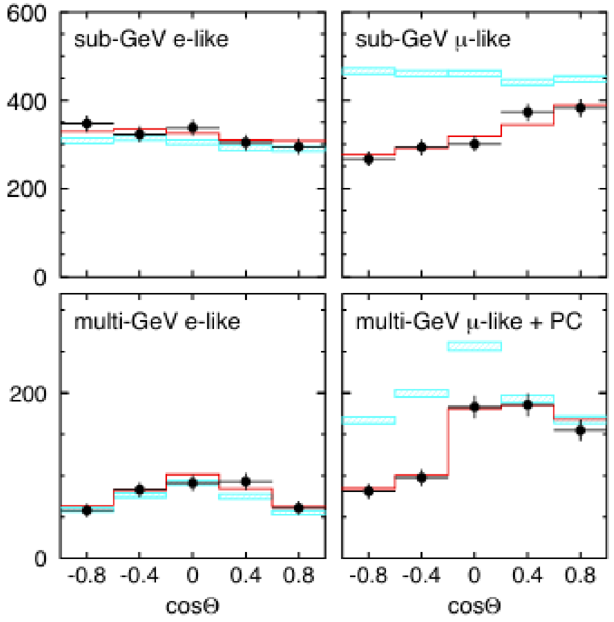

- **1930**: Predicted by Pauli in as explanation for β −decay
- **1956**: Detected by Cowan and Reines in as products in Savannah River nuclear reactors
- **1962**: First neutrino from proton beams were obtained
- **1962**: Discovery of ν_μ
- **2000**: Discovery of ν_τ, 25 years after the discovery of the 3rd lepton family

- **In 1998 Super-Kamiokande** observed a dependance between ν_μ counts and zenith angle

Neutrinos oscillate! → They have a **mass!**

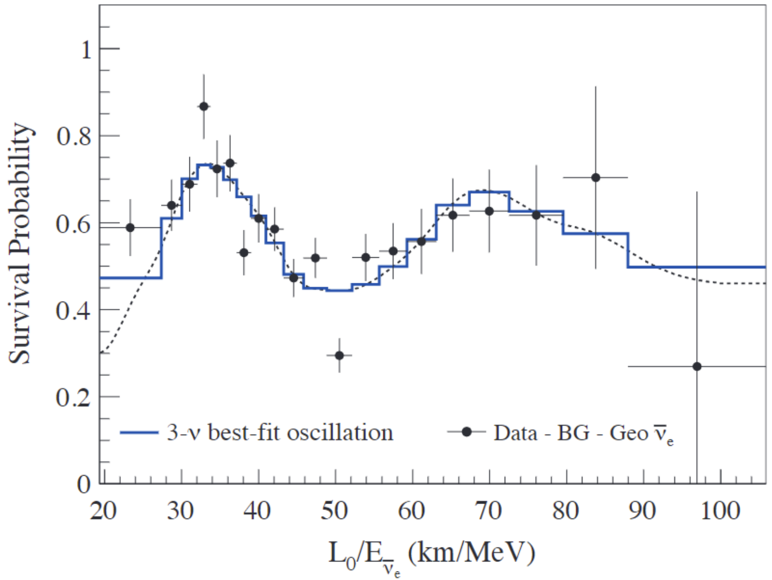

$\frac{L}{E}$ **dependency** observed by KamLAND

$$P_{\nu_\alpha \to \nu_\beta}(L, E) = \sin^2(2\theta)\sin^2\left(\frac{\Delta m^2 L}{4E}\right)$$

Neutrino Physics: Open Questions

The neutrino oscillation phenomenon arises since its **mass** and **flavor** eigenstates do not coincide

Oscillations are described by **PMNS matrix**

$$U = \begin{pmatrix} 1 & 0 & 0 \\ 0 & c_{23} & s_{23} \\ 0 & -s_{23} & c_{23} \end{pmatrix} \begin{pmatrix} c_{13} & 0 & s_{13}e^{-i\delta} \\ 0 & 1 & 0 \\ -s_{13}e^{i\delta} & 0 & c_{13} \end{pmatrix} \begin{pmatrix} c_{12} & s_{12} & 0 \\ -s_{12} & c_{12} & 0 \\ 0 & 0 & 1 \end{pmatrix}$$

- δ_{CP} can introduce a CP violating term

$$J \equiv J_{\mathrm{CP}}^{\max} \sin\delta$$
$$= \cos\theta_{12}\sin\theta_{12}\cos\theta_{23}\sin\theta_{23}\cos^2\theta_{13}\sin\theta_{13}\sin\delta$$

Terms different from zero for θ_{ij} allow to search for δ !

3 angles and **1 phase**

- **Charge-Parity violation?**

Imbalance in the production of matter and antimatter during the Big Bang

- Neutrino **mass ordering**

It is still unknown if ν_3 mass eigenstate is larger or smaller than the other two

- Octant of angle $\boldsymbol{\theta_{23}}$

- Are neutrinos **Dirac** or **Majorana** particles?

Cannot be tested by oscillation experiments

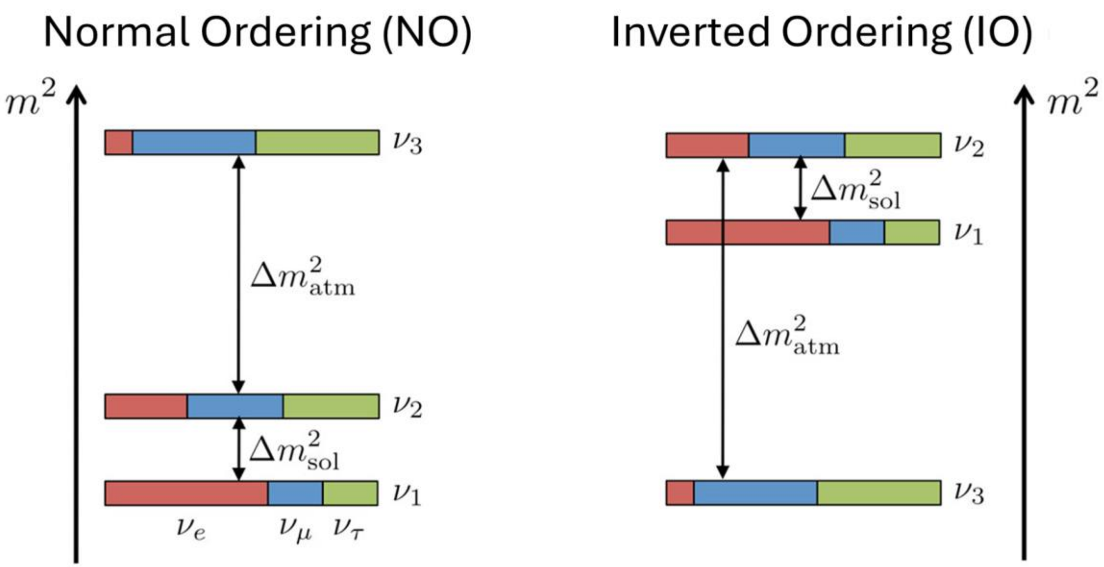

The T2K Experiment

T2K is a long-baseline neutrino experiment from J-PARC to Super-Kamiokande

Super-K

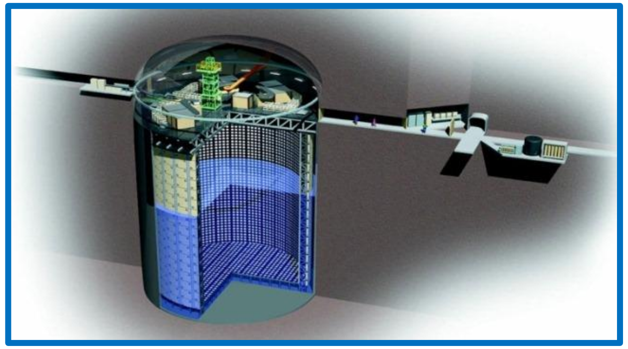

INGRID

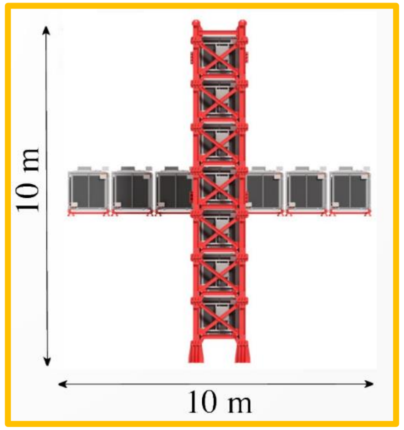

ND280

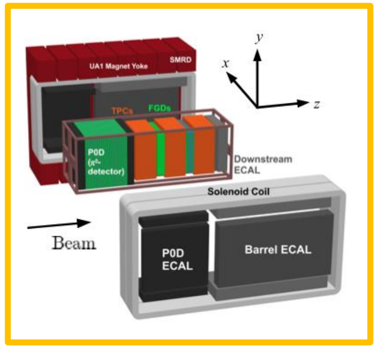

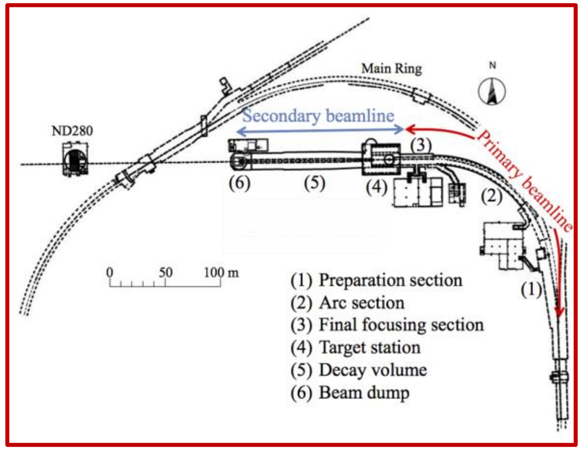

J-PARC

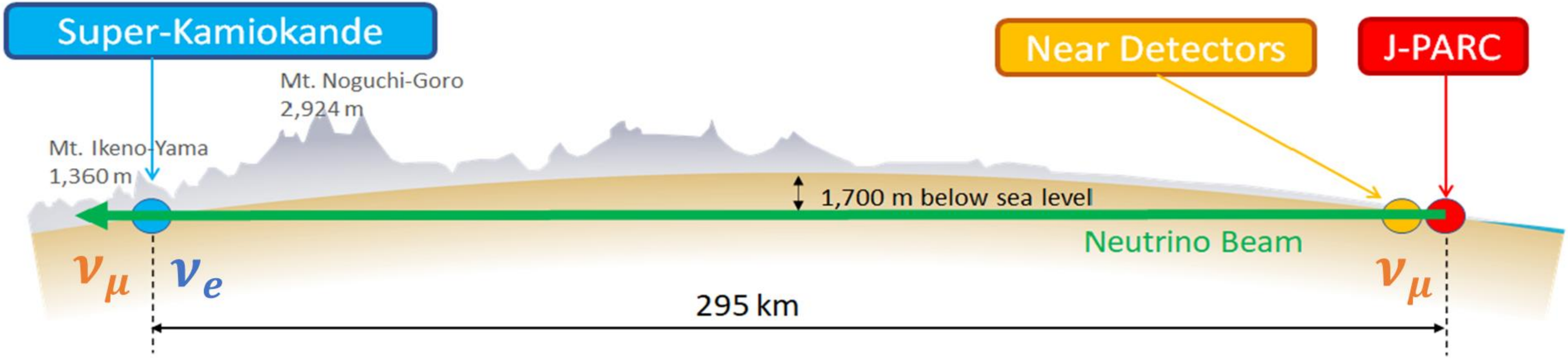

Latest T2K Results

$$U = \begin{pmatrix} 1 & 0 & 0 \\ 0 & c_{23} & s_{23} \\ 0 & -s_{23} & c_{23} \end{pmatrix} \begin{pmatrix} c_{13} & 0 & s_{13}e^{-i\delta} \\ 0 & 1 & 0 \\ -s_{13}e^{i\delta} & 0 & c_{13} \end{pmatrix} \begin{pmatrix} c_{12} & s_{12} & 0 \\ -s_{12} & c_{12} & 0 \\ 0 & 0 & 1 \end{pmatrix}$$

Long baseline experiment can provide information on those two parts of PMNS matrix

- ν_μ disappearance

  $\boldsymbol{\theta_{23}, \Delta m^2_{32}}$

- ν_e appearance

  $\boldsymbol{\theta_{13}, \delta_{CP}}$

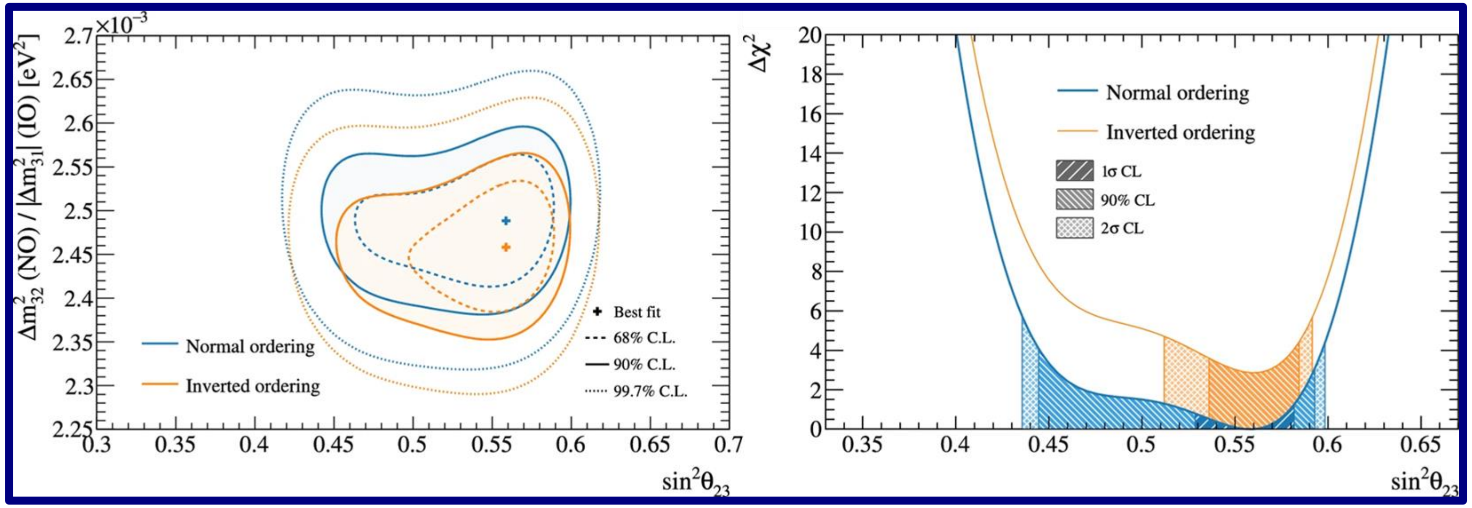

Latest T2K Results

$$U = \begin{pmatrix} 1 & 0 & 0 \\ 0 & c_{23} & s_{23} \\ 0 & -s_{23} & c_{23} \end{pmatrix} \begin{pmatrix} c_{13} & 0 & s_{13}e^{-i\delta} \\ 0 & 1 & 0 \\ -s_{13}e^{i\delta} & 0 & c_{13} \end{pmatrix} \begin{pmatrix} c_{12} & s_{12} & 0 \\ -s_{12} & c_{12} & 0 \\ 0 & 0 & 1 \end{pmatrix}$$

Long baseline experiment can provide information on those two parts of PMNS matrix

- ν_μ disappearance
  $\theta_{23}, \Delta m^2_{32}$
- ν_e appearance
  θ_{13}, δ_{CP}

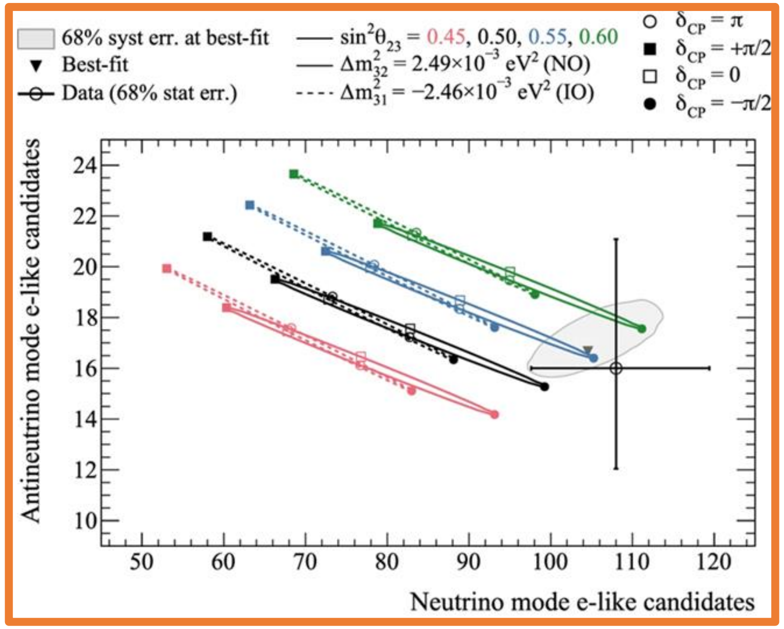

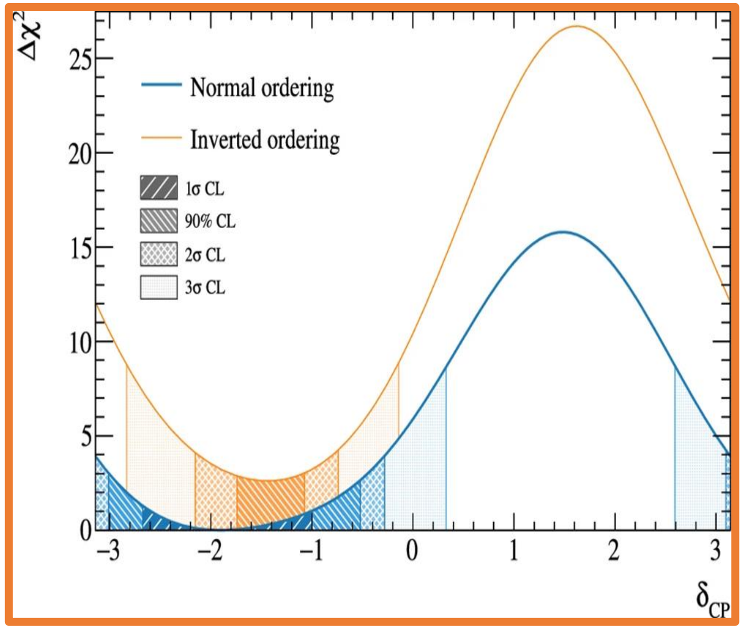

Next steps:

1. **T2K-Phase II**
   Beamline Upgrade
   ND280 Upgrade
2. **Beyond T2K**
   Hyper-Kamiokande

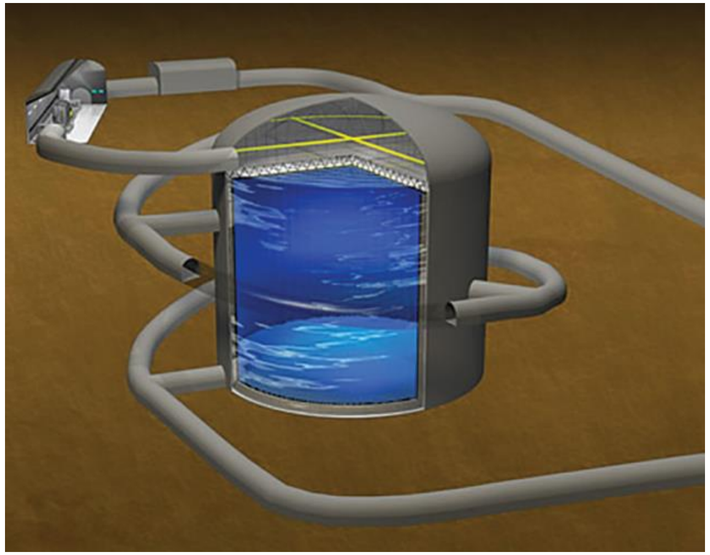

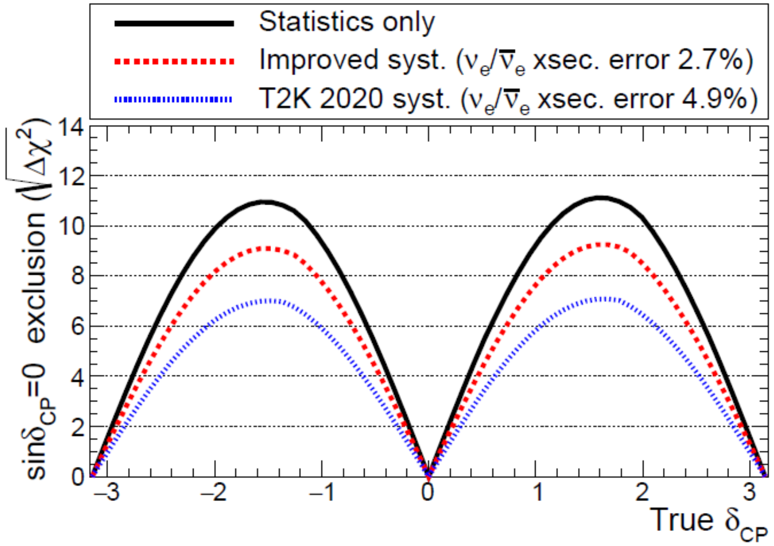

Hyper-Kamiokande preliminary!

Near Detector ND280 Upgrade

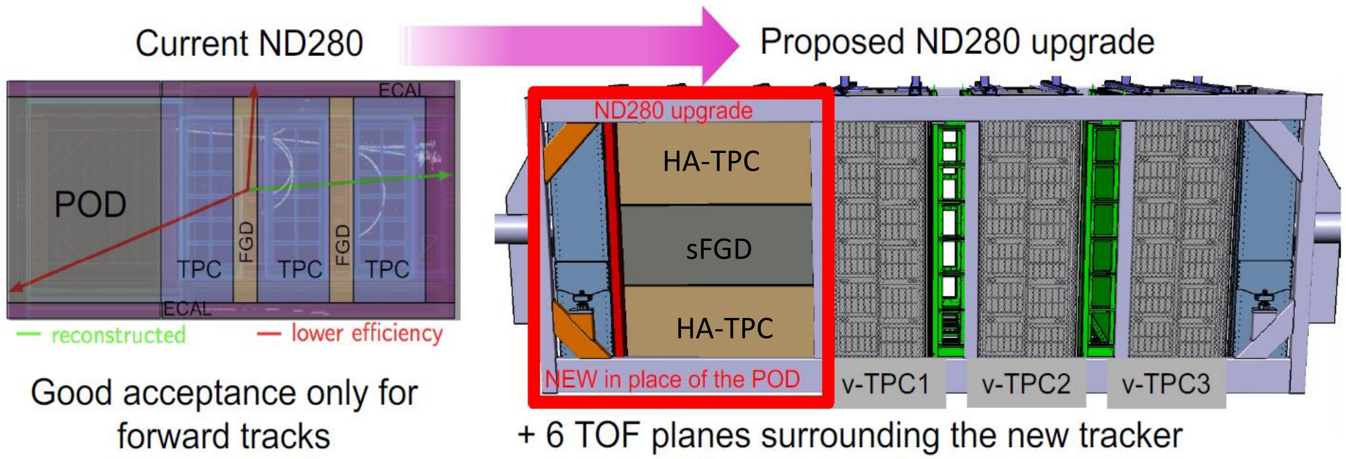

T2K Phase II

1. **Increased beam power:**
- Larger number of Protons on Target

2. **ND280 Upgrade:**
- Overall systematic uncertainty to **4%** (from 6%)

Large Acceptance angle

Reconstruction of **hadronic** part of interactions

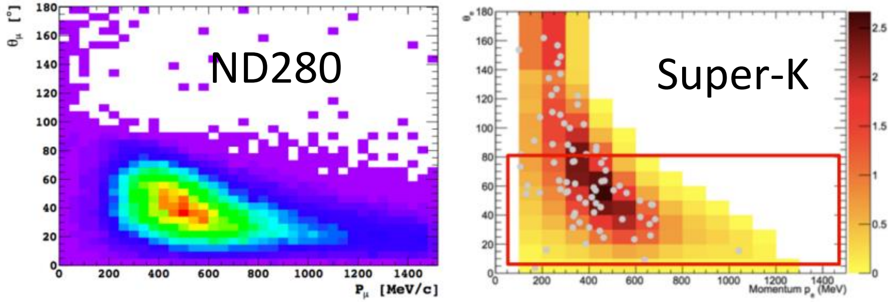

Muon momenta reconstruction

Near Detector ND280 Upgrade

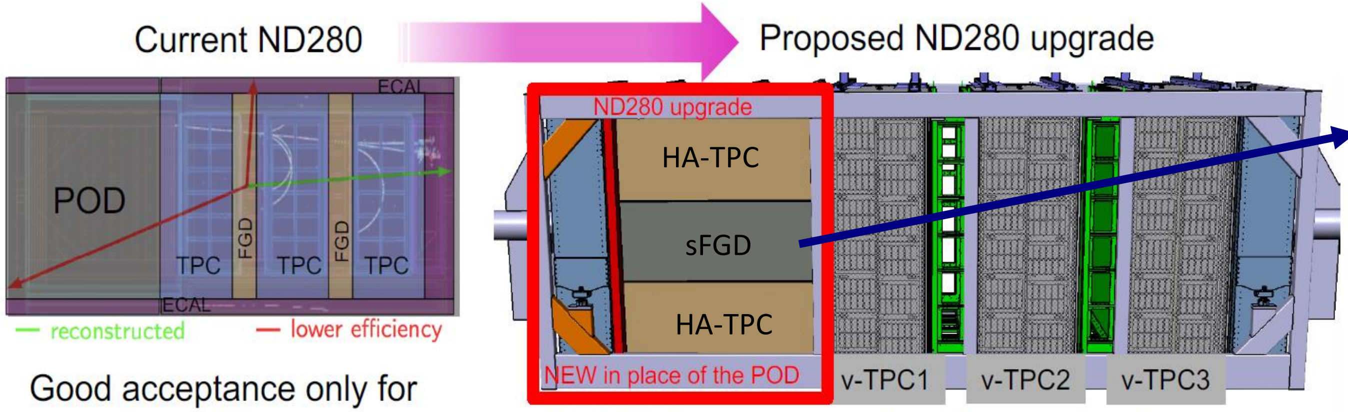

Good acceptance only for forward tracks

+ 6 TOF planes surrounding the new tracker

Super Fine Grain Detector (sFGD)

- Segmented target of cubic scintillators (1 cm side) for the improvement of hadronic part reconstruction
- Each cube is readout by 3 fibers

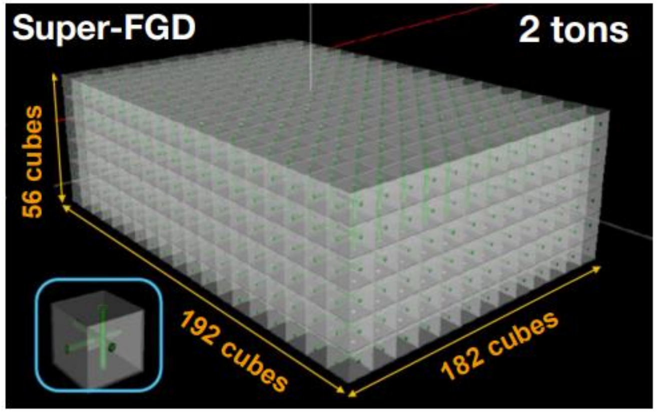

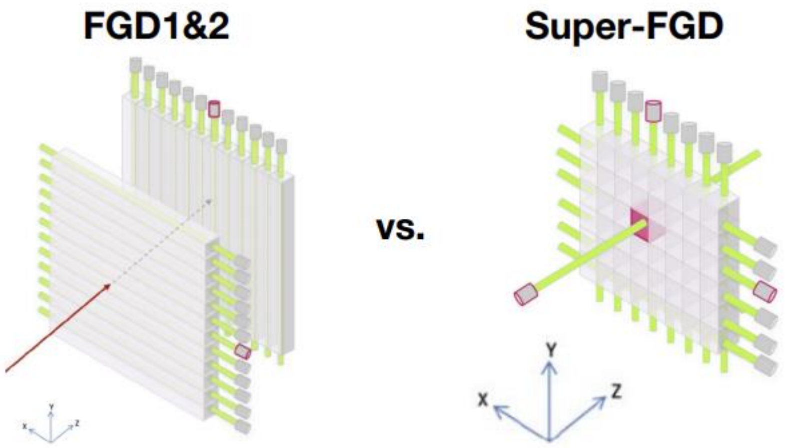

T2K Phase II

1. **Increased beam power:**
- Larger number of Protons on Target
2. **ND280 Upgrade:**
- Overall systematic uncertainty to **4%** (from 6%)

Large Acceptance angle

Reconstruction of **hadronic** part of interactions

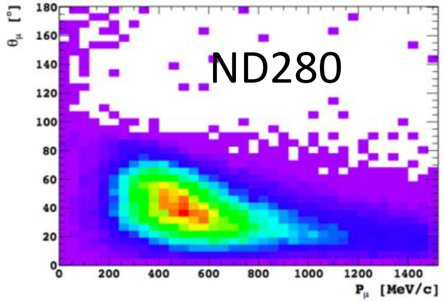

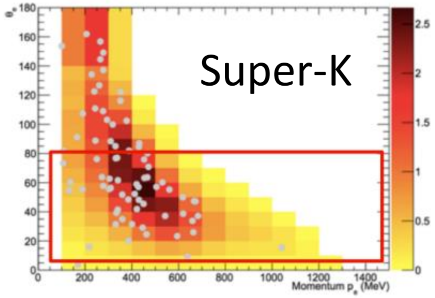

Muon momenta reconstruction

Near Detector ND280 Upgrade

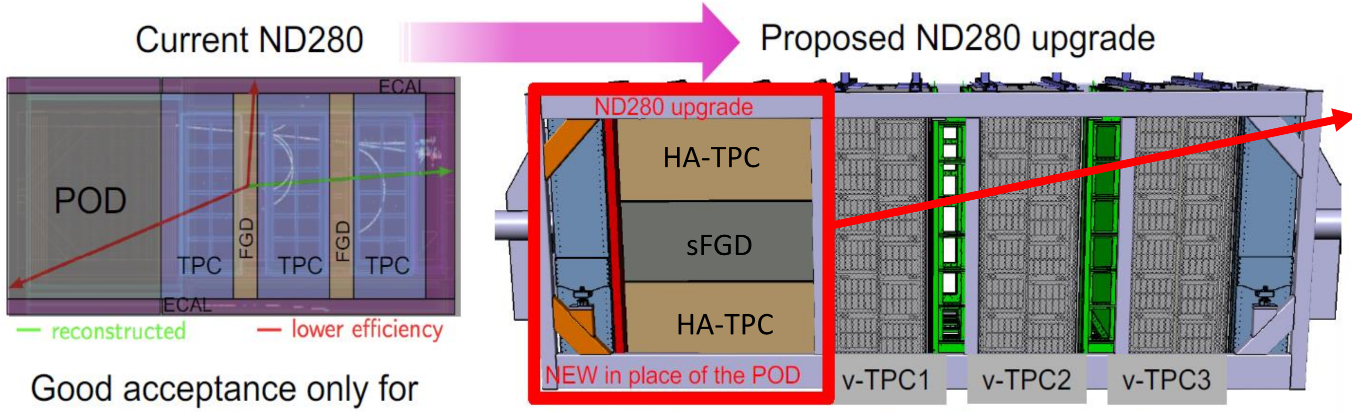

Good acceptance only for forward tracks

+ 6 TOF planes surrounding the new tracker

Time of Flight

- Six planes of scintillators to reduce the background
- Crossing time of charged particles

T2K Phase II

1. **Increased beam power:**
- Larger number of Protons on Target
2. **ND280 Upgrade:**
- Overall systematic uncertainty to **4%** (from 6%)

Large Acceptance angle

Reconstruction of **hadronic** part of interactions

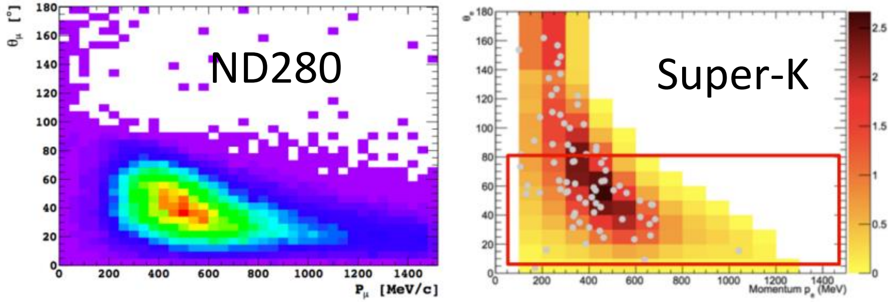

Muon momenta reconstruction

Near Detector ND280 Upgrade

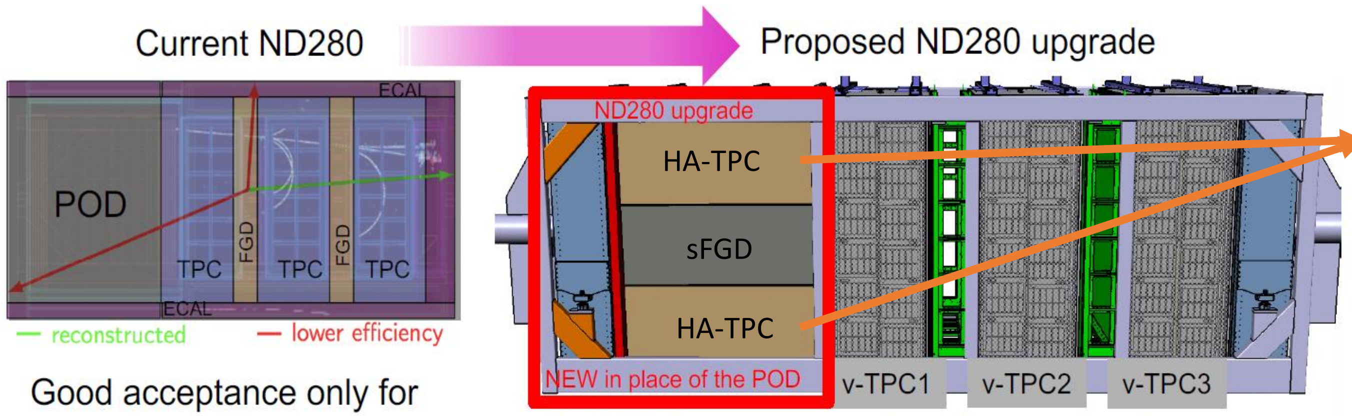

Good acceptance only for forward tracks

+ 6 TOF planes surrounding the new tracker

Two High Angle TPCs (HA-TPC)

- Placed at high angles respect to beam direction to identify leptons produced by neutrino interactions

T2K Phase II

1. **Increased beam power:**
- Larger number of Protons on Target
2. **ND280 Upgrade:**
- Overall systematic uncertainty to **4%** (from 6%)

Large Acceptance angle

Reconstruction of **hadronic** part of interactions

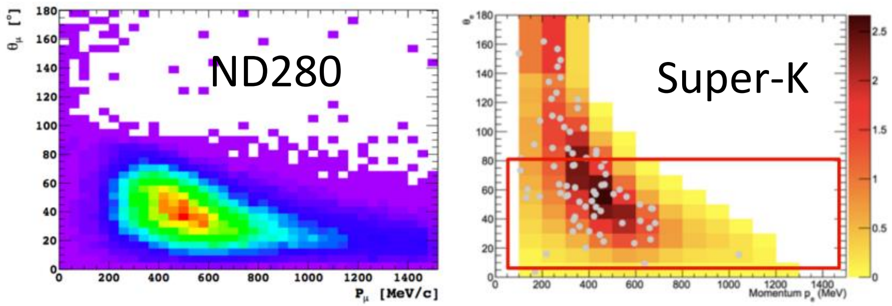

Muon momenta reconstruction

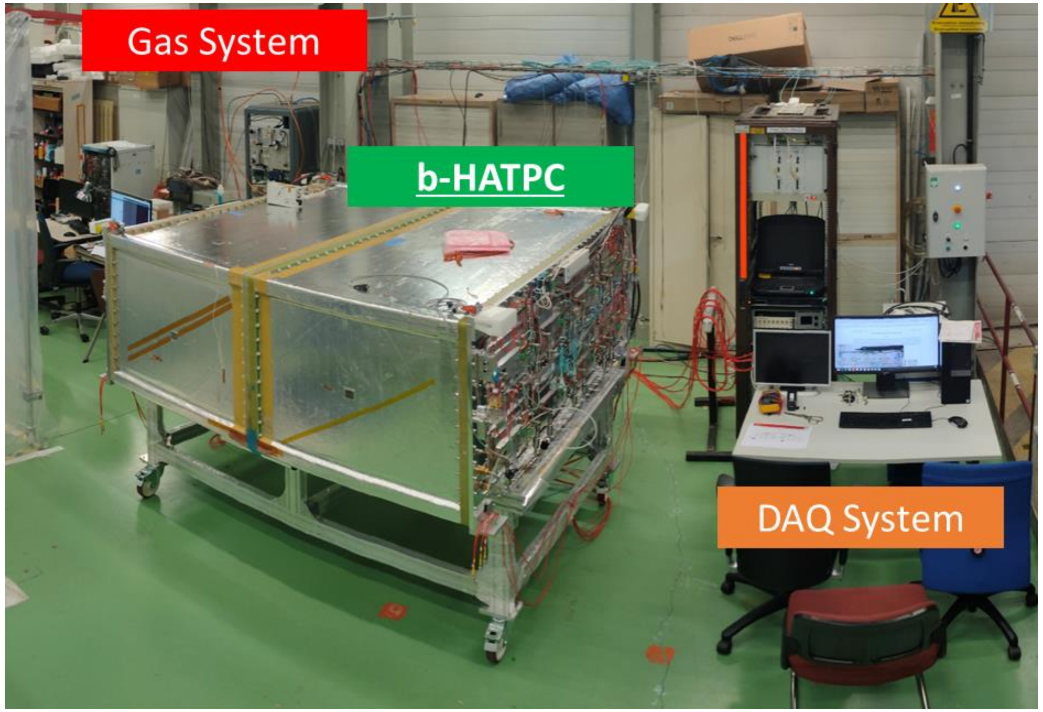

Commissioning setup 2023

1. Introduction to Neutrino Physics
2. T2K Experiment
3. **High-Angle Time Projection Chamber**
4. Field Cage production and characterization
5. Study on Field Cage 0 insulation issue
6. Study on Electric field of Field Cages
7. Track Reconstruction algorithm with Machine Learning

Time Projection Chambers

Time Projection Chambers are detectors that use a gas medium as a target of interactions with traversing charged particles

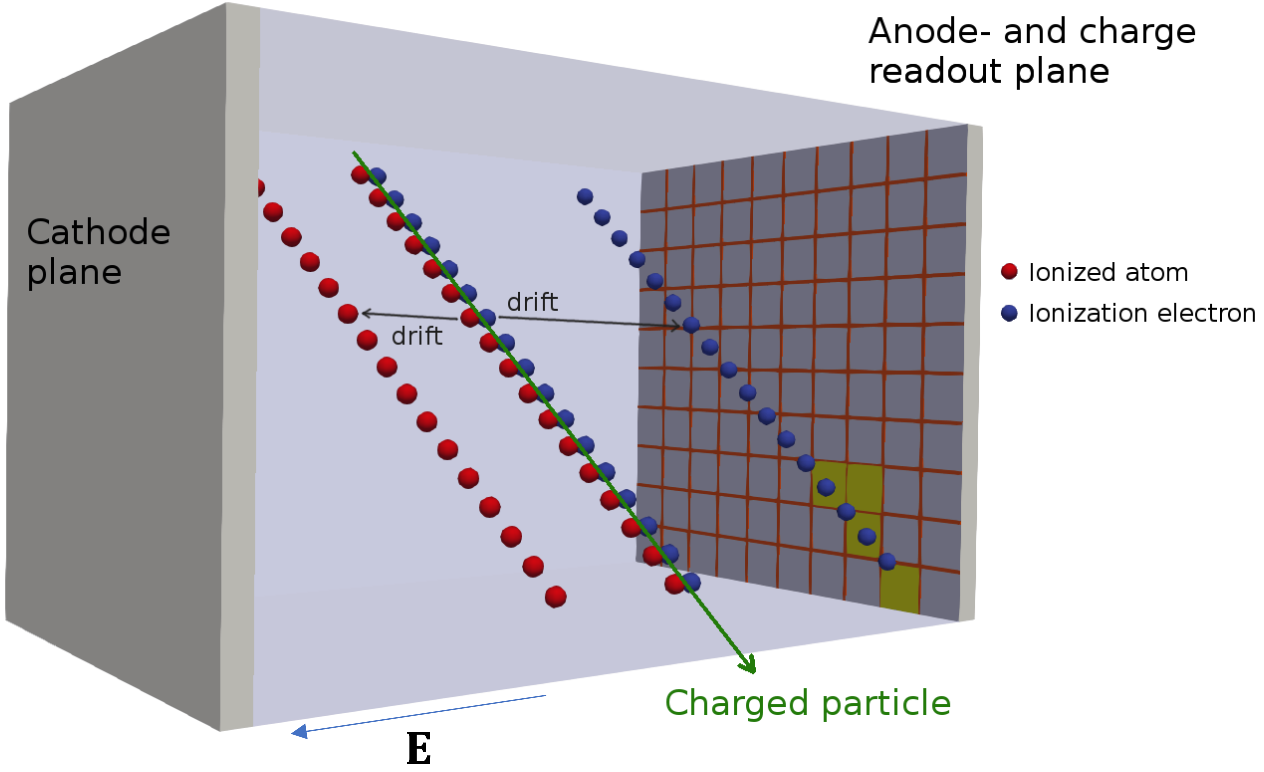

2. Due to the presence of Electric field, electrons are **drifted** towards the anode according to Langevin's equation:

$$\mathrm{m}\frac{\mathrm{d}\mathbf{u}}{\mathrm{dt}} = e\mathbf{E} + e[\mathbf{u} \times \mathbf{B}] - K\mathbf{u}$$

$$\downarrow$$

$$\mathbf{u} = \frac{e}{m}\tau|\mathbf{E}|\frac{1}{1+\omega^2\tau^2}\left(\hat{\mathbf{E}} + \omega\tau[\hat{\mathbf{E}} \times \hat{\boldsymbol{B}}] + \omega^2\tau^2(\hat{\mathbf{E}} \cdot \hat{\mathbf{B}})\hat{\mathbf{B}}\right)$$

if E and B are parallel: $\mathbf{u} = \frac{e}{m}\tau|\mathbf{E}| = \mu|\mathbf{E}|$

1. Charged particles lose energy due to multiple inelastic processes:

- **excitation and/or ionization** of gas molecules: electrons and positive ions are created

3. Electrons are **multiplied** and **collected** by readout sensors

High Angle Time Projection Chambers (HA-TPC)

Requirements:

- **Momentum resolution** $\frac{\sigma_p}{p} < 9\%$ at 1 GeV/c → neutrino energy estimation

  ↓

  Spatial resolution O(800 μm) → 3D track reconstruction

- **Energy resolution** $\sigma_{\frac{dE}{dx}} < 10\%$ → PID of electrons and muons
- **Low material budget walls**

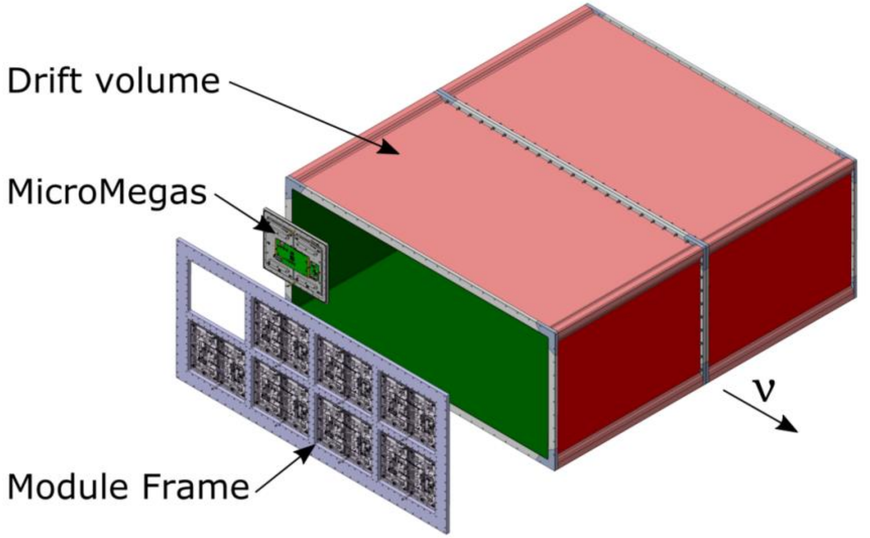

Parameter	Value
Overall x × y × z (m)	2.0 × 0.8 × 1.8
Drift distance (cm)	90
Magnetic Field (T)	0.2
Electric field (V/cm)	275
Gas Ar-CF_4-iC_4H_{10} (%)	95 - 3 - 2
Drift Velocity $cm/\mu s$	7.8
Transverse diffusion ($\mu m/\sqrt{cm}$)	265
Micromegas gain	1000
Micromegas dim. z×y (mm)	340 × 410
Pad z × y (mm)	10 × 11
N pads	36864
el. noise (ENC)	800
S/N	100
Sampling frequency (MHz)	25
N time samples	511

1. **Field Cage**
   - Thin walls and less space subtracted to active volume
2. **Resistive MicroMegas**

   ERAM: Encapsulated Resistive Anode MicroMegas
   - Charge spread on resistive layer to enhance spatial resolution
   - Spark protection

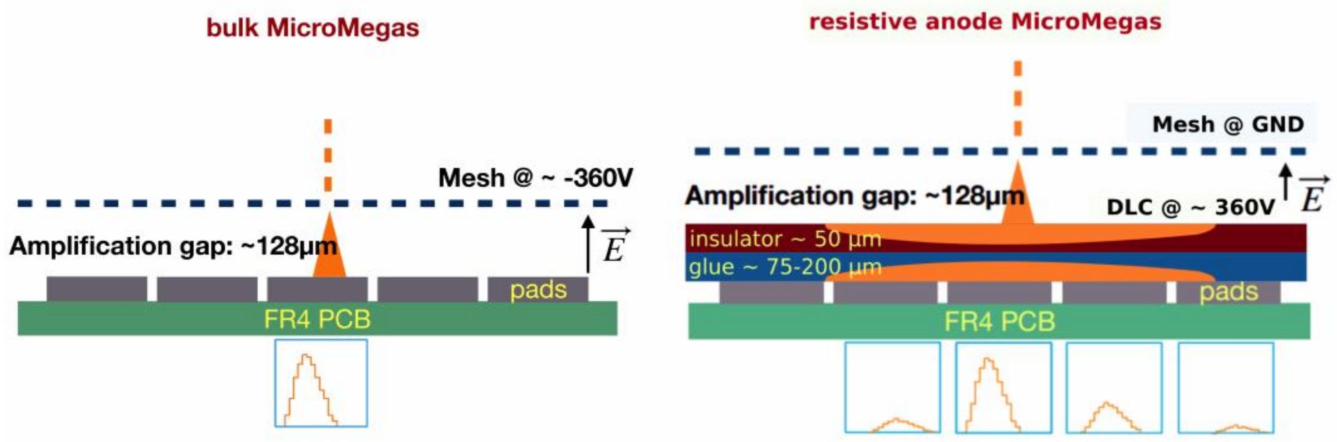

HA-TPC timeline

Design and Prototyping phase | **Building phase**

Timeline

- **CERN 2018**
  Performance of **spreading** for right pad dimensions
- **DESY 2019**
  Performance of foil of 400 kΩ/sq but not final electronics
- **DESY 2021**
  Electron beam with energy 0.5-5 GeV
  Superconductive magnet
- **CERN 2021**
  Muon beam
  No Magnetic field
  External tracker
- **CERN 2022**
  8 ERAMs at the same time
- **2023/2024**
  Installation at J-PARC

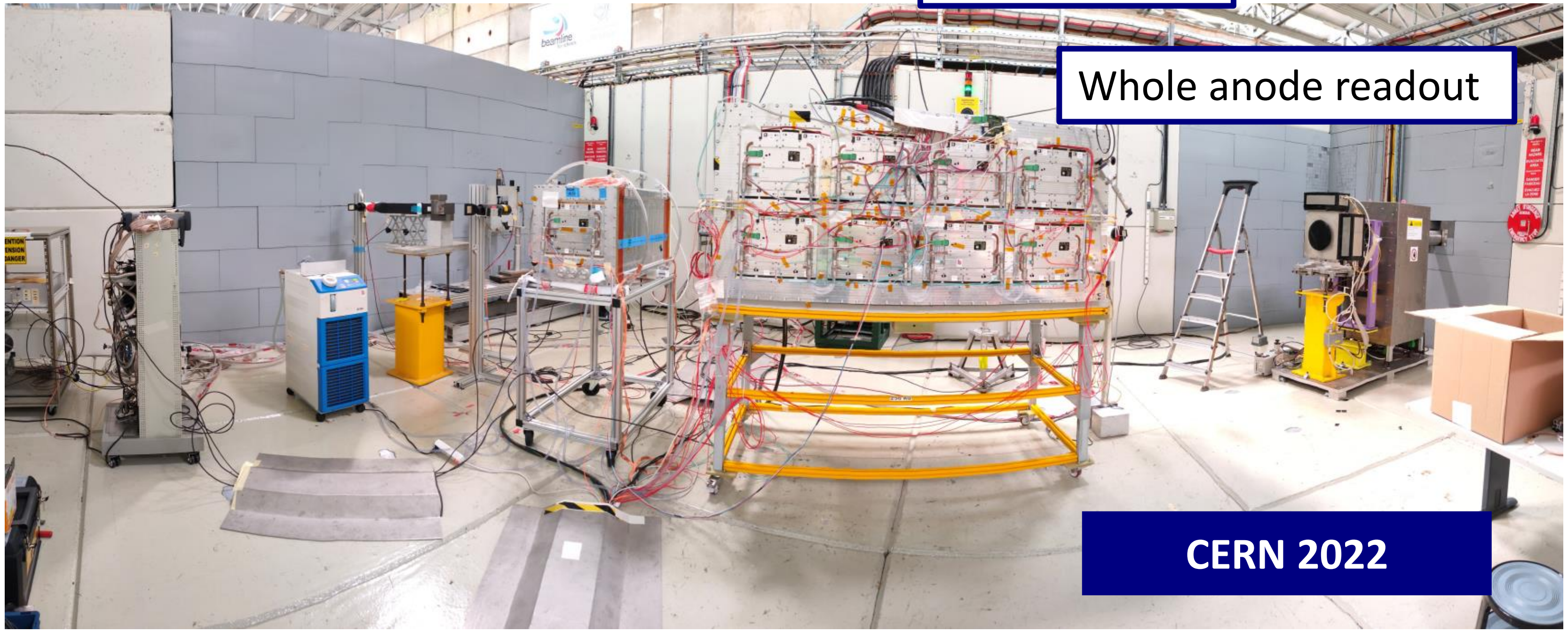
Whole anode readout

CERN 2022

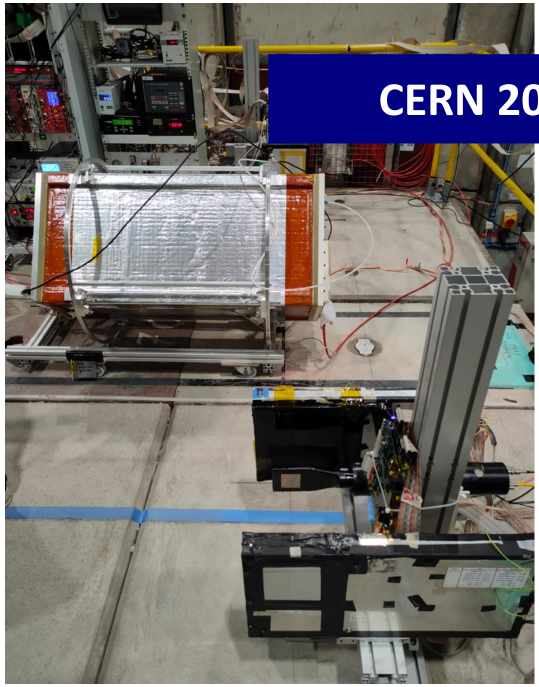
CERN 2021

HA-TPC installation

Installation of HA-TPC in ND280 at J-PARC

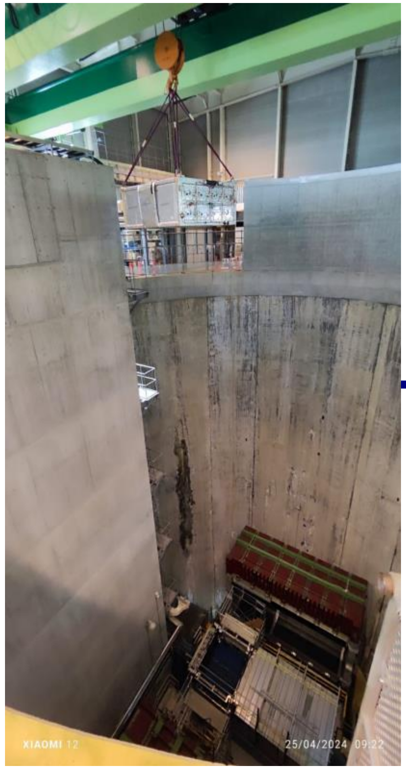

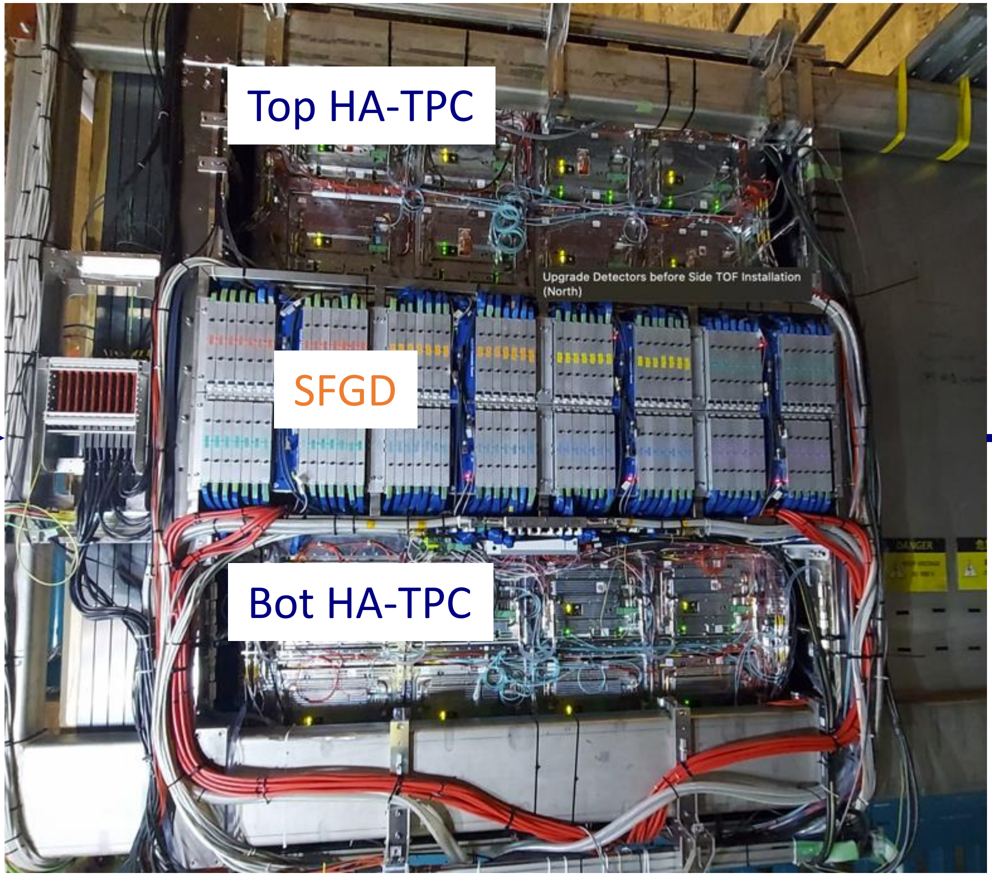

Top HA-TPC

Neutrino data since May 2024

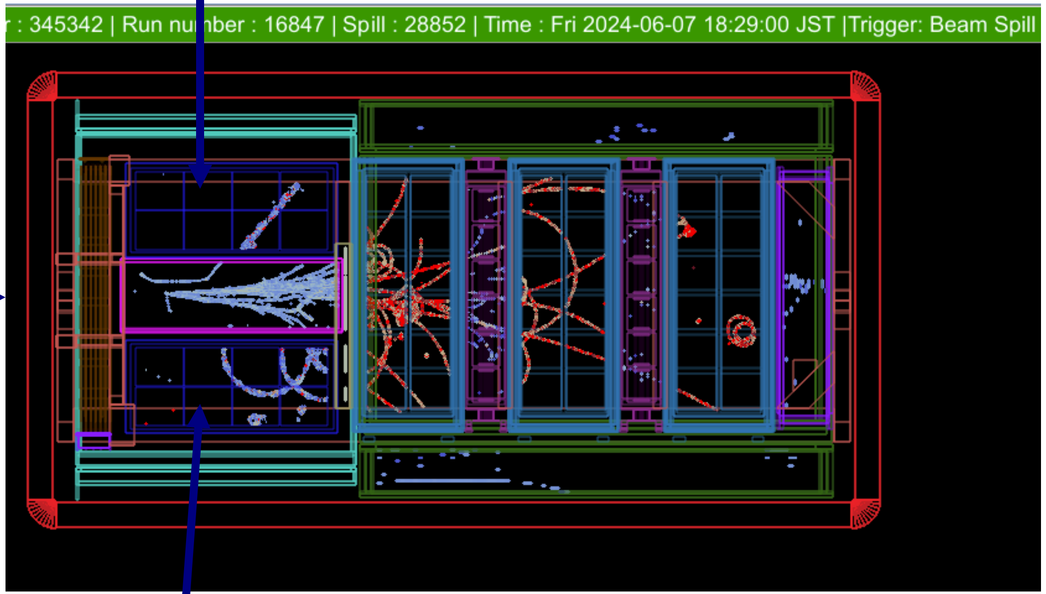

Bot HA-TPC

Side view of full ND280 event display

1. Introduction to Neutrino Physics
2. T2K Experiment
3. High-Angle Time Projection Chamber
4. **Field Cage production and characterization**
5. Study on Field Cage 0 insulation issue
6. Study on Electric field of Field Cages
7. Track Reconstruction algorithm with Machine Learning

Field Cage Production

The next part of the presentation is dedicated to illustrate my work:

1. Building of the field cages of HA-TPC
2. Characterization of their insulating properties
3. Characterization of their mechanical properties

of the 4 field cages used in the realization of the two HA-TPCs

The first field cage (FC0) presented a critical electrical issue, which helped us to improve the final design and the building procedure

Field Cage Production

Field cages are made of lightweight composite materials, therefore they require multiple steps over a period of about three months to be completed

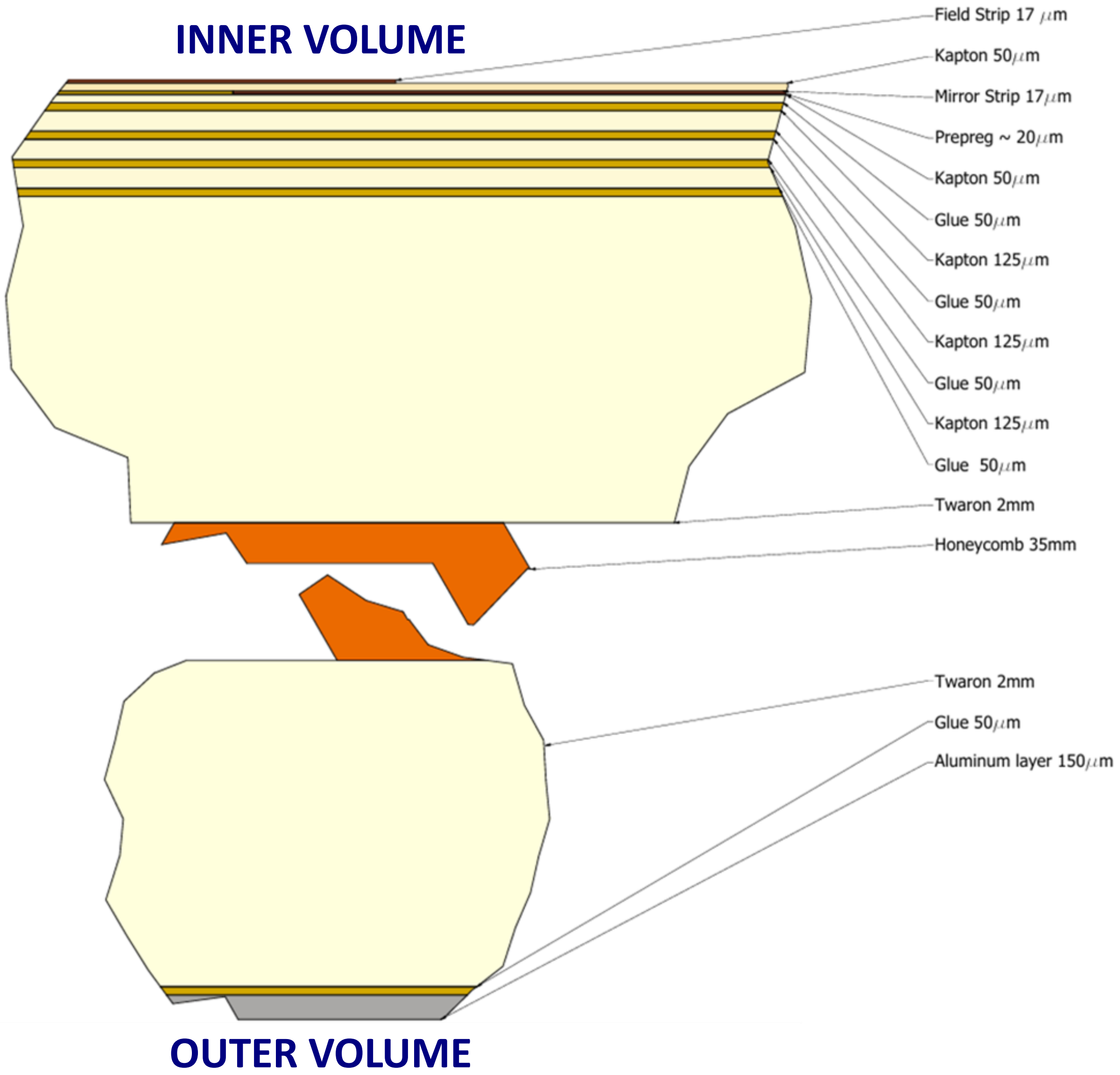

Mold

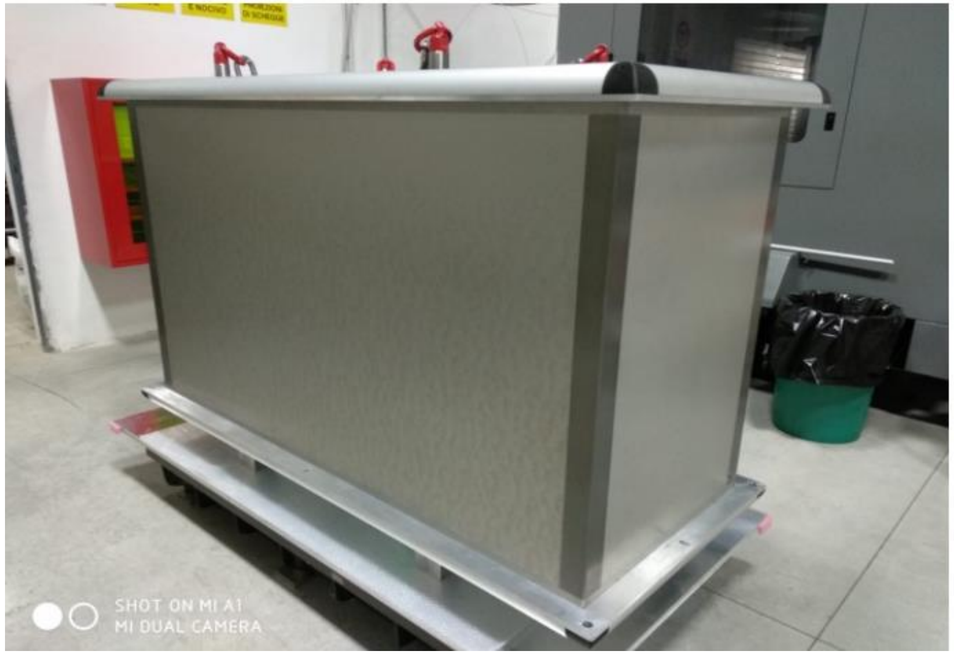

Central support structure with high accuracy reference

Field Cage Production

Field cages are made of lightweight composite materials, therefore they require multiple steps over a period of about three months to be completed

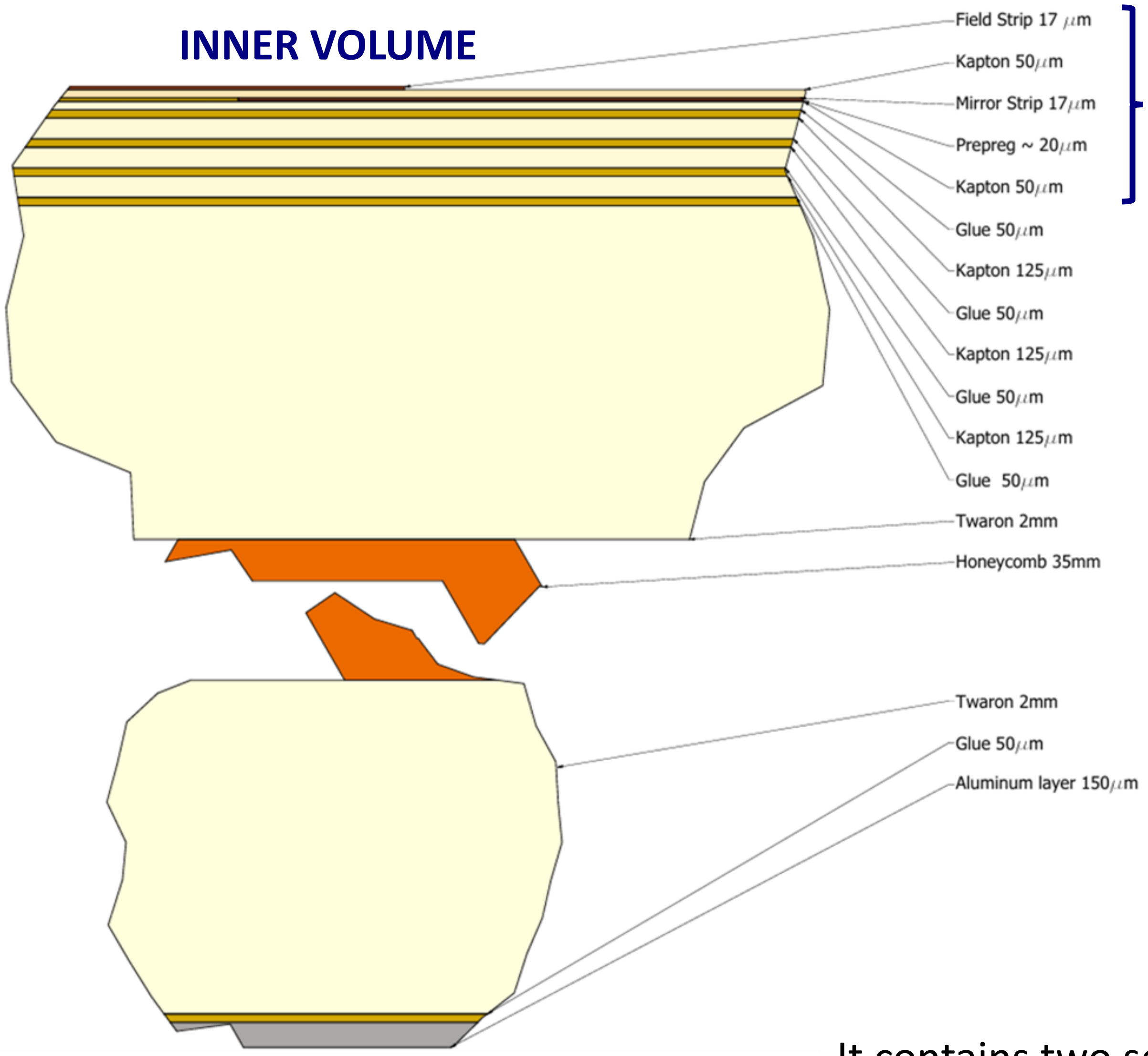

Strip foil

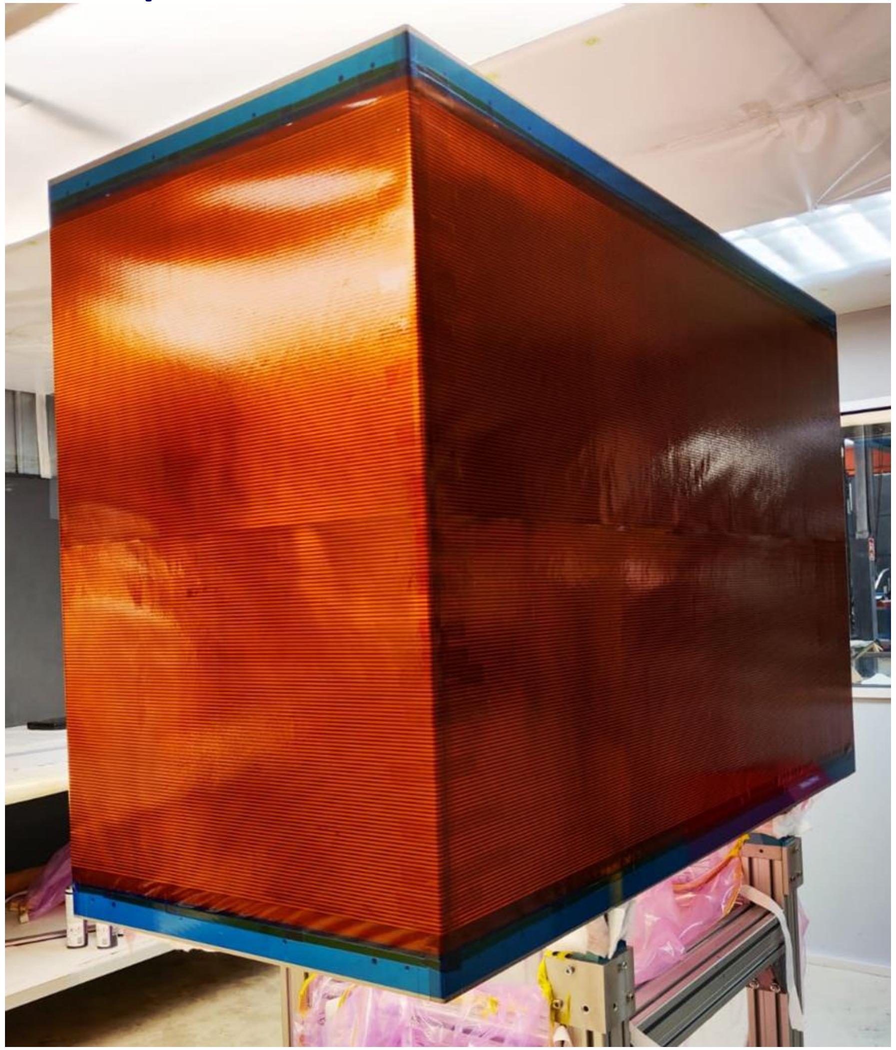

It contains two sets of copper strips to shape the Electric field

Field Cage Production

Field cages are made of lightweight composite materials, therefore they require multiple steps over a period of about two months to be completed

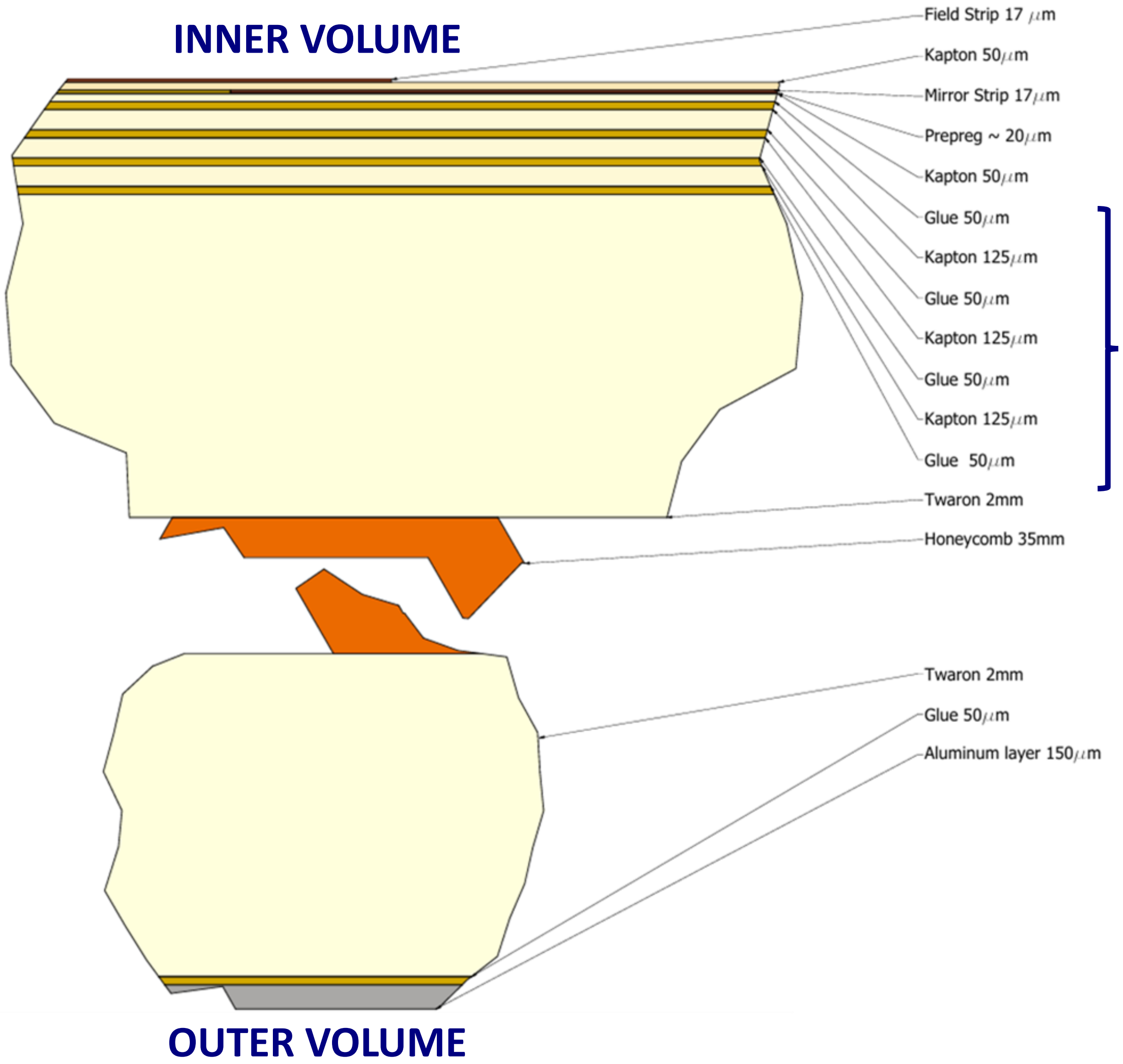

Additional Kapton for protection

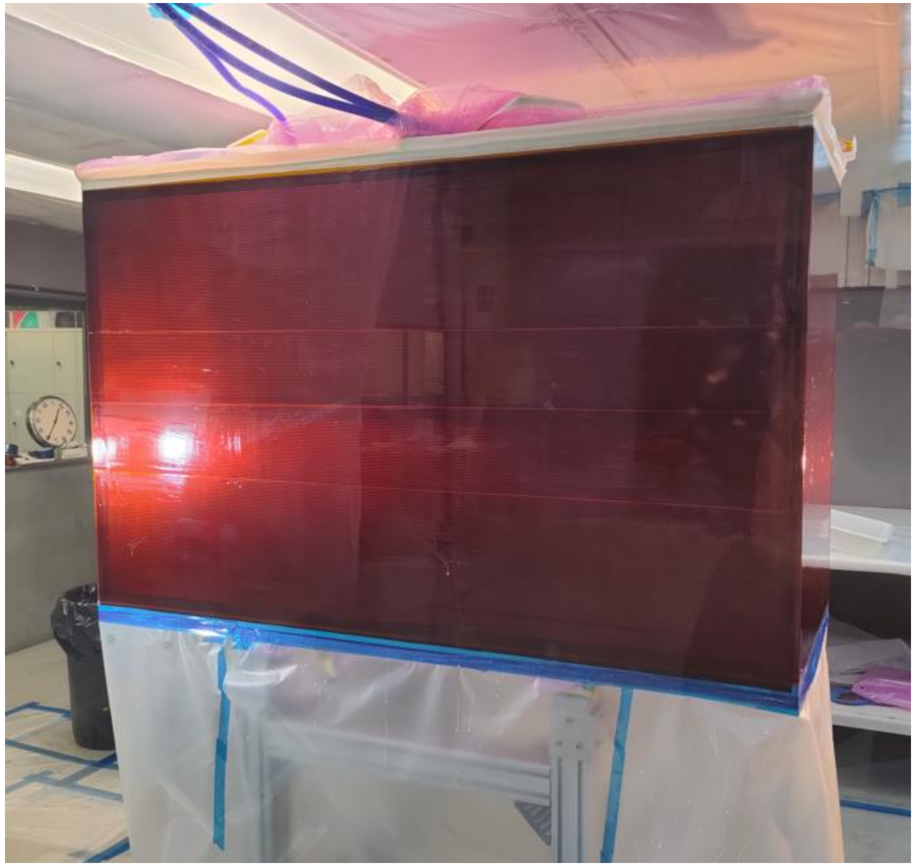

Additional Kapton layers for optimal insulation

Field Cage Production

Field cages are made of lightweight composite materials, therefore they require multiple steps over a period of about two months to be completed

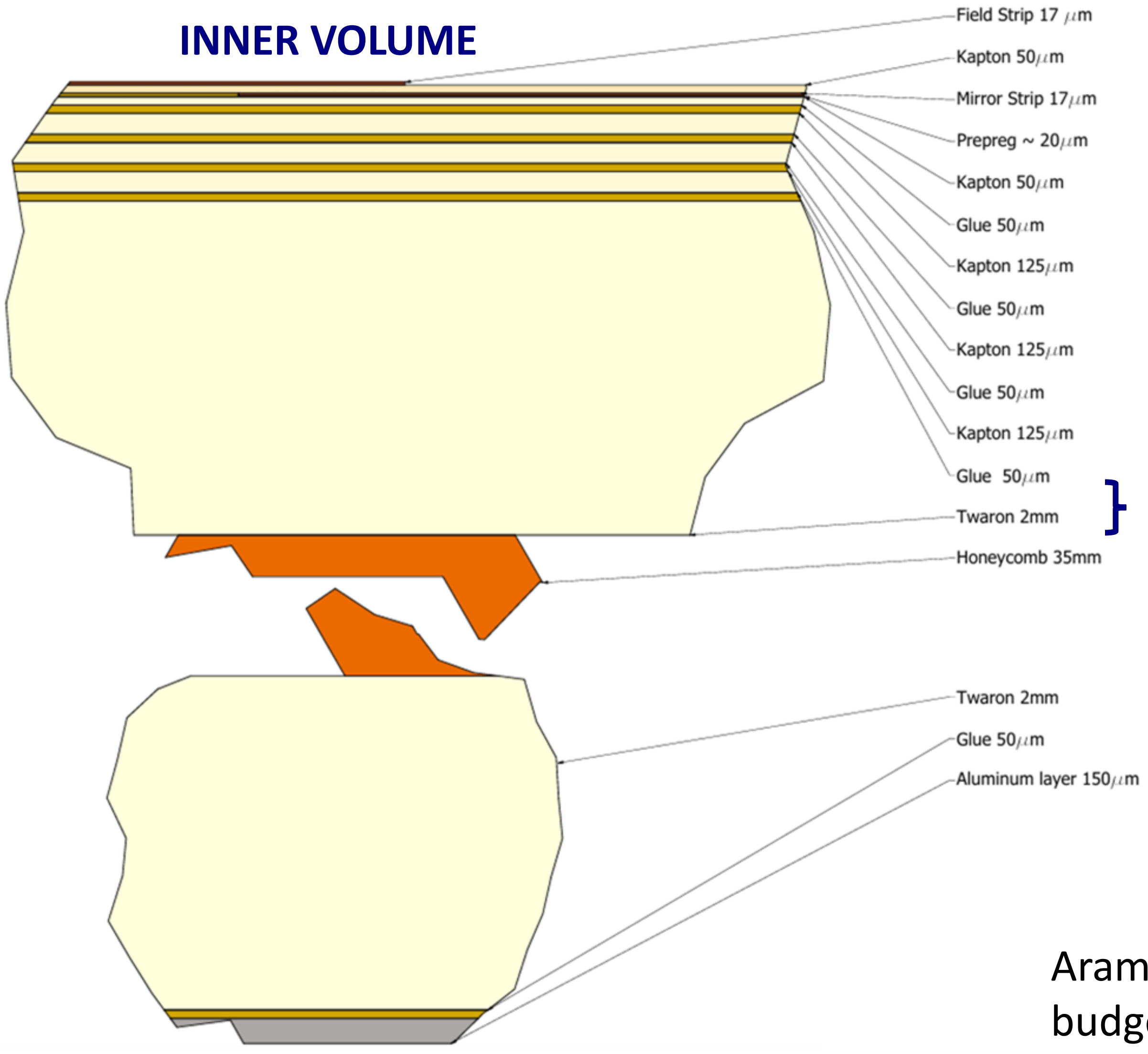

Internal Twaron layer

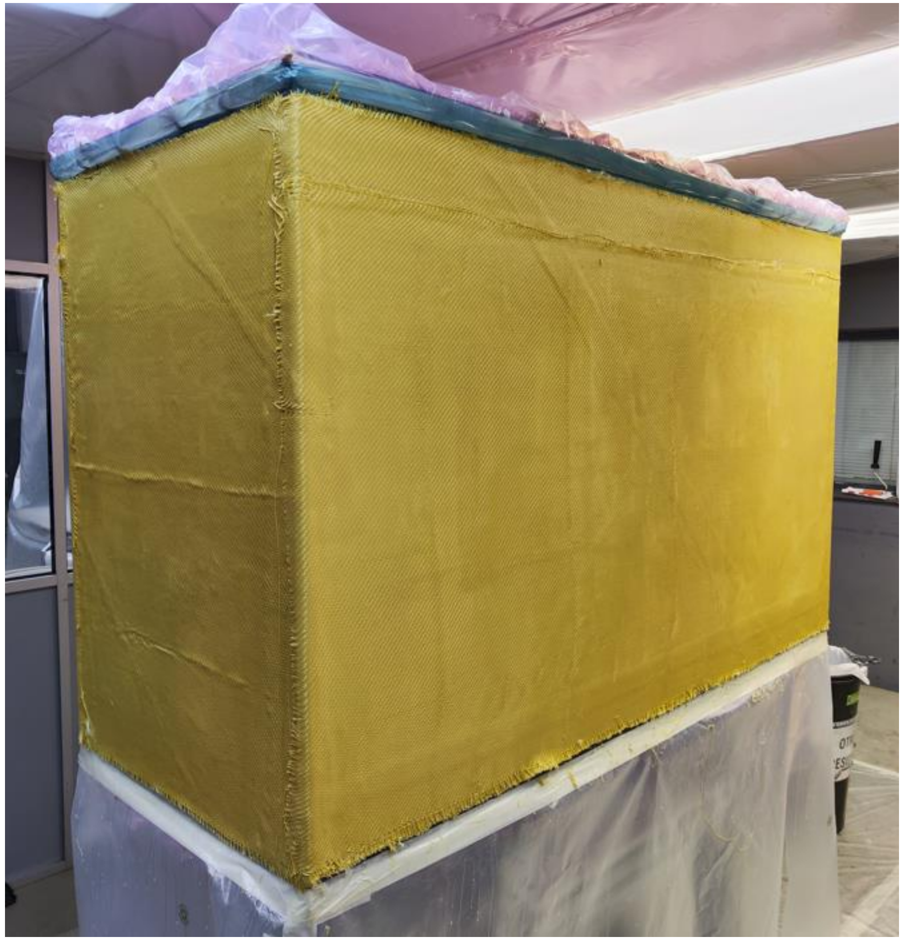

Aramid fabric for optimal mechanical support while maintaining low budget materials and insulating properties

Field Cage Production

Field cages are made of lightweight composite materials, therefore they require multiple steps over a period of about two months to be completed

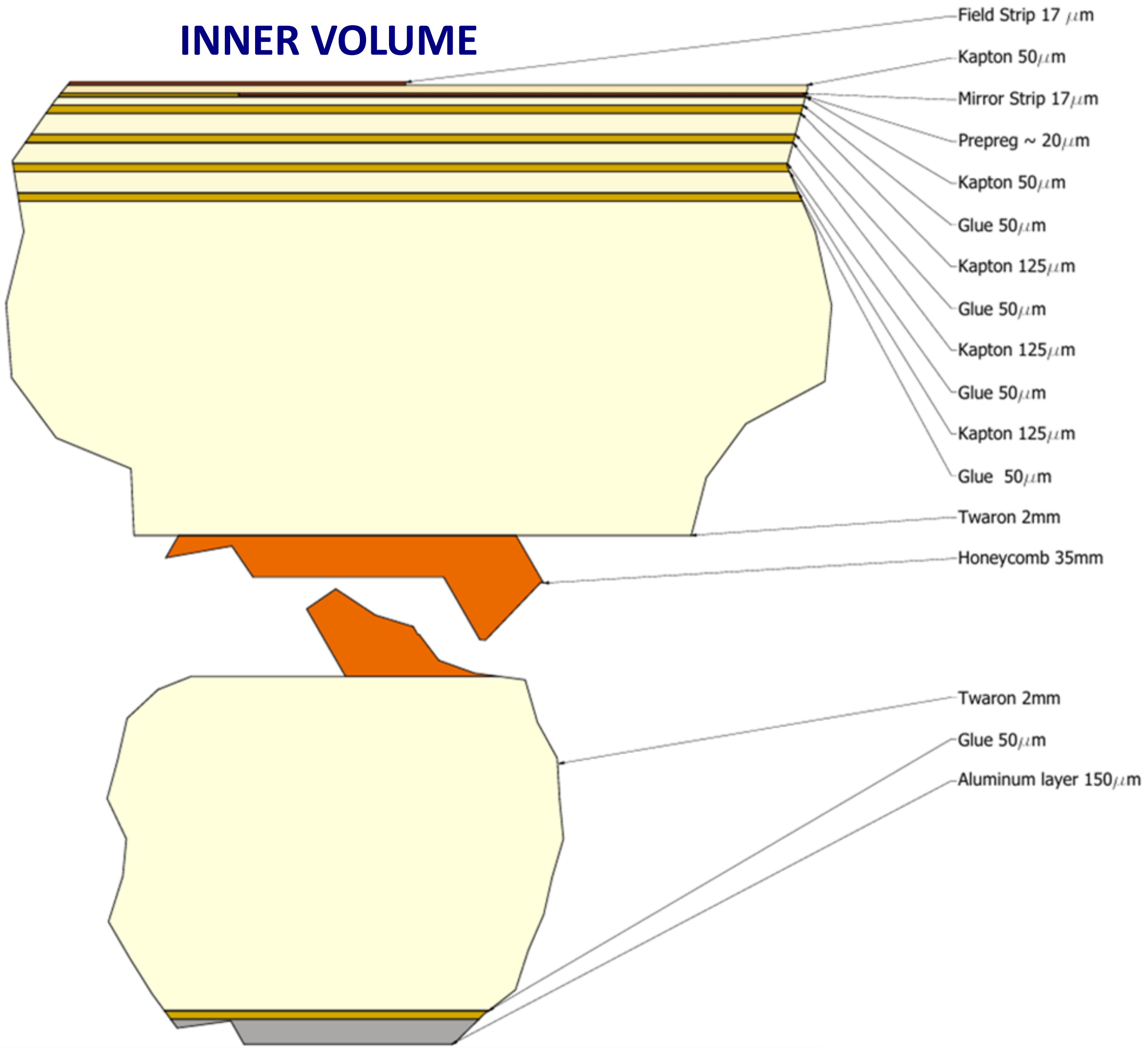

Flanges

Fiberglass structure

Field Cage Production

Field cages are made of lightweight composite materials, therefore they require multiple steps over a period of about two months to be completed

INNER VOLUME

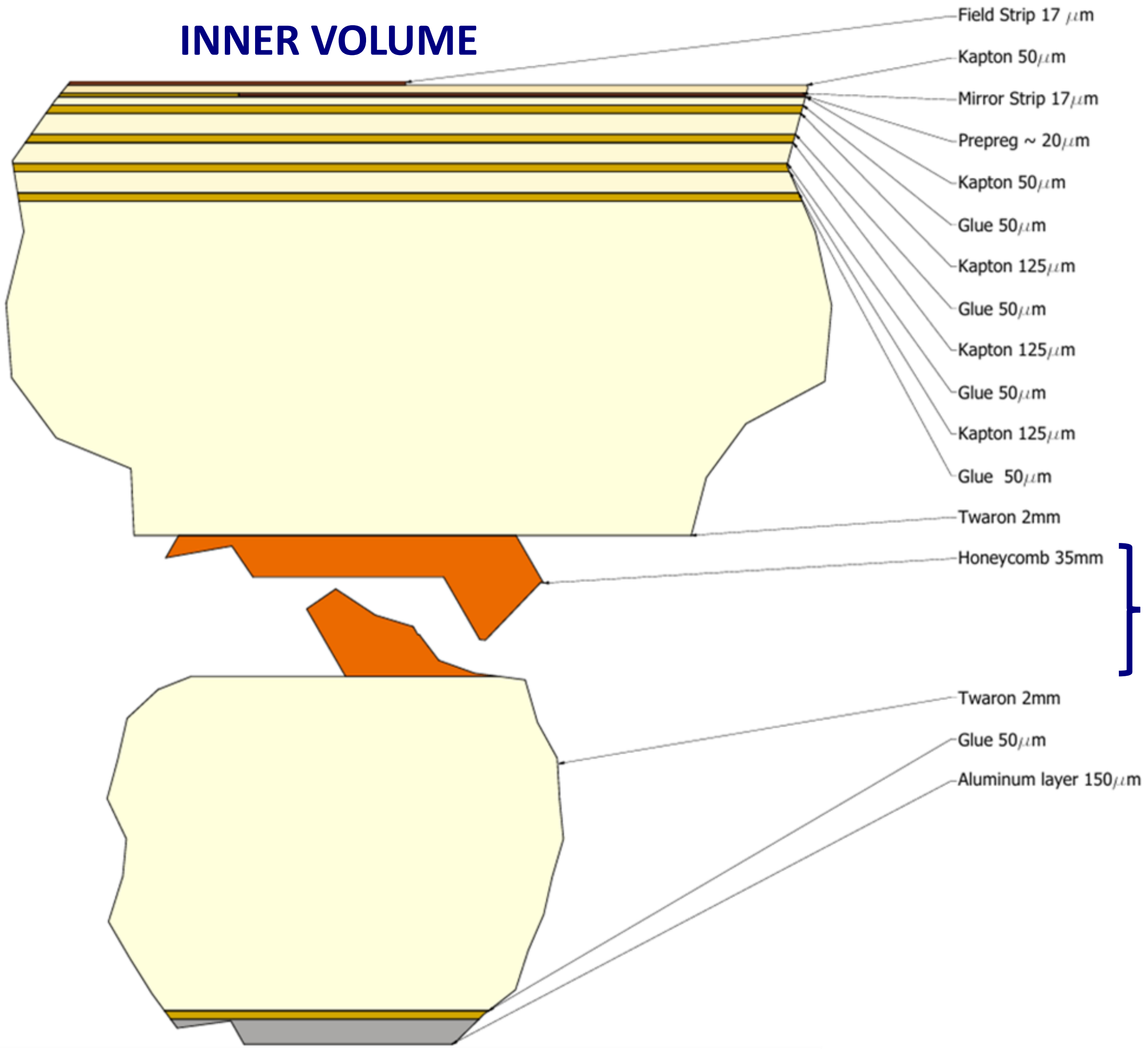

OUTER VOLUME

HoneyComb

Lightweight structural material

Field Cage Production

Field cages are made of lightweight composite materials, therefore they require multiple steps over a period of about two months to be completed

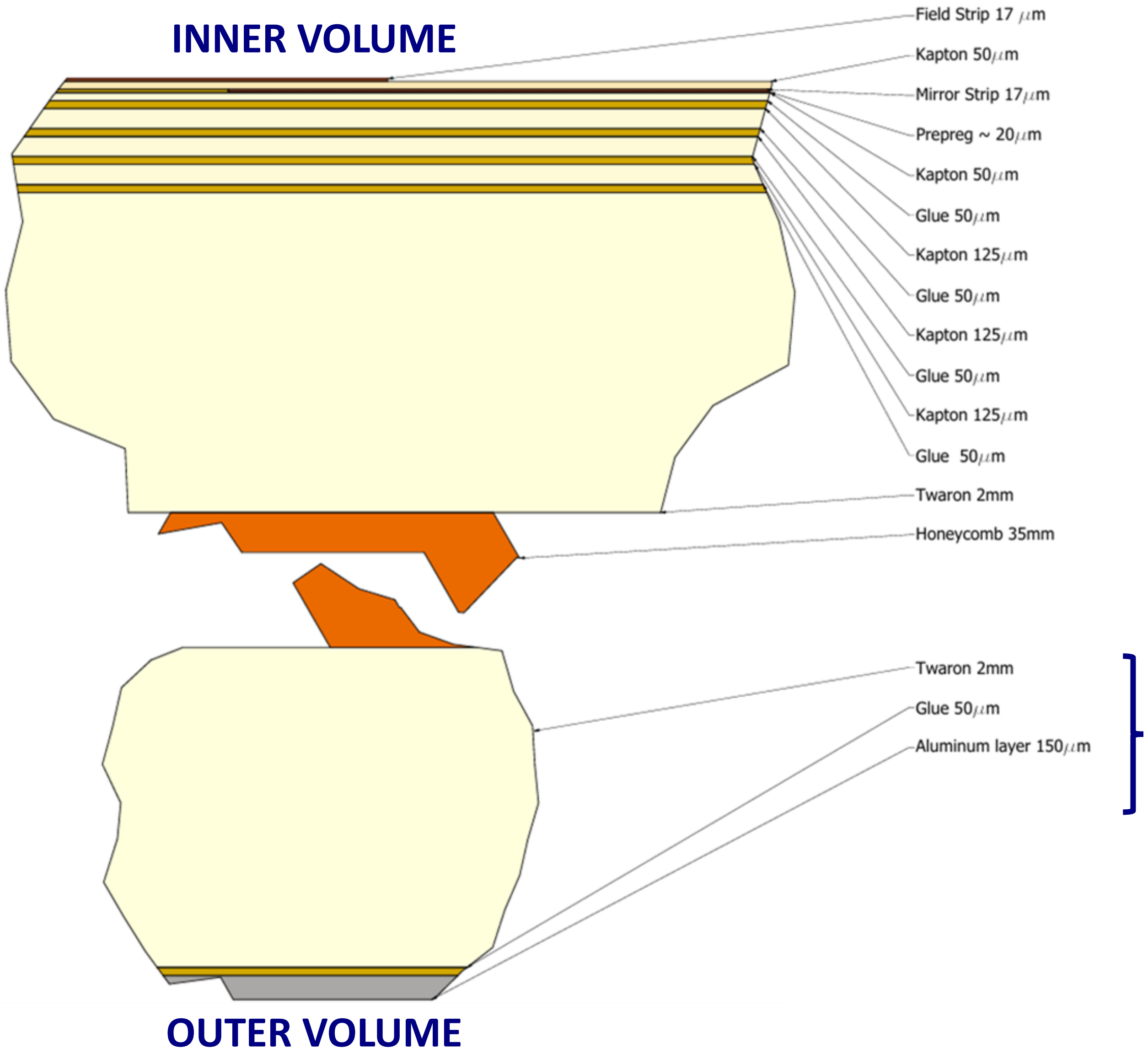

External layers

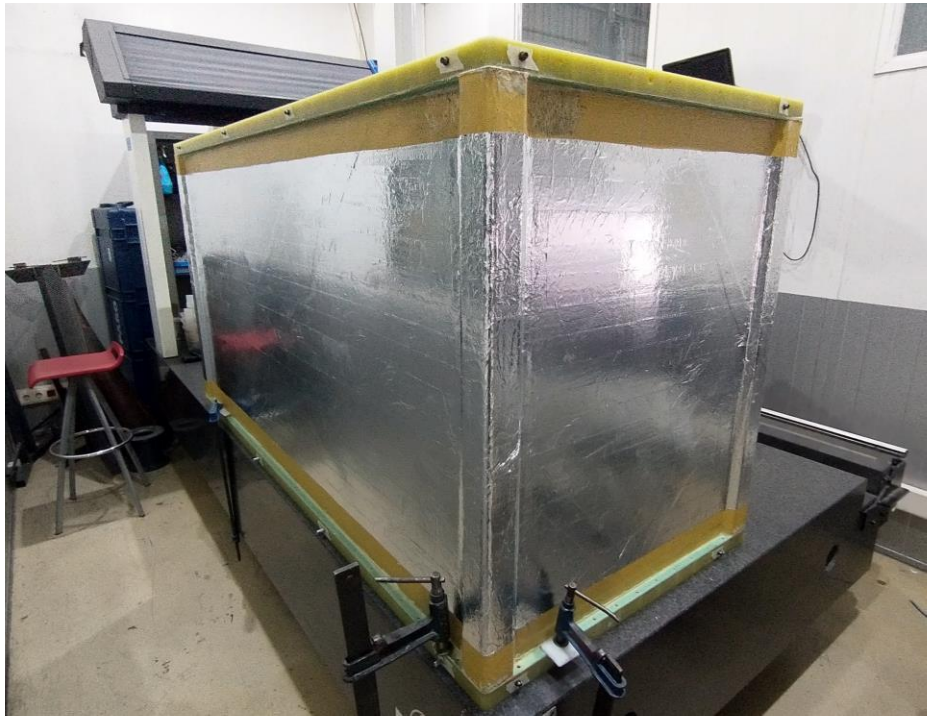

Additional Twaron layers and Aluminum shielding

HA-TPC assembly

Field cages are made of lightweight composite materials, therefore they require multiple steps over a period of about two months to be completed

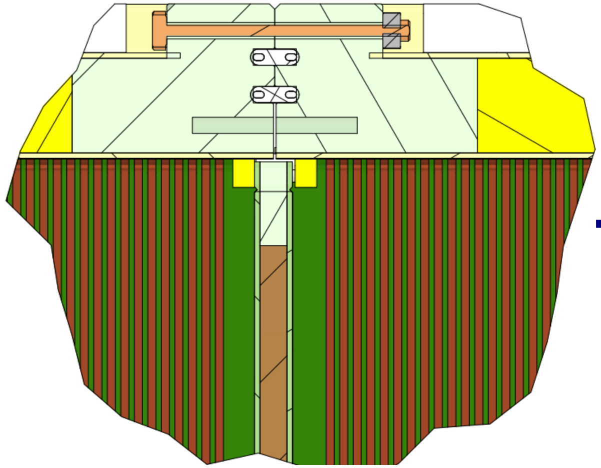

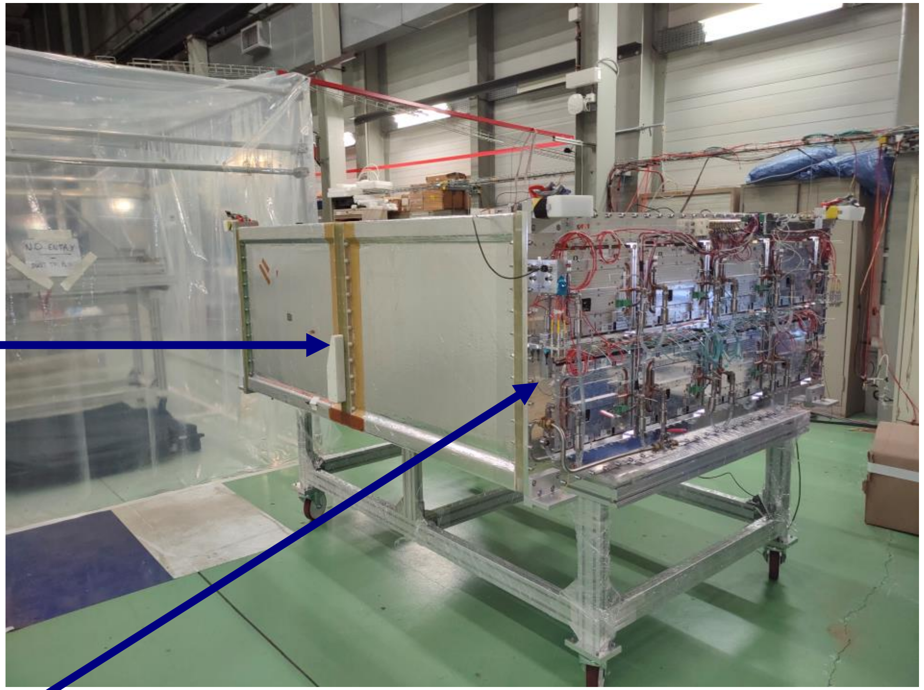

HA-TPCs are formed by two field cages with a central common cathode and two endplates

Mechanical tests

Deformation due to under- or over-pressure on field cage walls that might influence the direction of electric field

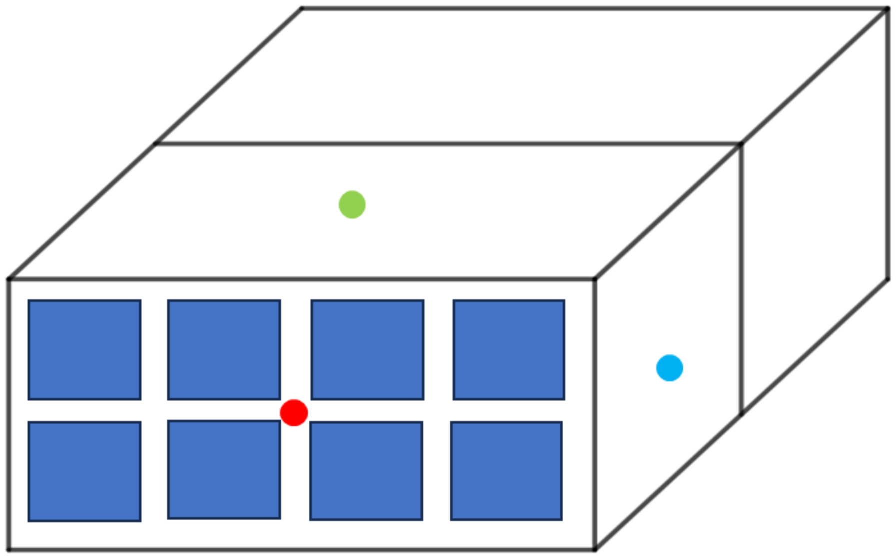

Data:

Max deformation of large faces: $\sim 50 \frac{\mu\mathrm{m}}{\mathrm{mbar}}$

Max deformation of small faces: $\sim 8 \frac{\mu\mathrm{m}}{\mathrm{mbar}}$

Almost linear in the studied pressure range

FULL axial contribution of the cathode panel

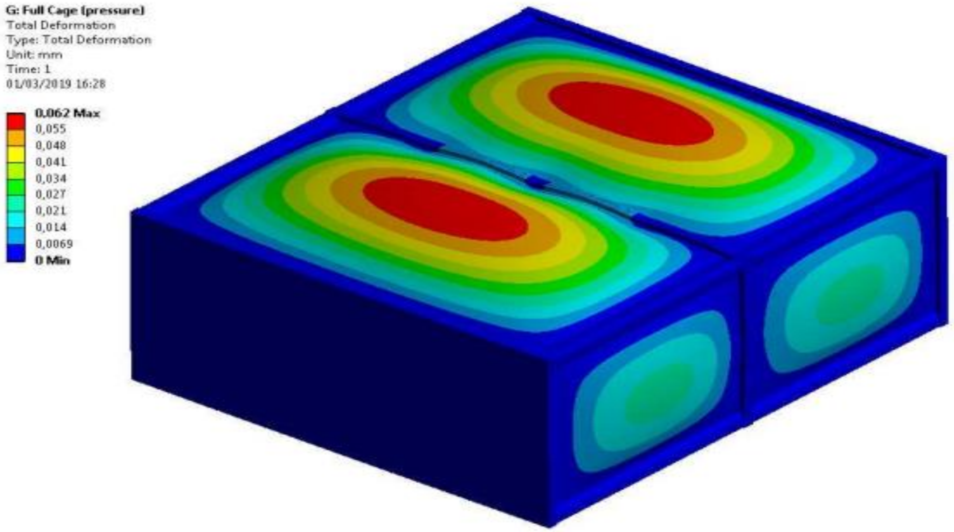

Max total deformation ~60 μm

Simulation:

Max deformation of large faces: $\sim 50 \frac{\mu\mathrm{m}}{\mathrm{mbar}}$

Central cathode only partially constrains flanges deformation

Evaluation of Insulating Properties

Particular attention was dedicated to the insulating properties of the inner materials:

- Strip foil
- Additional Kapton layers
- Inner Twaron layer
- Resins

to assess:

The issue was here in the first Field Cage

1. Surface resistivity

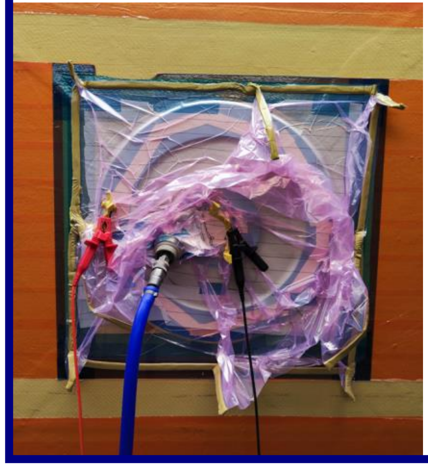

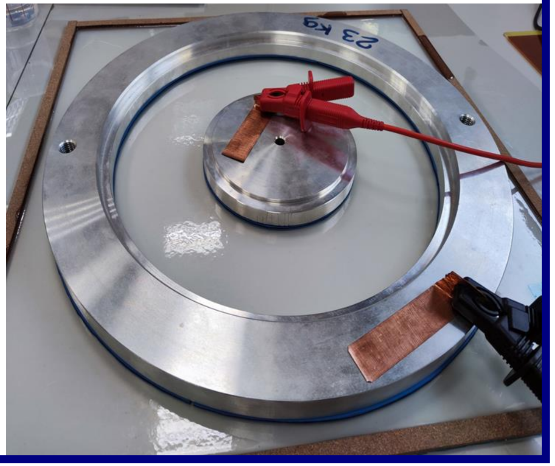

2. Volumetric resistivity

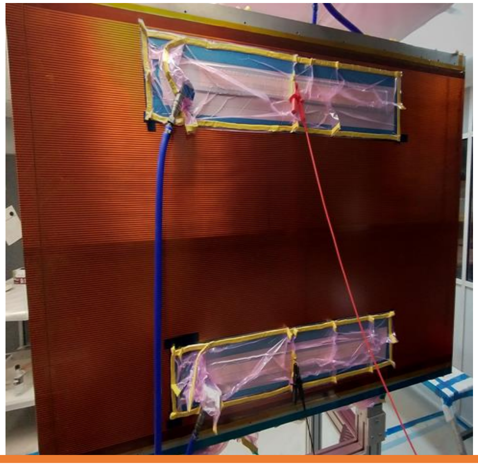

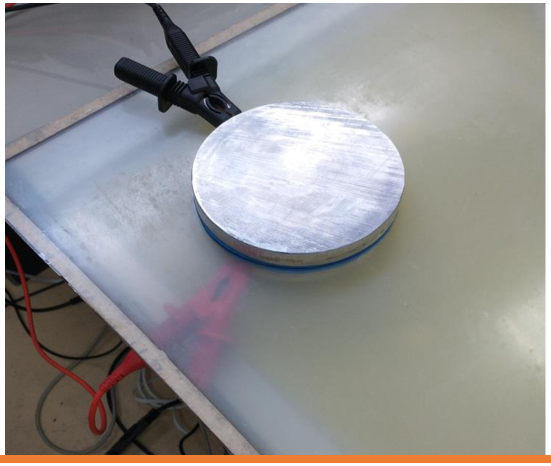

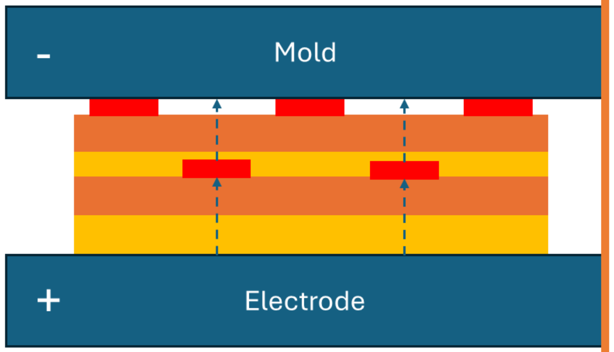

Resin Resistivity

1. Surface resistivity

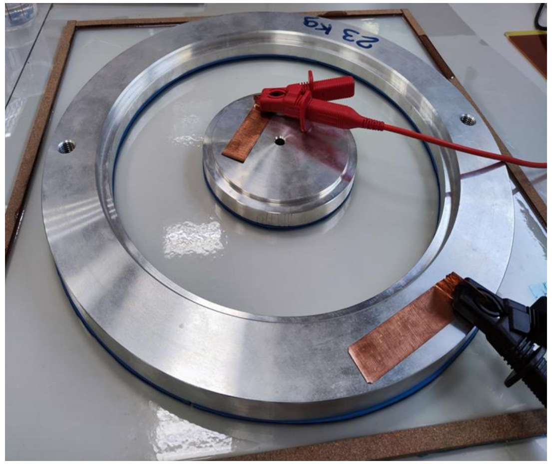

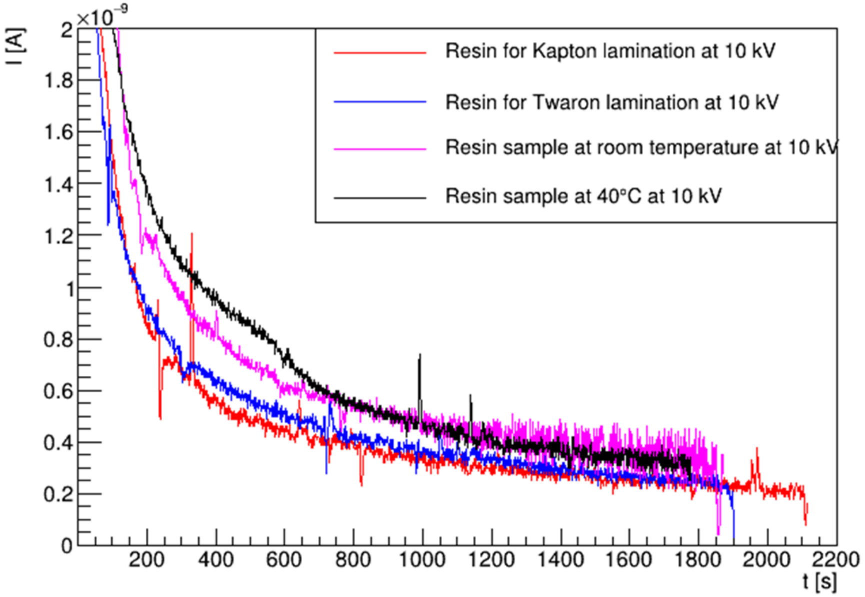

Dataset	Voltage [kV]	Current [pA]	R_S [Ω/□]
Twaron lamination	10	84 ± 1	$(9.9 \pm 0.1) \cdot 10^{14}$
Kapton lamination	10	104 ± 5	$(8.0 \pm 0.4) \cdot 10^{14}$
Room T curing	10	169 ± 7	$(4.9 \pm 0.2) \cdot 10^{14}$
40°C curing	10	96 ± 5	$(8.7 \pm 0.4) \cdot 10^{14}$

Expected values from an insulating material!

2. Volumetric resistivity

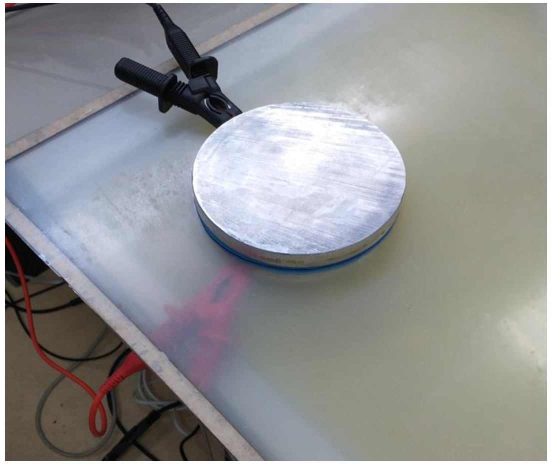

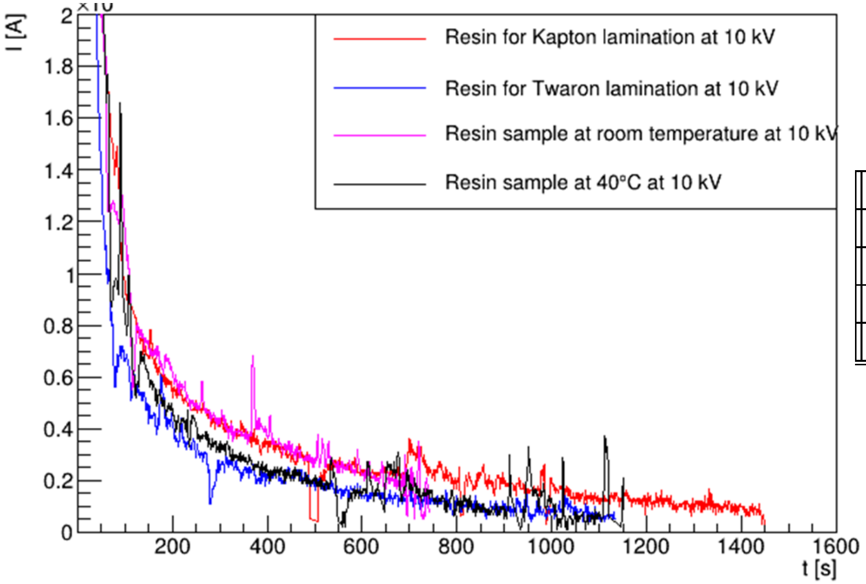

Dataset	Voltage [kV]	Current [pA]	ρ_{vol} [Ω·cm]
Twaron lamination	10	220 ± 2	$(7.133 \pm 0.007) \cdot 10^{16}$
Kapton lamination	10	252 ± 1	$(6.223 \pm 0.002) \cdot 10^{16}$
Room T curing	10	348 ± 4	$(4.520 \pm 0.006) \cdot 10^{16}$
40°C curing	10	330 ± 2	$(4.760 \pm 0.003) \cdot 10^{16}$

1. Introduction to Neutrino Physics
2. T2K Experiment
3. High-Angle Time Projection Chamber
4. Field Cage production and characterization
5. **Study on Field Cage 0 insulation issue**
6. Study on Electric field of Field Cages
7. Track Reconstruction algorithm with Machine Learning

Field Cage 0

Field Cage 0 was the first full scale field cage realized, which showed a critical flaw in its insulating properties and stability over time

- Small scale prototypes did not demonstrate a similar issue
- The main difference is the strips length, **5 times larger** than in the prototypes

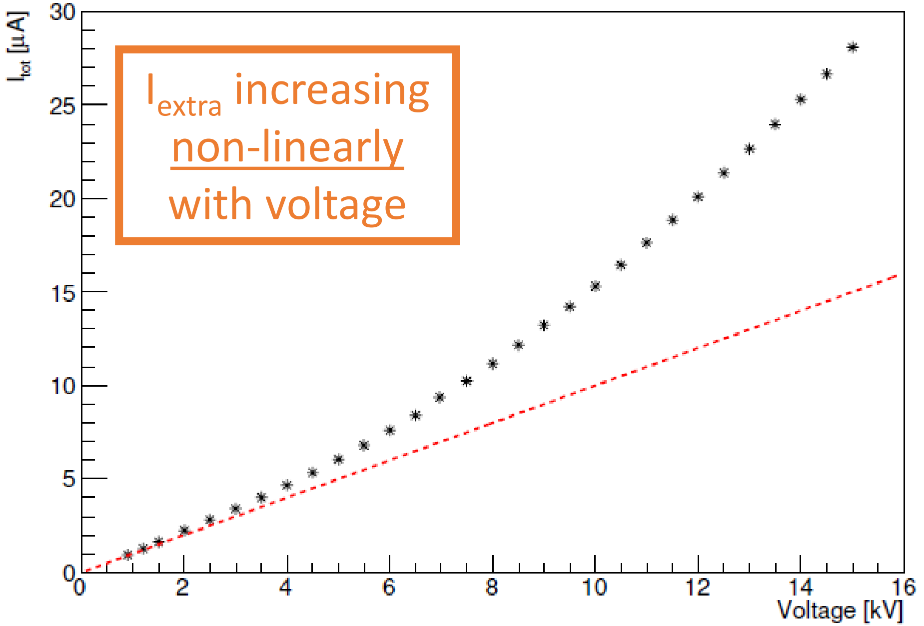

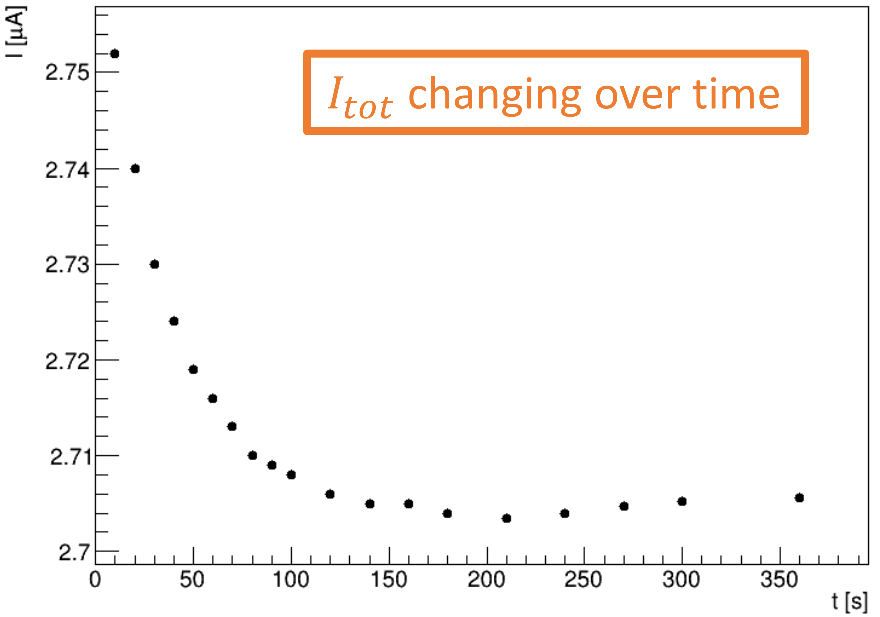

The degradation of insulating properties was caused by the use of an **antistatic spray** during the construction procedure, which **contaminated** the layers making them **resistive**

Field Cage 0

Field Cage 0 was the first full scale field cage realized, which showed a critical flaw in its insulating properties and stability over time

- Small scale prototypes did not demonstrate a similar issue
- The main difference is the strips length, **5 times larger** than in the prototypes

Non uniform voltage degradation

↓

Deformation of Electric field

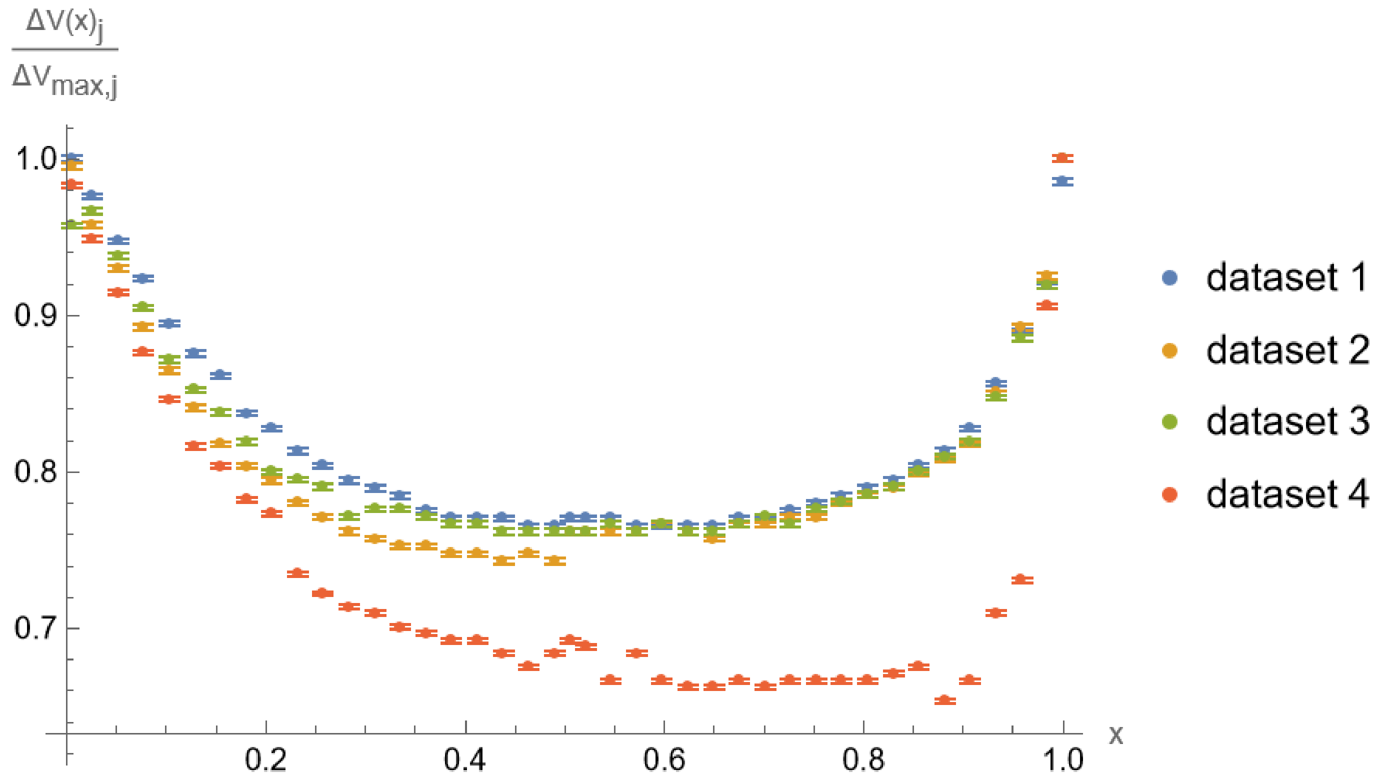

To investigate the issue, several steps were performed:

1. **Measurements** on current on the voltage divider
2. **Removal of glued field cage layers** to probe the ones underneath
3. **Development of models** to explain possible resistive paths inside field cage walls

Single Resistor measurements

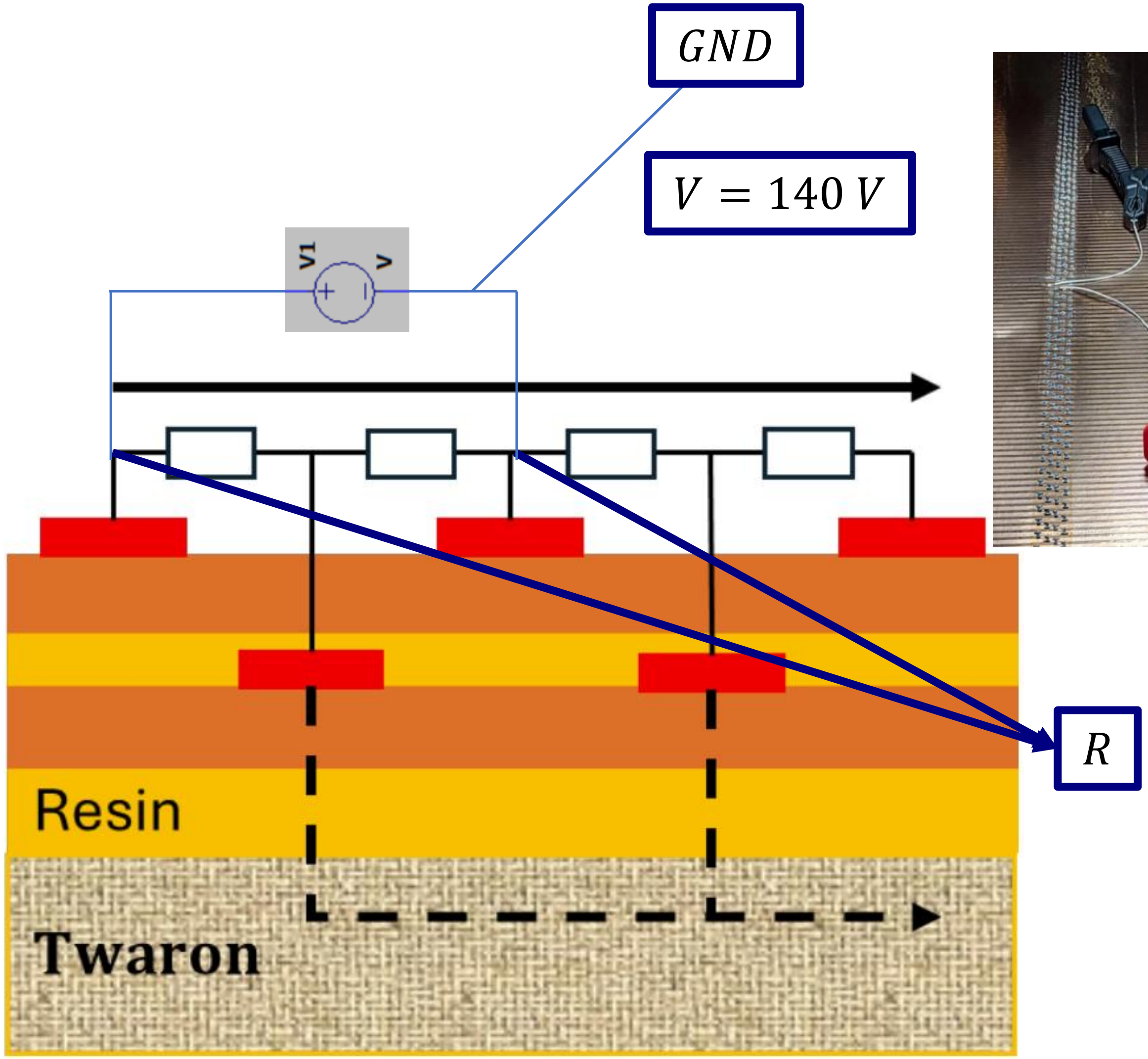

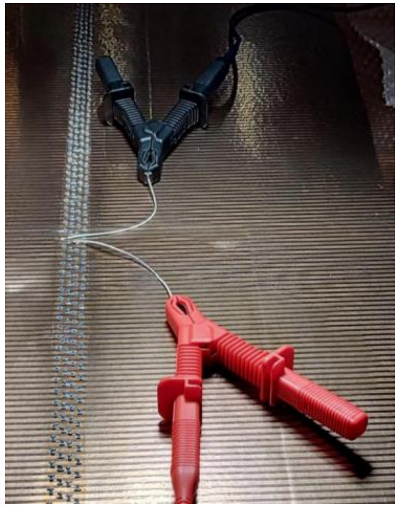

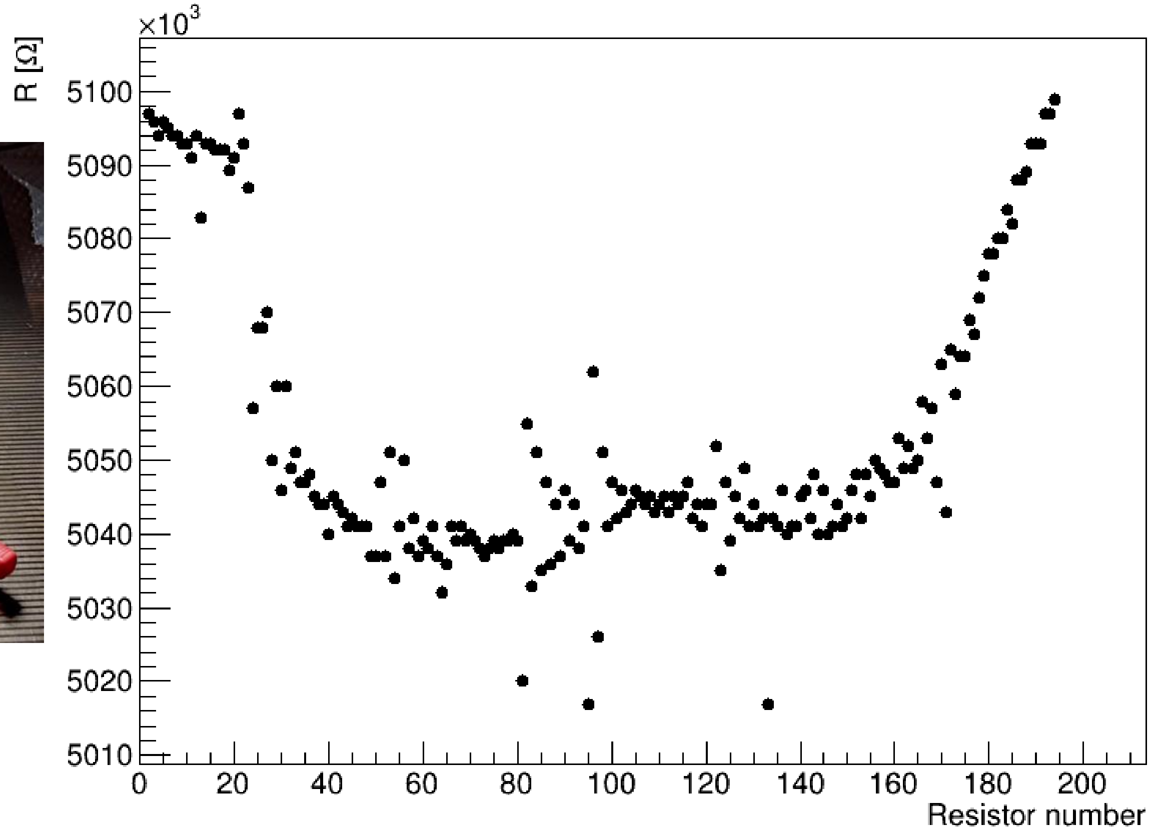

Resistors before soldering were selected to have resistance values with a tolerance $\sim 0.1\%$

Resistors after soldering on the voltage divider feature tolerance **>1%**

Global model of FC0

A model of the whole field cage has been realized by considering two resistive paths:

1. ***"Vertical leakage K"*:** Leakage current through the Kapton coverlay
2. ***"Horizontal leakage T"*:** Leakage current on layers parallel to the strip foil

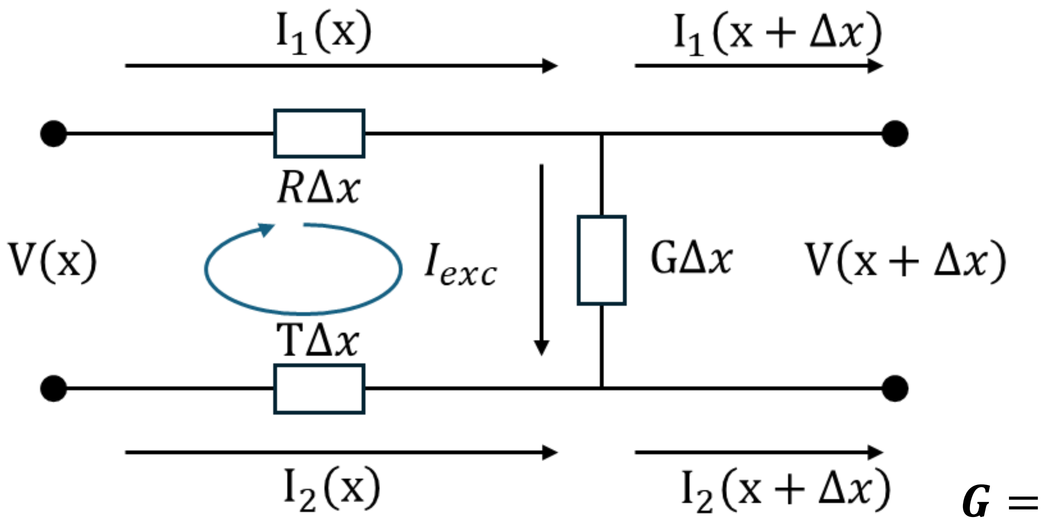

$\boldsymbol{G = 1/K}$

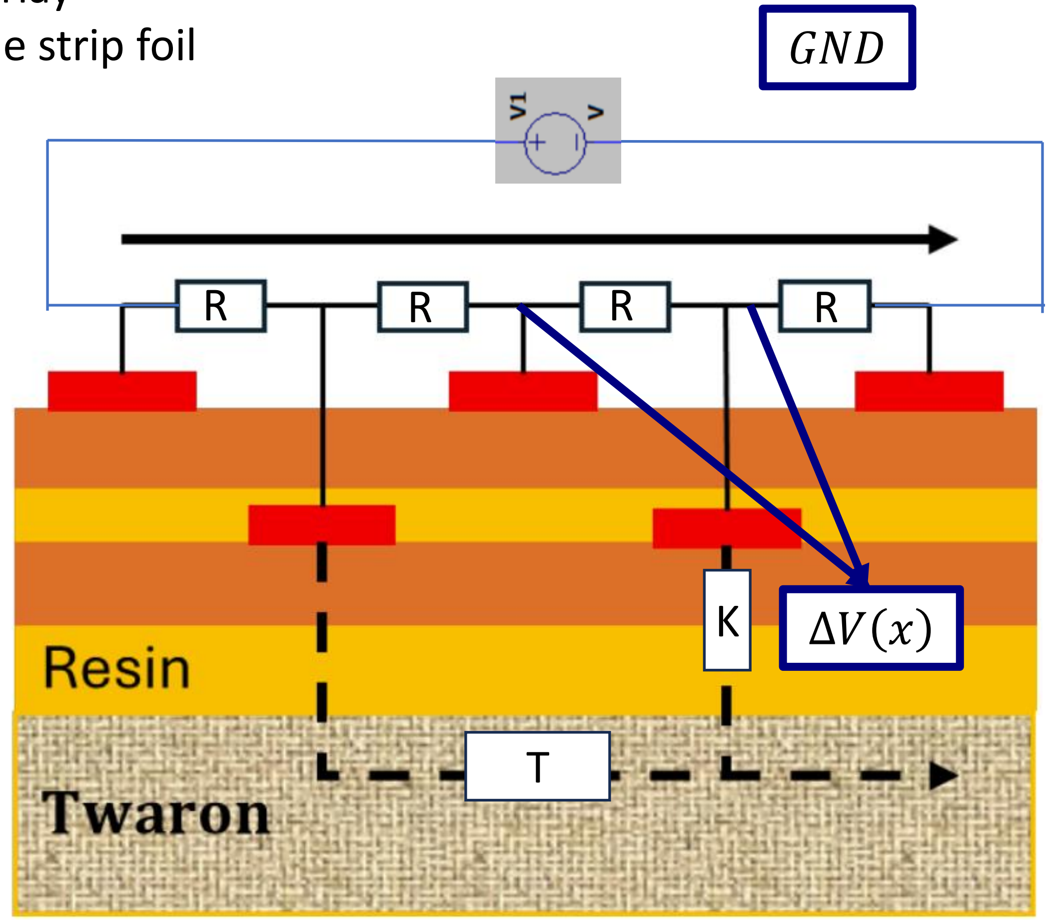

Two conditions to describe the model:

1. (K, T) uniform
2. (K_i, T_i) non uniform as a function of *x*

“Vertical” Resistivity

Measurements on FC0

Strip Foils of different Thickness

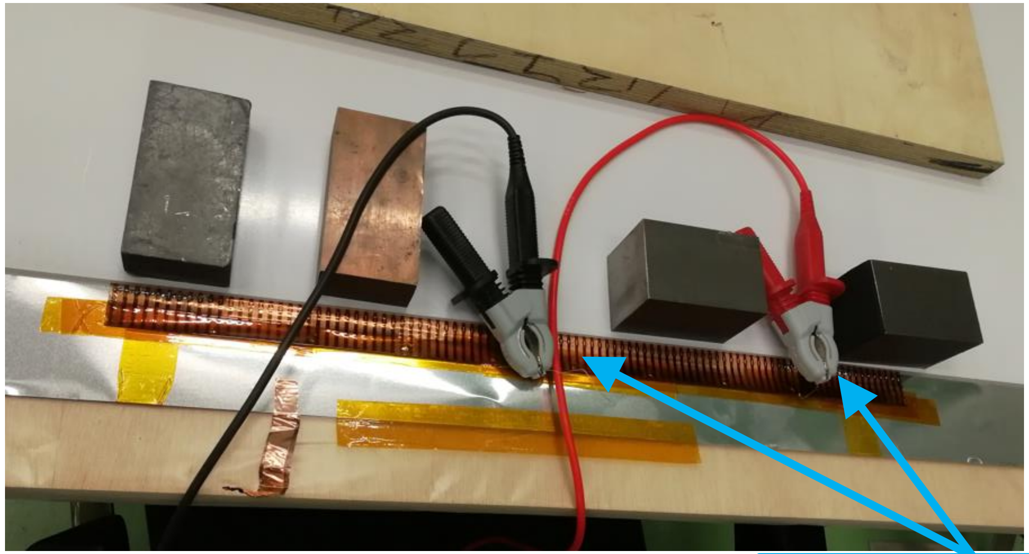

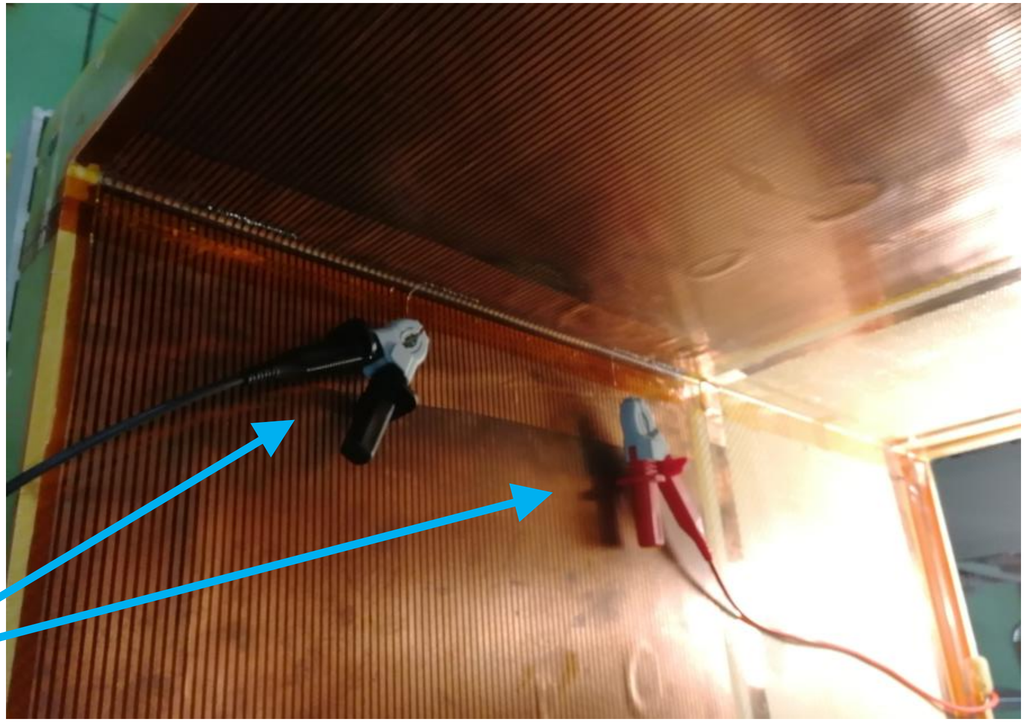

2 electrodes – HV applied

Measurements on Kapton resistivity were performed

“Vertical” Resistivity

Several measurements were performed on Kapton sheets or directly on strip foils

Foil #3
(like Foil #2 in FC#0)

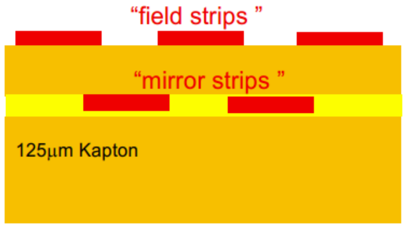

Foil #4
To be used for recovering FC#0

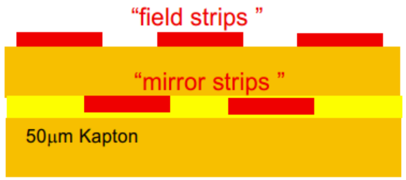

Foil #5
To be used for Next FC#1

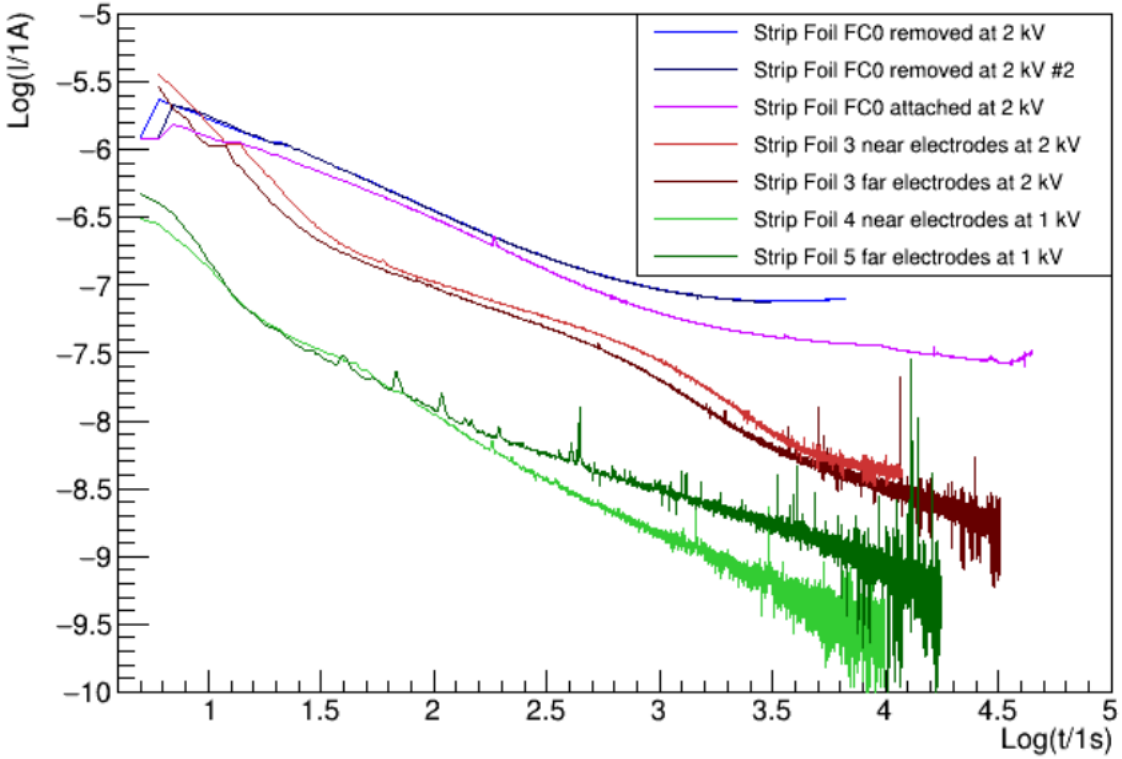

- Despite the **same coverlay thickness**, strip foil 2 used in FC0 and the new strip foil 3 behave very differently!

Converted into ***“strip equivalent” (i.e. one cell):***

Dataset	R_{strip} [GΩ]
Kapton 25 μm, round electrodes	14.79 ± 0.07
Strip foil 2, removed	128.03 ± 0.03
Strip foil 2, attached	350.4 ± 0.1
Strip foil 3	2320 ± 2

Compatible with theoretical value of Kapton

"Horizontal" Resistivity

External Twaron layer (not corrupted in FC0)

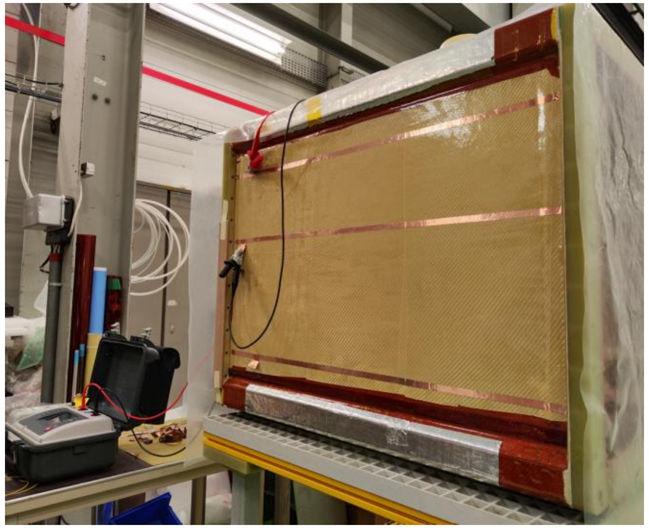

Internal Twaron layer (corrupted in FC0)

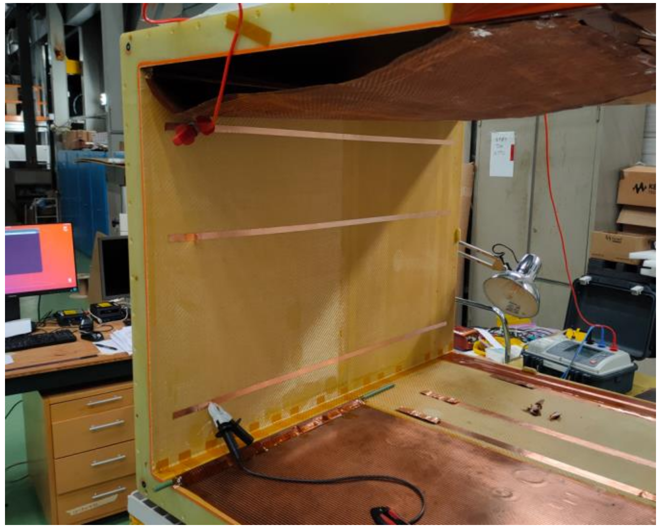

A lot of measurements with many different geometries and different places were performed studied.

There were important proofs that the **external** and **internal** Twaron layers behave differently

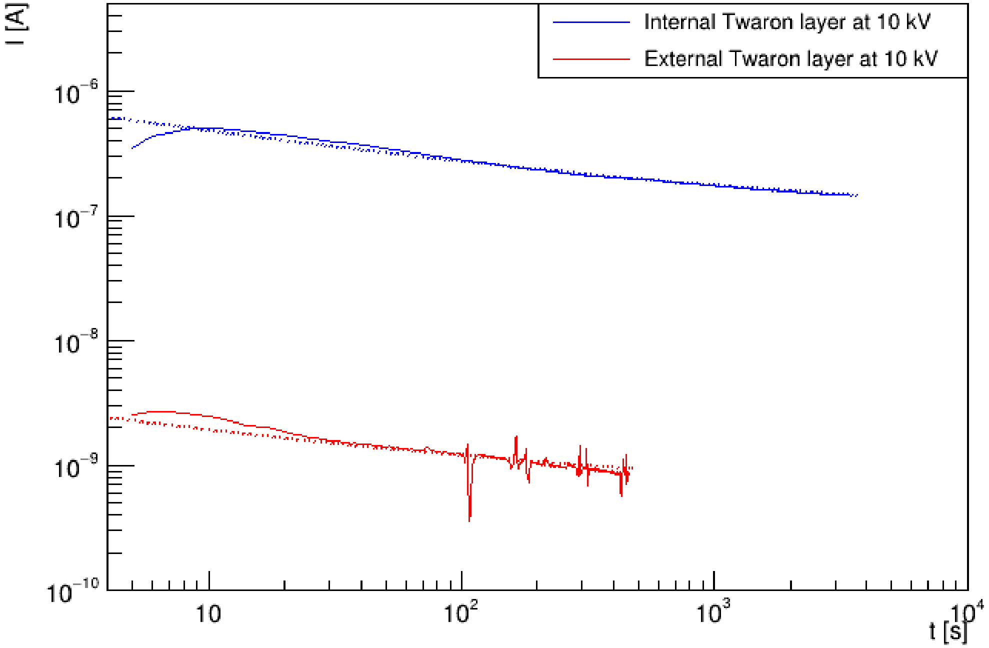

Converted into ***"strip equivalent" (i.e. one cell):***

Dataset	R_{strip} [MΩ]
Internal Twaron (30 kV)	120
Internal Twaron (5 kV)	600
External Twaron	24900

Global model: (K, T) constant

Considering such assumption, the model has an analytical solution:

$$\begin{cases} V\left(\frac{1}{2}\right) = 0 \\ I_2(0) = 0 \\ I_1(0) = I_1(1) \end{cases}$$

Symmetry condition (for $V\left(\frac{1}{2}\right) = 0$)

Initial and final condition on current (for $I_2(0) = 0$ and $I_1(0) = I_1(1)$)

$$V_0 = R \int_0^1 I_1(x)$$

Relation between HV applied and current

$$\boldsymbol{I_1(x)} = \frac{V_0}{R} \cdot \frac{R \cosh\left(\alpha\left(\frac{1}{2} - x\right)\right) + T \cosh\left(\frac{\alpha}{2}\right)}{\frac{2R}{\alpha} \sinh\left(\frac{\alpha}{2}\right) + T \cosh\left(\frac{\alpha}{2}\right)} \qquad \alpha = \sqrt{\frac{R+T}{K}}$$

Values ***"strip equivalent"***:

Dataset	$\bar{T}_{all}^{strip}$ [MΩ]	$\bar{K}_{strip}^{all}$ [MΩ]
1-2-3	16.0±0.4	9000±2000
4	11.2±0.5	2400±800

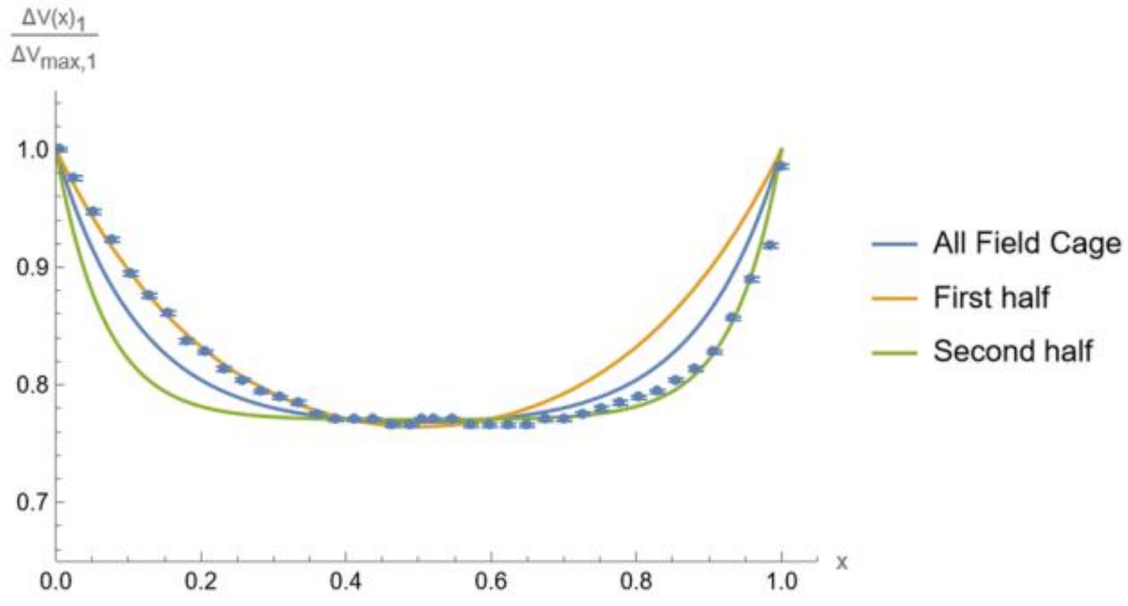

Dataset 1

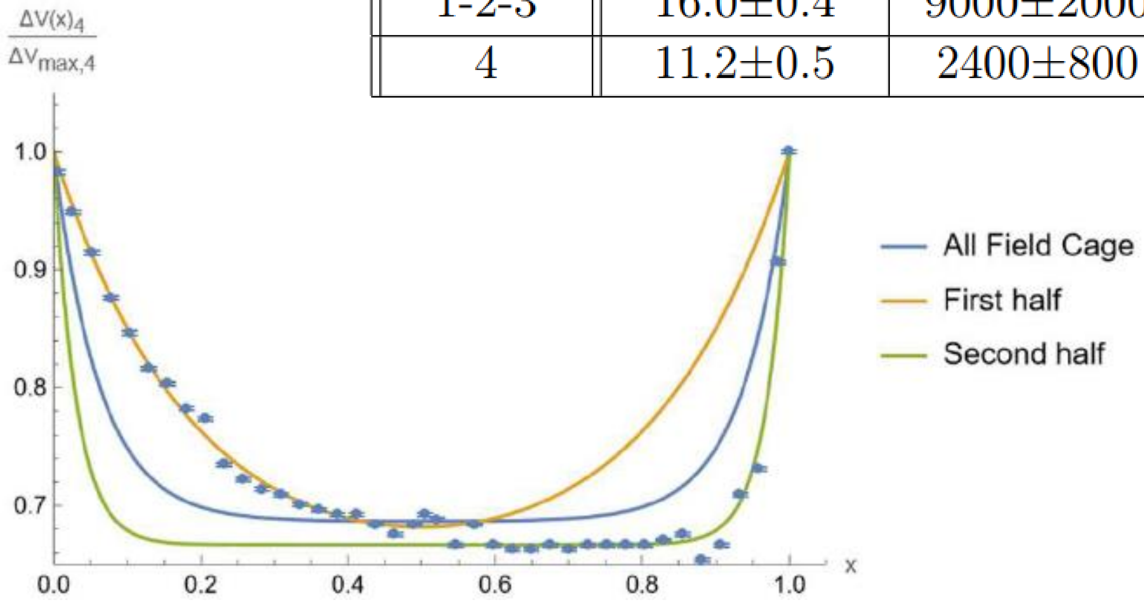

Dataset 4

Parameter λ: from measurements on Kapton and Twaron

In order to eliminate the degeneracy in the model, it is necessary to impose that (K_i, T_i) vary with the same rate λ

Dataset	R_{strip} [MΩ]
Internal Twaron (30 kV)	120
Internal Twaron (5 kV)	600
External Twaron	24900

Dataset	R_{strip} [GΩ]
Kapton 25 μm, round electrodes	14.79 ± 0.07
Strip foil 2, removed	128.03±0.03
Strip foil 2, attached	350.4±0.1
Strip foil 3	2320 ± 2

$$\lambda_{exp} = \frac{T}{K} \sim 8 \times 10^{-3}$$

The residual degeneracy is now fixed!

(K_i, T_i) values are not constant at the edges!

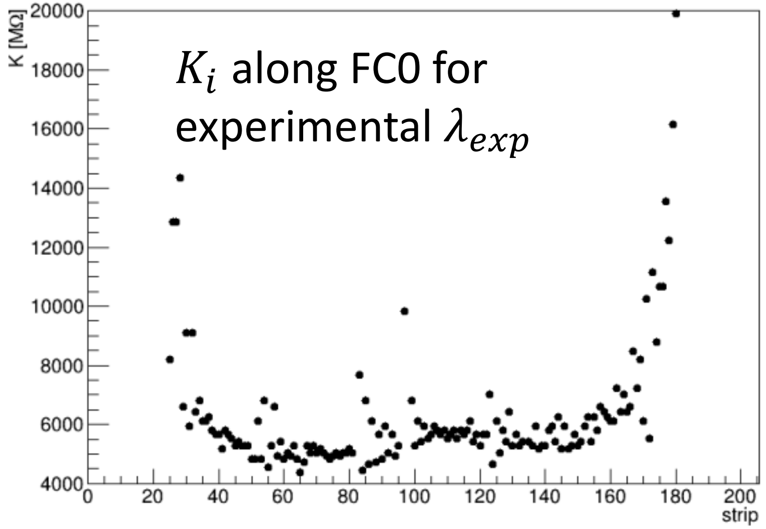

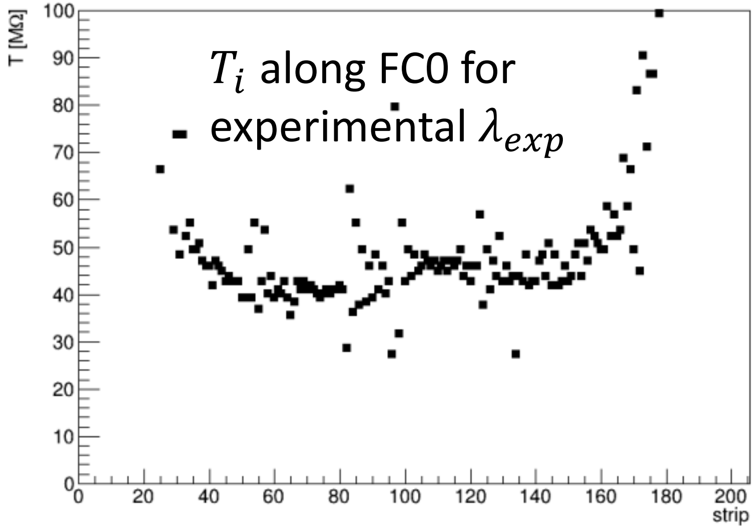

Parameter λ: from measurement of total current

From **global measurements:**

Extract best λ such that $I_{meas}^{tot} = I_{predicted}^{tot}$

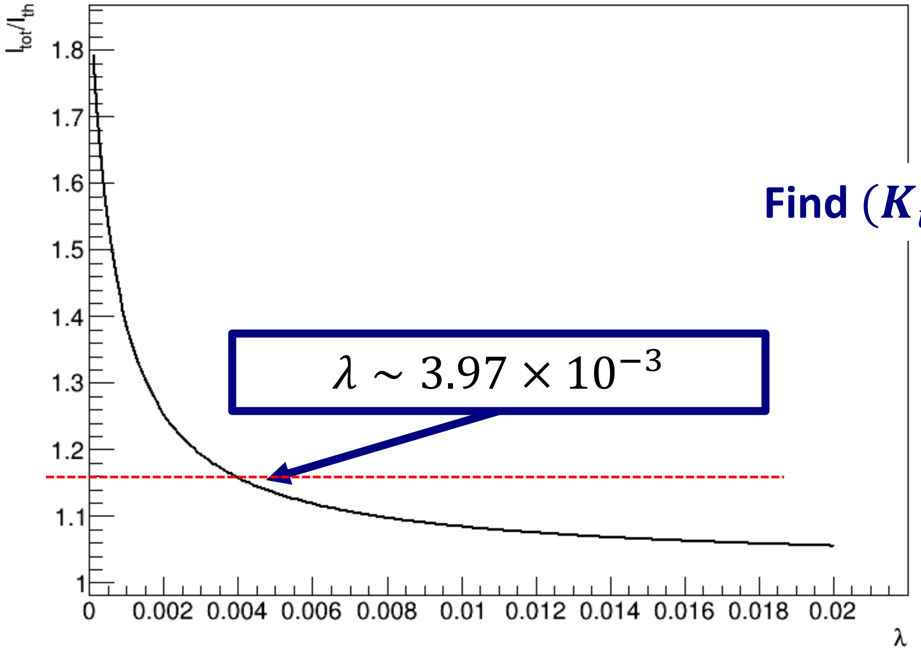

Find (K_i, T_i) for the best λ

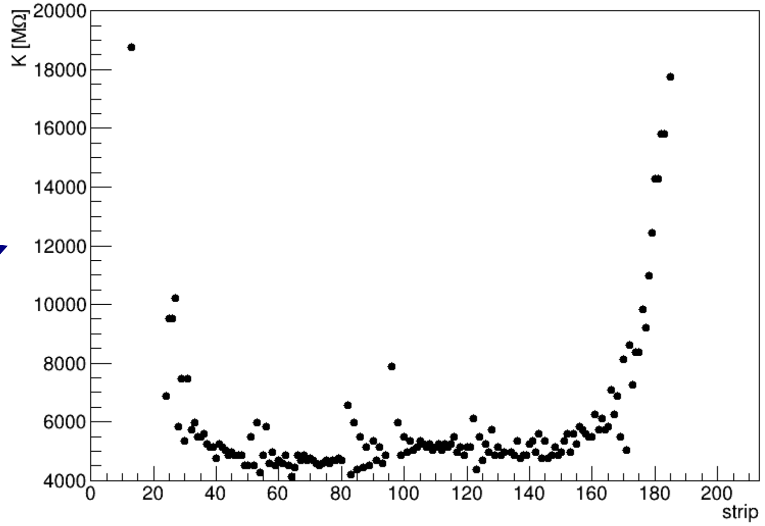

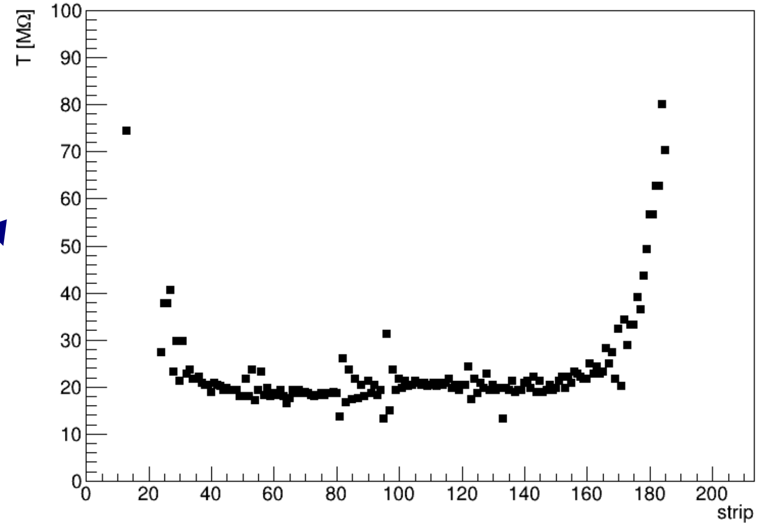

(K_i, T_i) increase on the edge:

Compatible with a spray placed more abundantly in the centre of the strip foil

$K_{central} = (4970 \pm 60)\text{M}\Omega$ $\qquad T_{central} = (19.7 \pm 0.2)\text{M}\Omega$

Comparing the two Global models

The best fits of the global model under the two assumptions are both compatible with the measured extra current

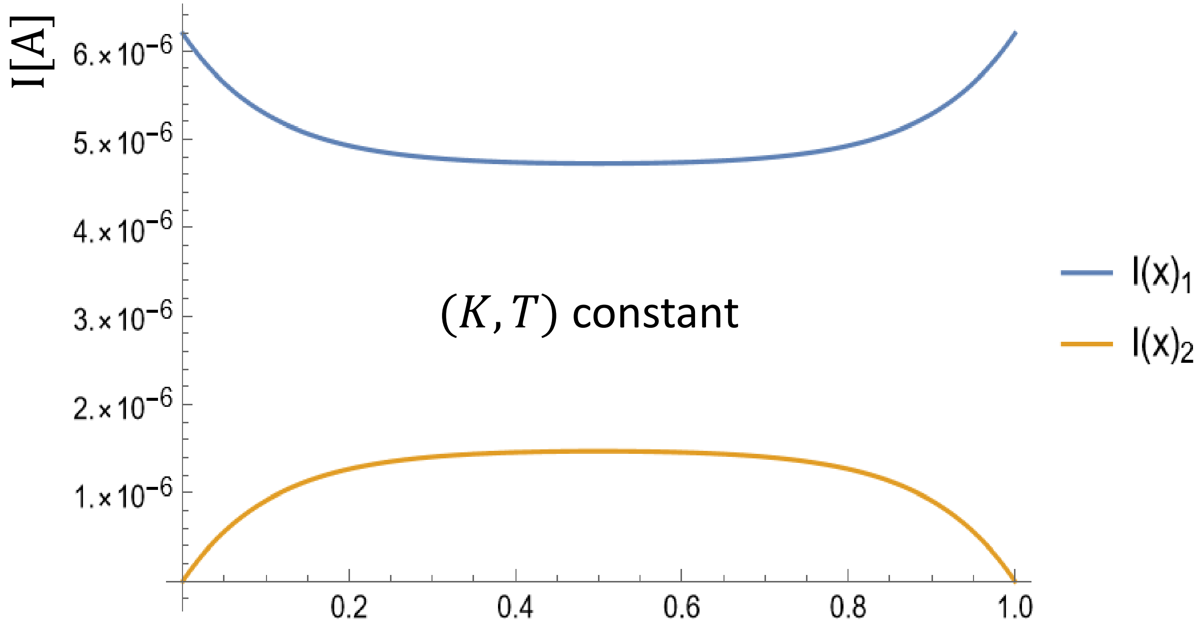

(K, T) constant

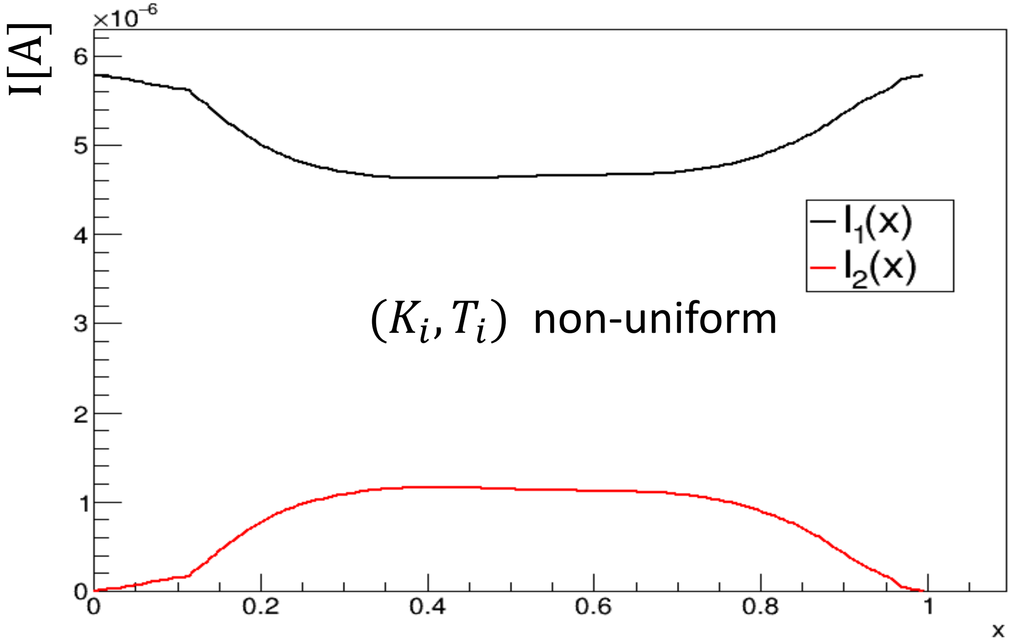

(K_i, T_i) non-uniform

Dataset	$\bar{T}_{all}^{strip}$ [MΩ]	$\bar{K}_{strip}^{all}$ [MΩ]
1-2-3	16.0±0.4	9000±2000
4	11.2±0.5	2400±800

After further degradation at 25 kV

$$K_{central} = (4970 \pm 60)\text{M}\Omega$$

$$T_{central} = (19.7 \pm 0.2)\text{M}\Omega$$

+ **much larger** at the edges

Conclusions and FC0 refurbishment

Two models for the explanation of the Field Cage 0 extra current were introduced

The two kind of datasets applied to the two models present similar results

- The trend for K and T local resistances is compatible with an antistatic spray placed more in the centre than in the edges
- Newly produced strip foils resistivities are compatible with the Kapton resistivity from datasheet

However, estimation of resistivity for Kapton and Twaron from independent are one order of magnitude larger than the one predicted by models

Excellent results in refurbishment of FC0

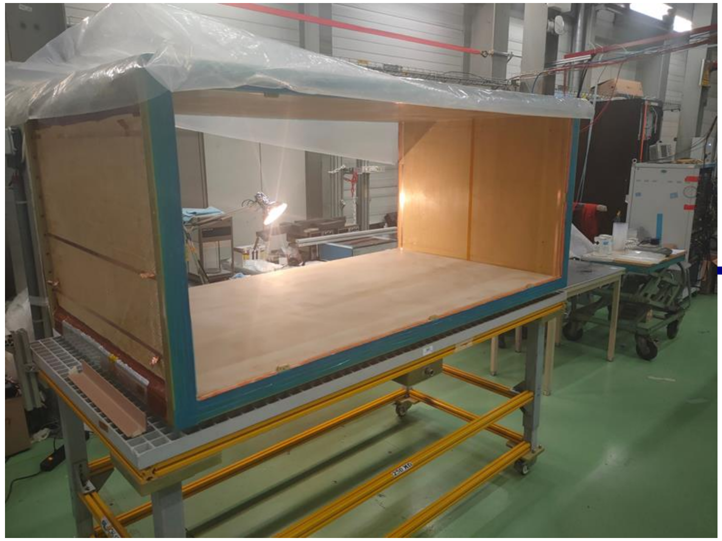

FC0 refurbishment

Two models for the explanation of the Field Cage 0 extra current were introduced

The two kind of datasets applied to the two models present similar results

- The trend for K and T local resistances is compatible with an antistatic spray placed more in the centre than in the edges
- Newly produced strip foils resistivities are compatible with the Kapton resistivity from datasheet

In the new configuration for FC0 there is **no dependency between resistivity and position**

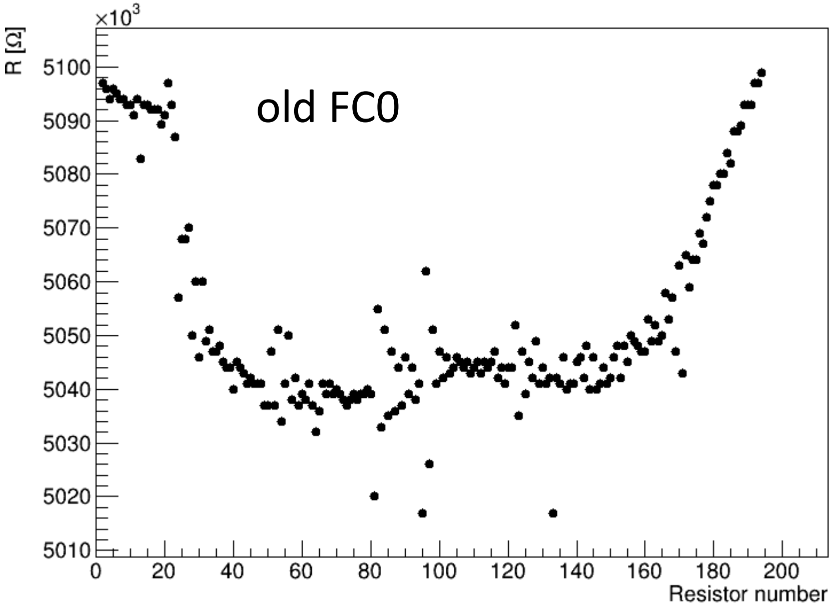

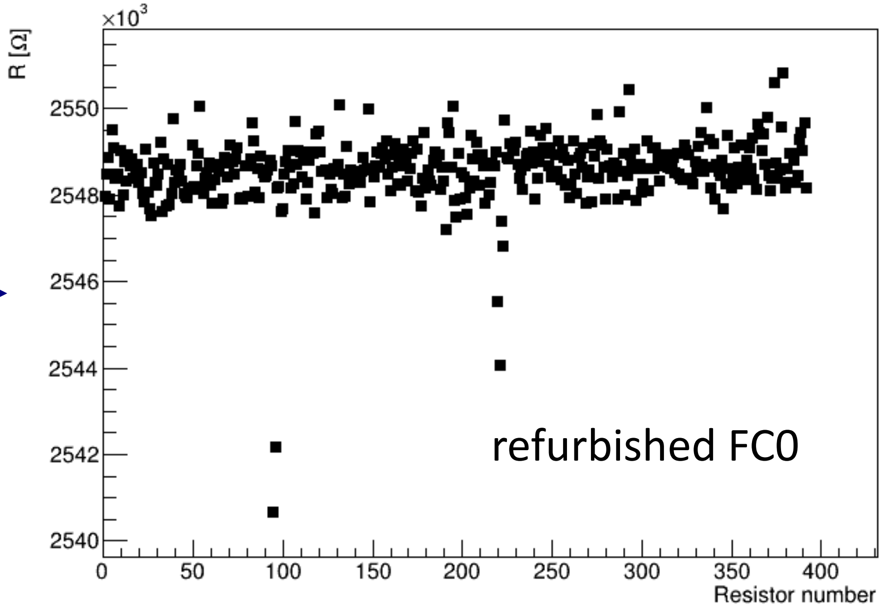

1. Introduction to Neutrino Physics
2. T2K Experiment
3. High-Angle Time Projection Chamber
4. Field Cage production and characterization
5. Study on Field Cage 0 insulation issue
6. **Study on Electric field of Field Cages**
7. Track Reconstruction algorithm with Machine Learning

Electric Field Performance

1. The study of cosmics data in HA-TPCs showed an **unexpected behavior** for tracks passing close to the cathode $\Delta x < 20$ cm
2. First, the **quantification of track distortion** was performed on the readout plane and on the drift direction
3. Several **sources** were investigated:
   - Space charge effects
   - Modification of cathode side design from TDR Finite Element Methods simulations

The issue could have been solved by an hardware intervention before installation, but due to the very tight schedule it was not spotted in time

- First strip starts close to the cathode
- Cathode close to the wall

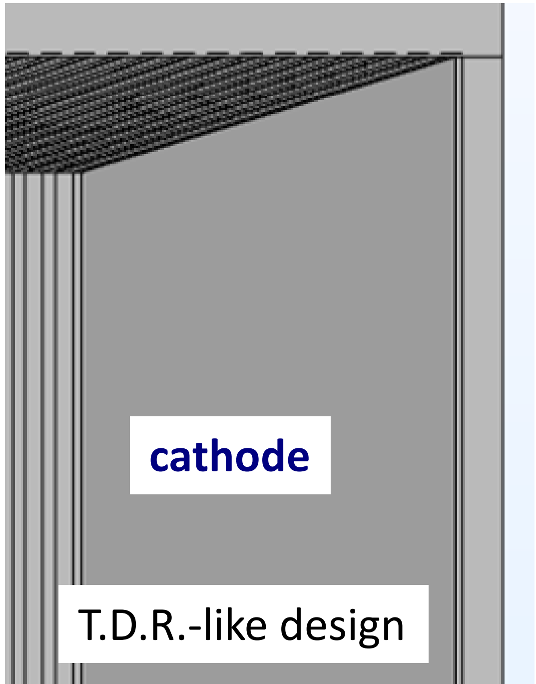

- First strip starts 8 mm away from cathode
- Cathode 12 mm away from to the wall

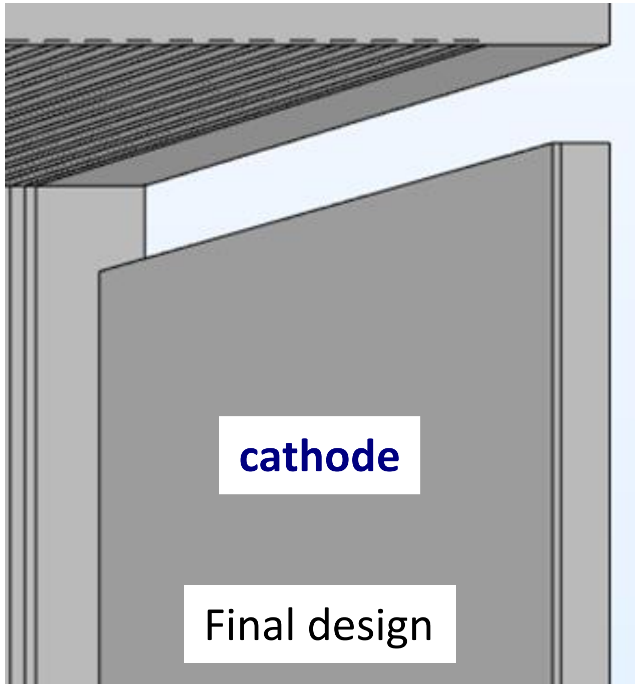

Analysis of cosmics run (no B field)

Using the standard reconstruction for cosmics with **no B**, it was observed an **apparent curvature** for tracks near the cathode and the field cage walls

EP2

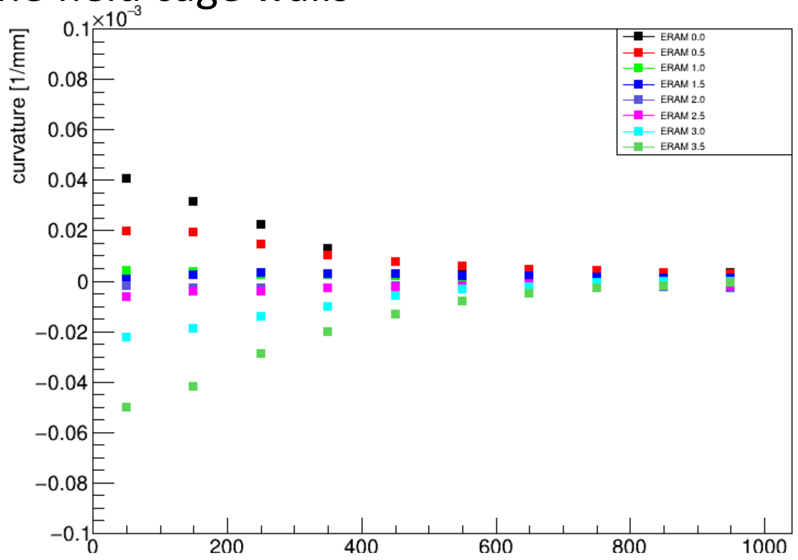

EP3

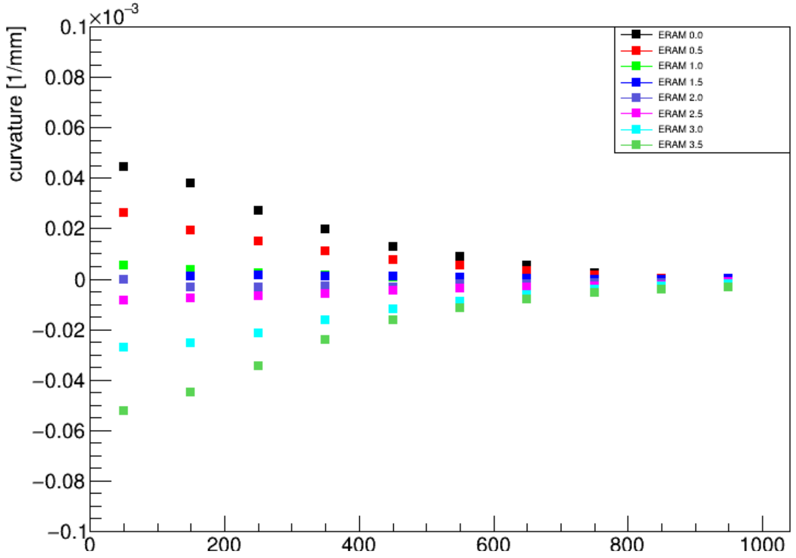

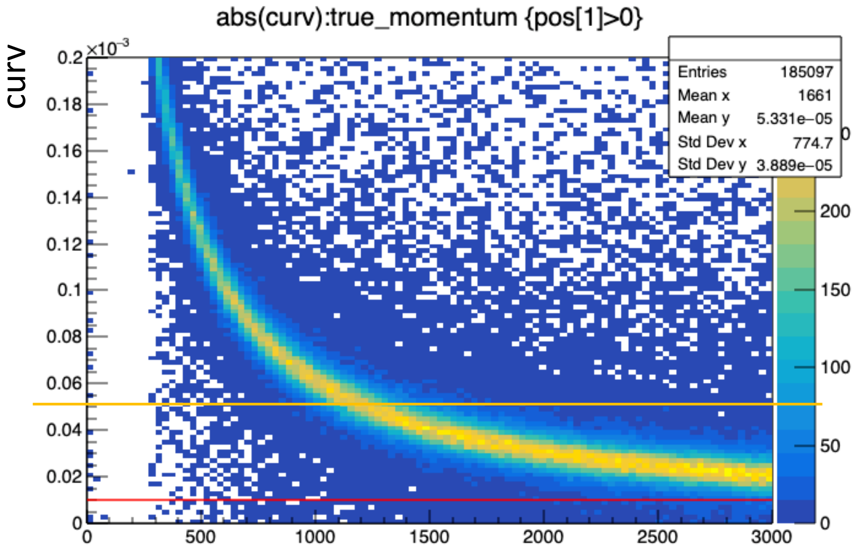

MeV/c

EP0

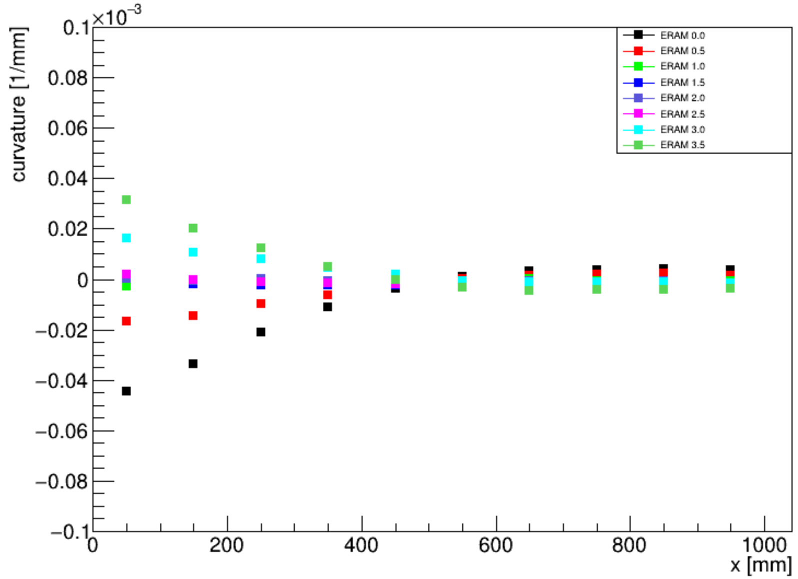

EP1

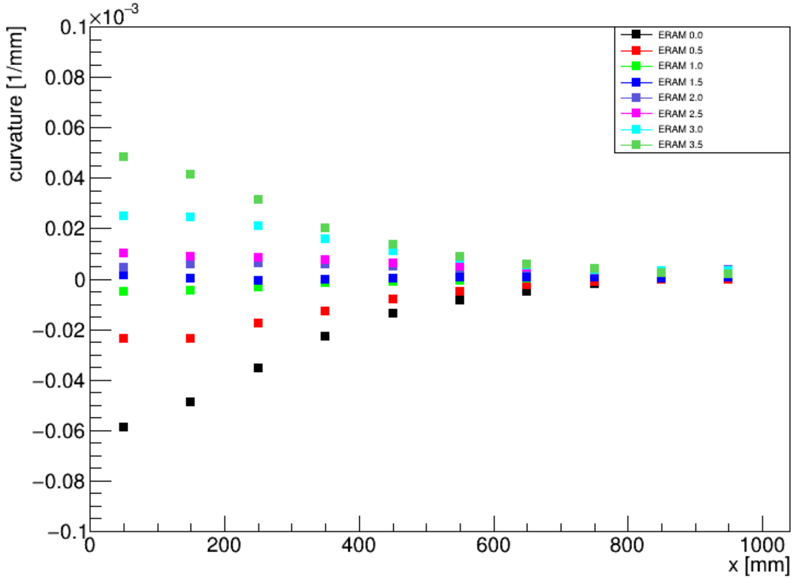

For vertical tracks the effect is compatible with 1000 MeV/c muons

$$|u_y| > 0.95$$

$$\text{curv}[mm^{-1}] = \frac{1}{R}$$

Space charge effects

Ions escaping the amplification region create a current in the active volume that might influence the Electric field

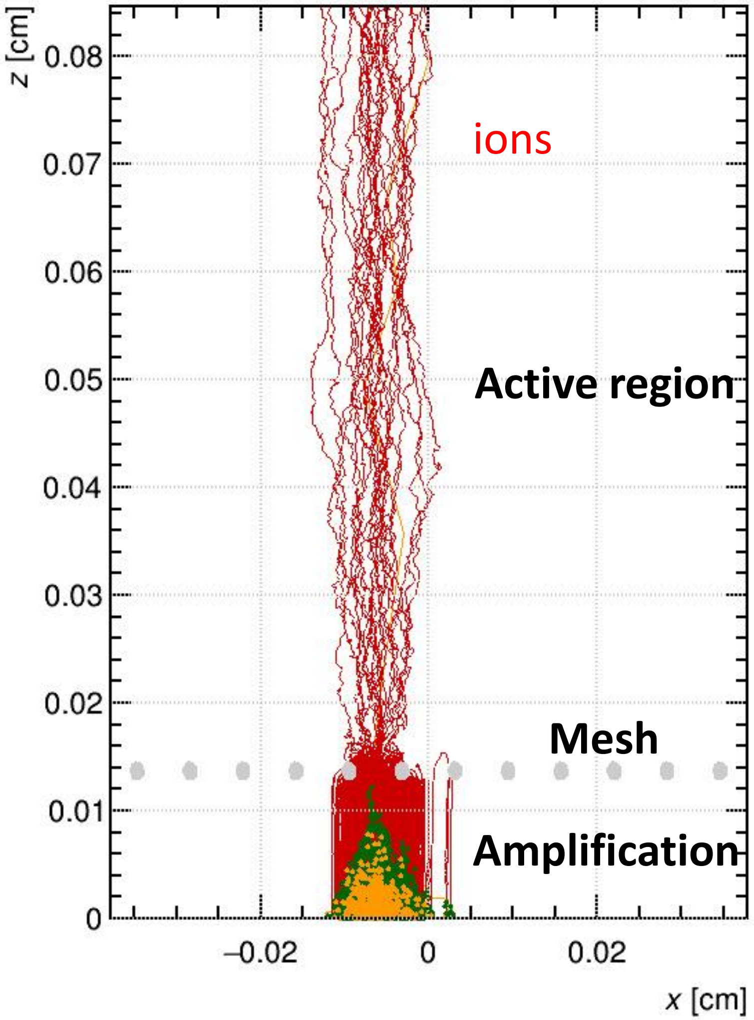

Considering:

- rate of primary e^- created by cosmic rays per unit of volume $R \sim 2 \times 10^6 \mathrm{m}^{-3}\mathrm{s}^{-1}$
- ratio of ions escaping from the mesh per avalanche $G^+_{esc} \sim 100$
- ions drift velocity $v^+_D \sim 1\,\frac{\mathrm{m}}{\mathrm{s}}$
- a drift region of length $L \sim 1\mathrm{m}$

The ion charge density is

$$\rho^+ = \frac{eRG^+_{esc}L}{v^+_D} \sim 2.1 \times 10^{-11}\,\frac{\mathrm{C}}{\mathrm{m}^3} \rightarrow \boxed{I^+ \sim 20\ \mathrm{pA}}$$

Very small effect!

For E_z component:

$$|E^+_{z,MAX}| \sim 0.13\,\frac{\mathrm{V}}{\mathrm{m}} \ll |\mathrm{E_{nom}}| = 27500\,\frac{\mathrm{V}}{\mathrm{m}}$$

This effect is negligible

Simulation of Field Cages in COMSOL

To understand the origin of such residuals distributions, a detailed 3D simulation of the Electric field in the full scale TPC was implemented with COMSOL Multiphysics software

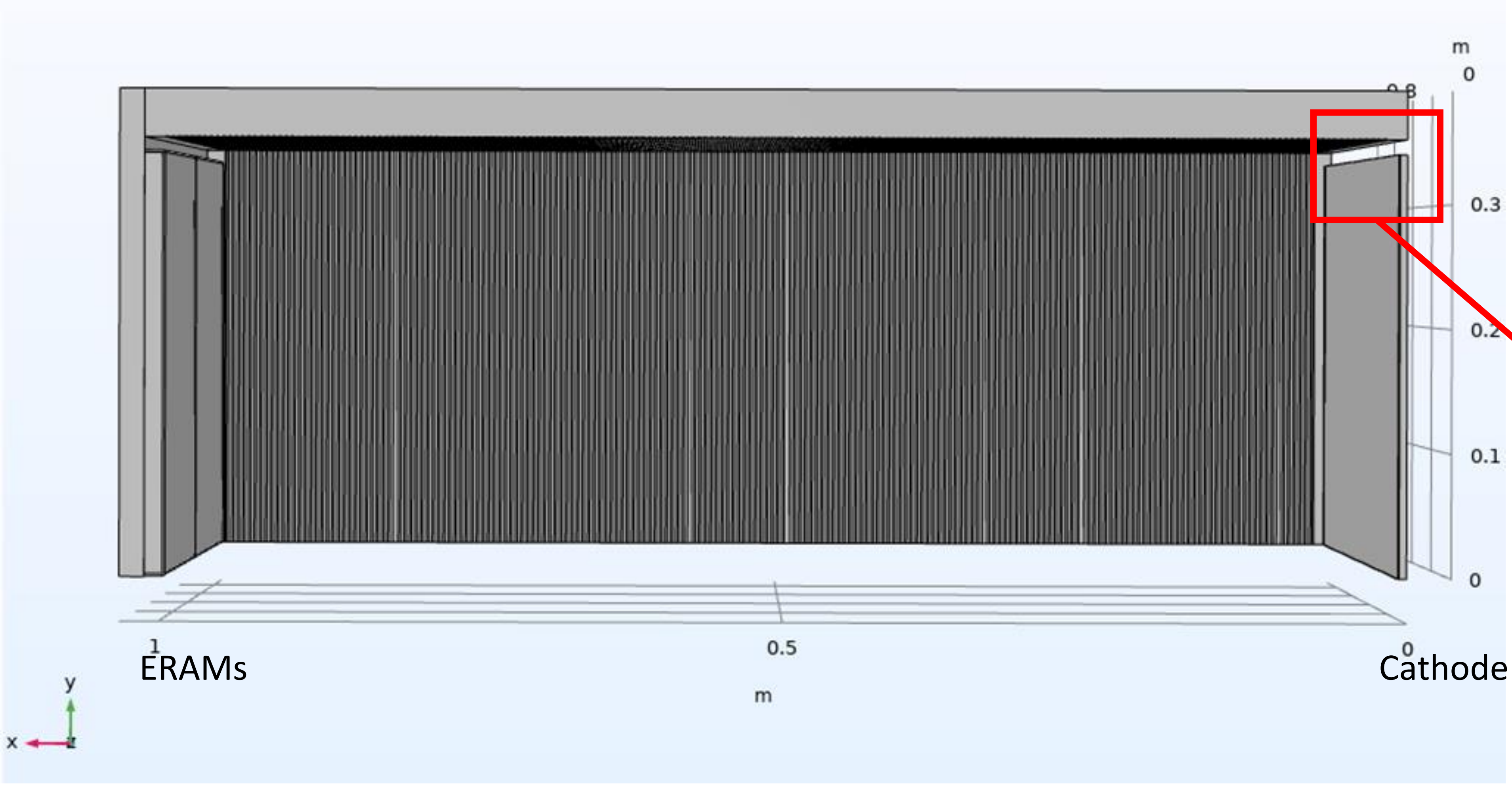

x: 1011 mm
y: 352 mm
z: 875 mm

Dimensions of a Field Cage obtained by metrology

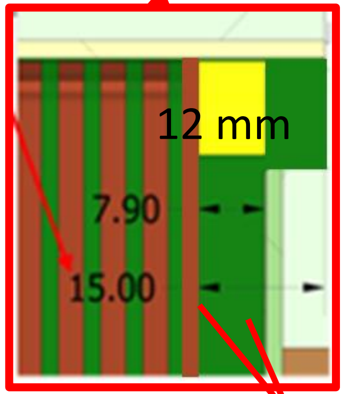

Thanks to symmetries, out of 16 ERAMs we can simulate 1/8 of them (a quarter of a single field cage)

Same V!

But it shouldn't…

Simulated Electric field

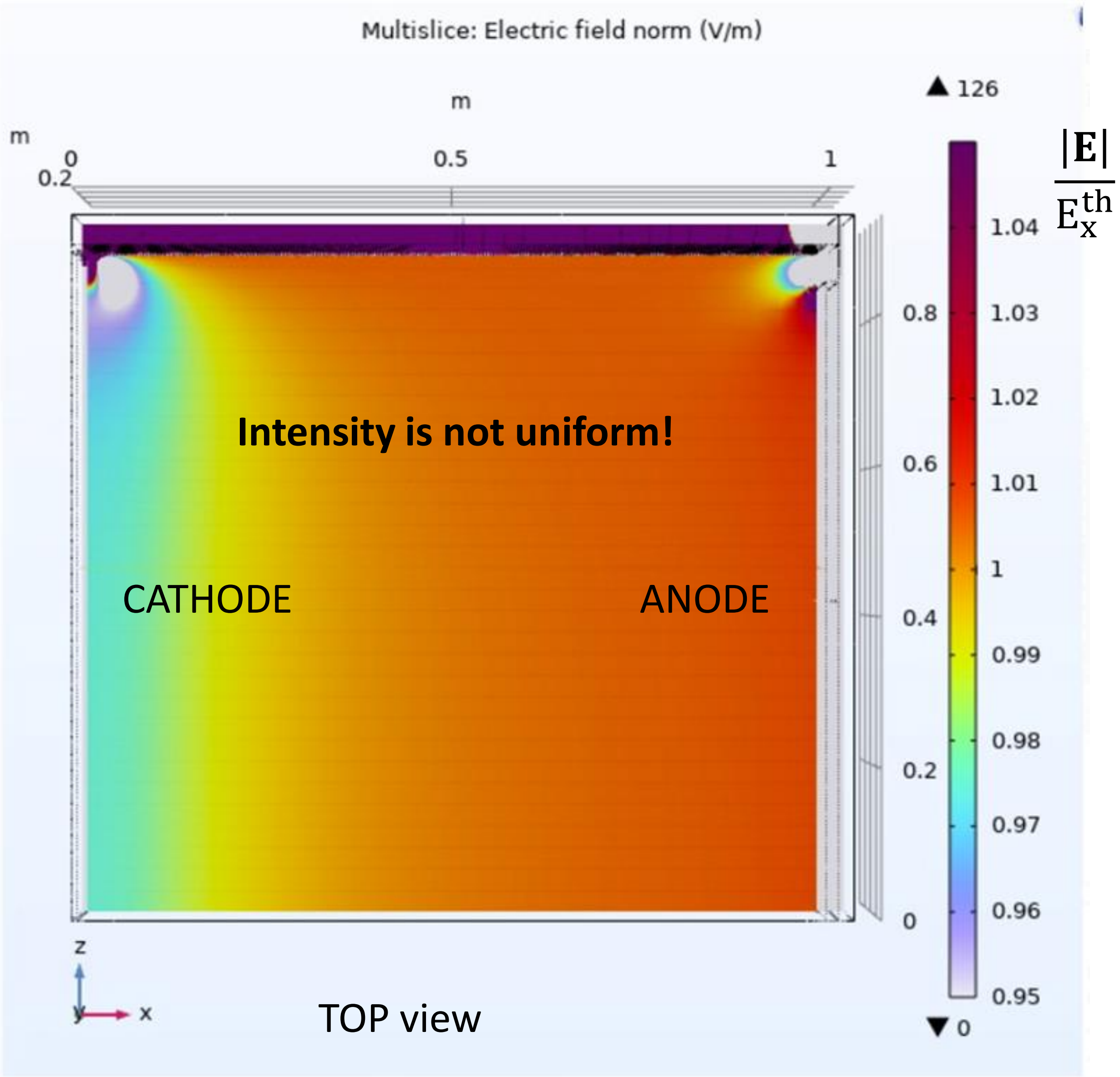

Deformation on corners in both anode and cathode

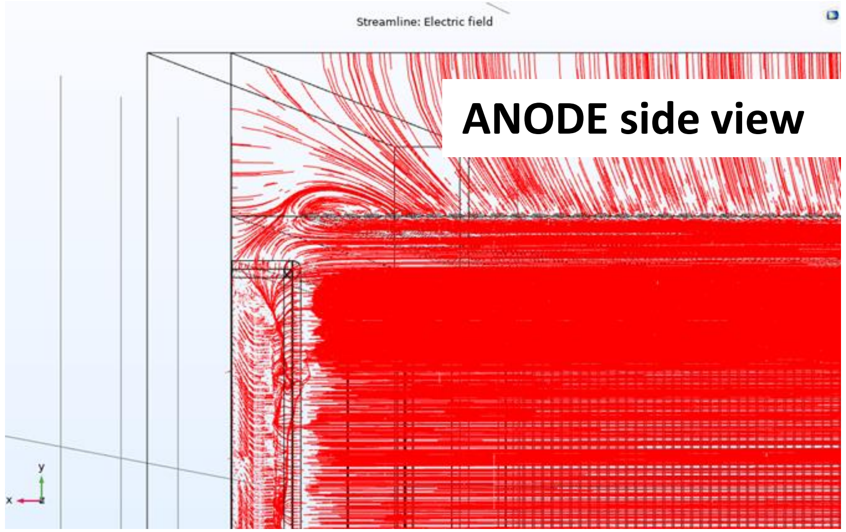

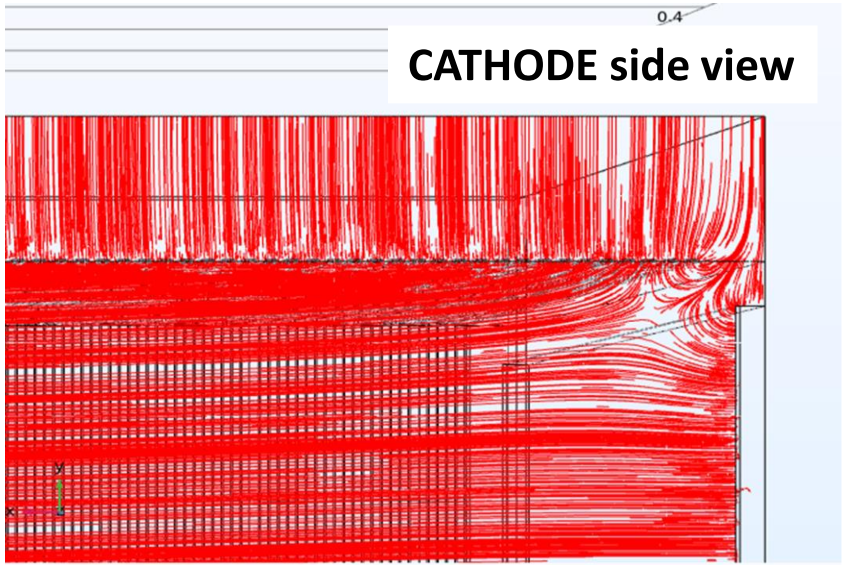

Analysis of cosmics run (no B field)

After the implementation of Electric field map in reconstruction software, the results are greatly improved

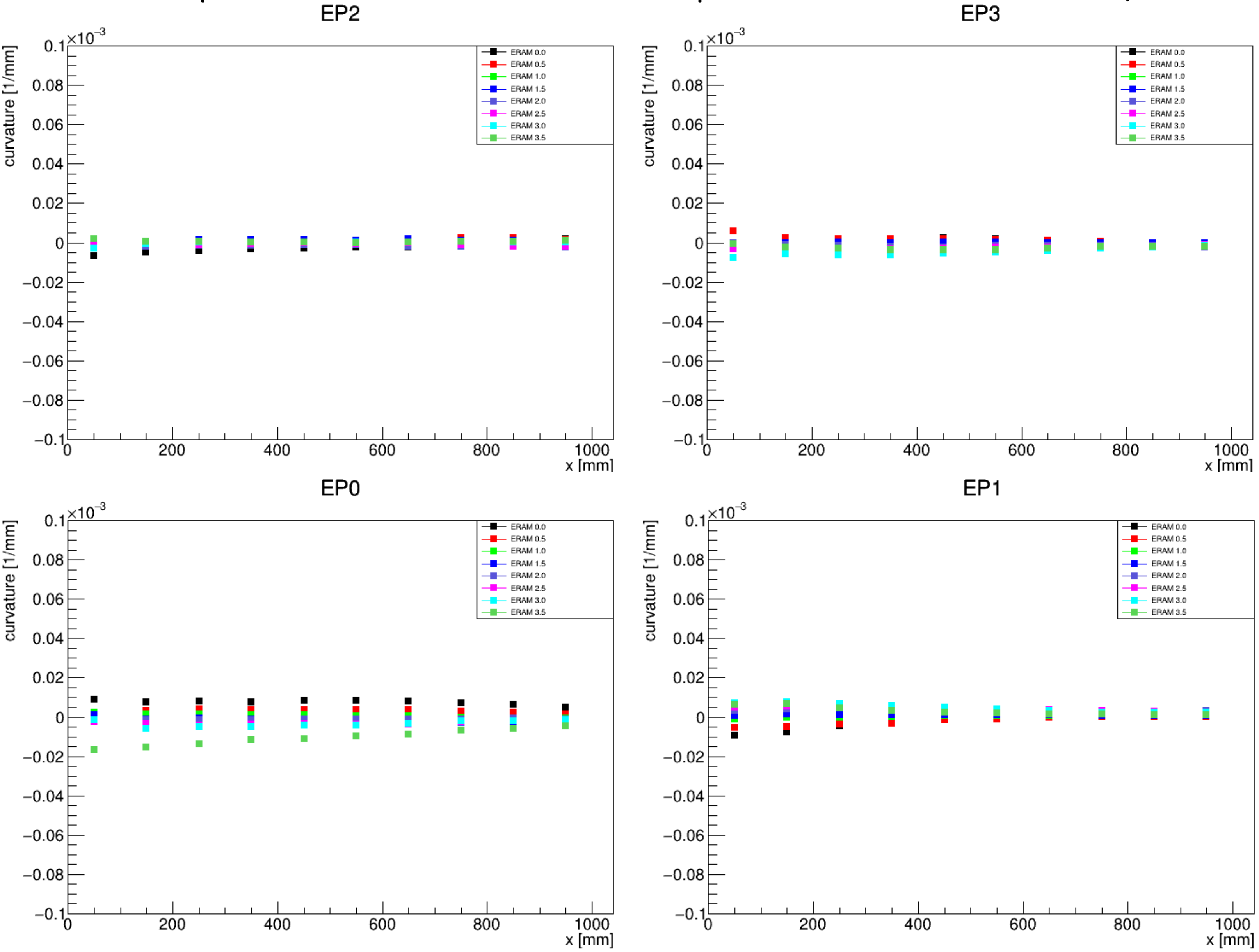

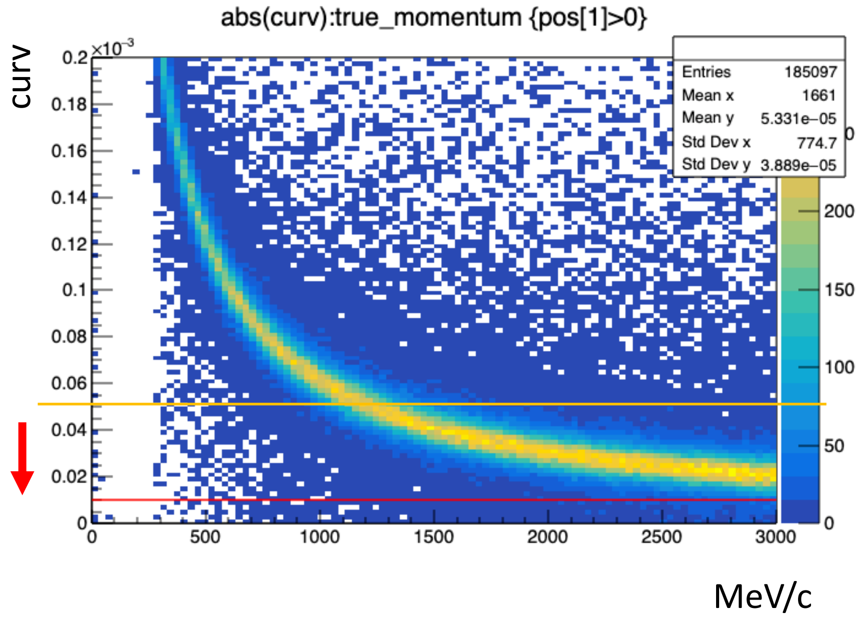

A large improvement!

Analysis of cosmics run on ERAM plane (no B)

Since tracks are expected to be linear, a **linear** fit of cosmics is performed using as data point the cluster position from reconstruction software

- Tracks *almost* vertical are chosen ($|u_y| > 0.95$) with at least 50 clusters
- System of reference is **rotated**
- Residuals are collected and divided by x position
- Average value (bias) in a group of 2x2 pads is estimated

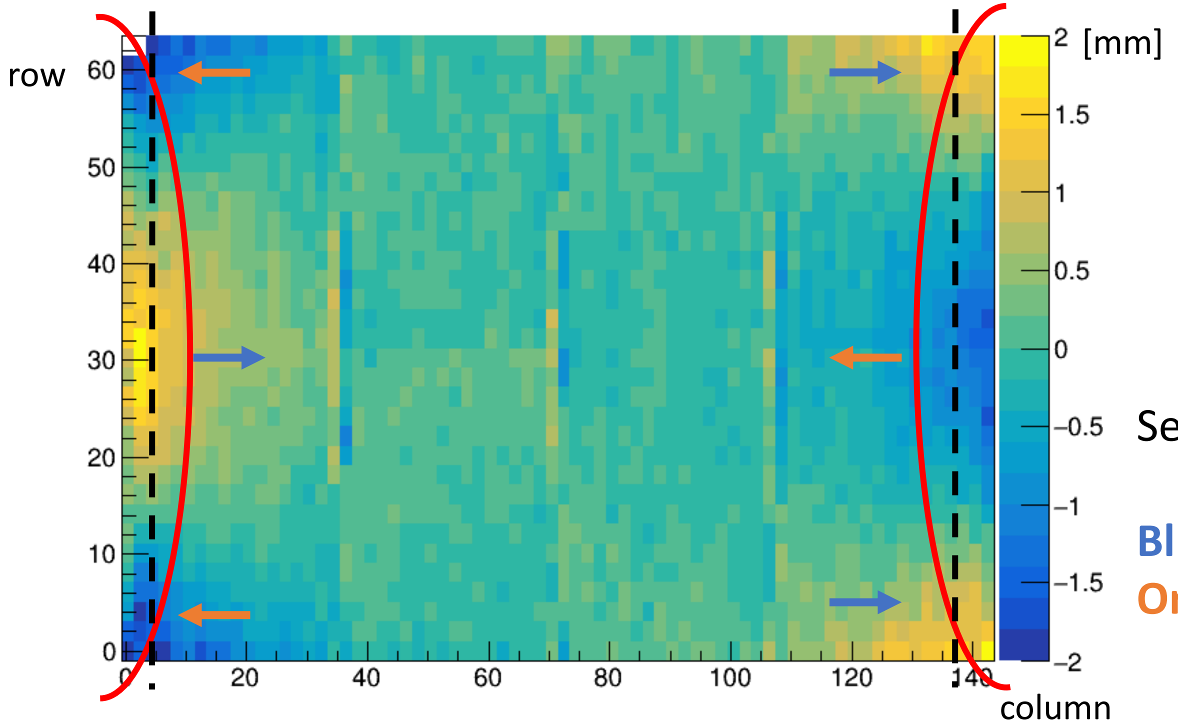

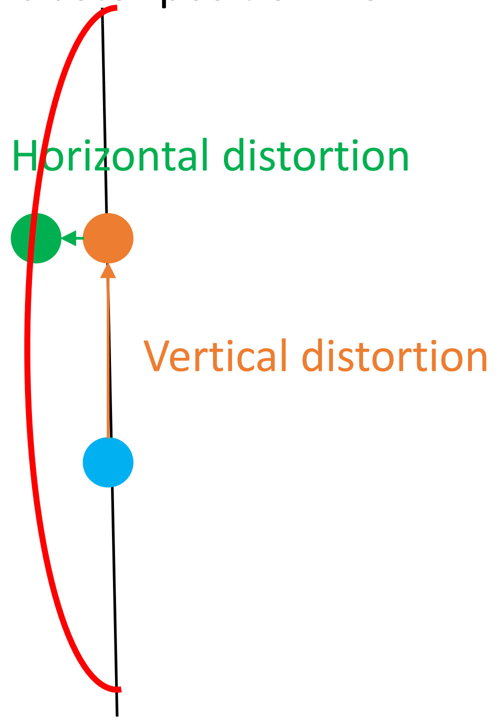

Evaluating only horizontal displacement!

Selecting tracks at maximum 20 cm away from cathode

Blue arrow means displacement to the **right**
Orange arrow displacement to the **left**

Analysis of cosmics run on ERAM plane (no B)

Since tracks are expected to be linear, a **pol1** fit of cosmics is performed using as data point the cluster position from hatRecon

- Tracks *almost* vertical are chosen ($|u_y| > 0.95$) with at least 50 clusters
- System of reference is **rotated**
- Residuals are collected and divided by x position
- Average value (bias) in a group of 2x2 pads is estimated

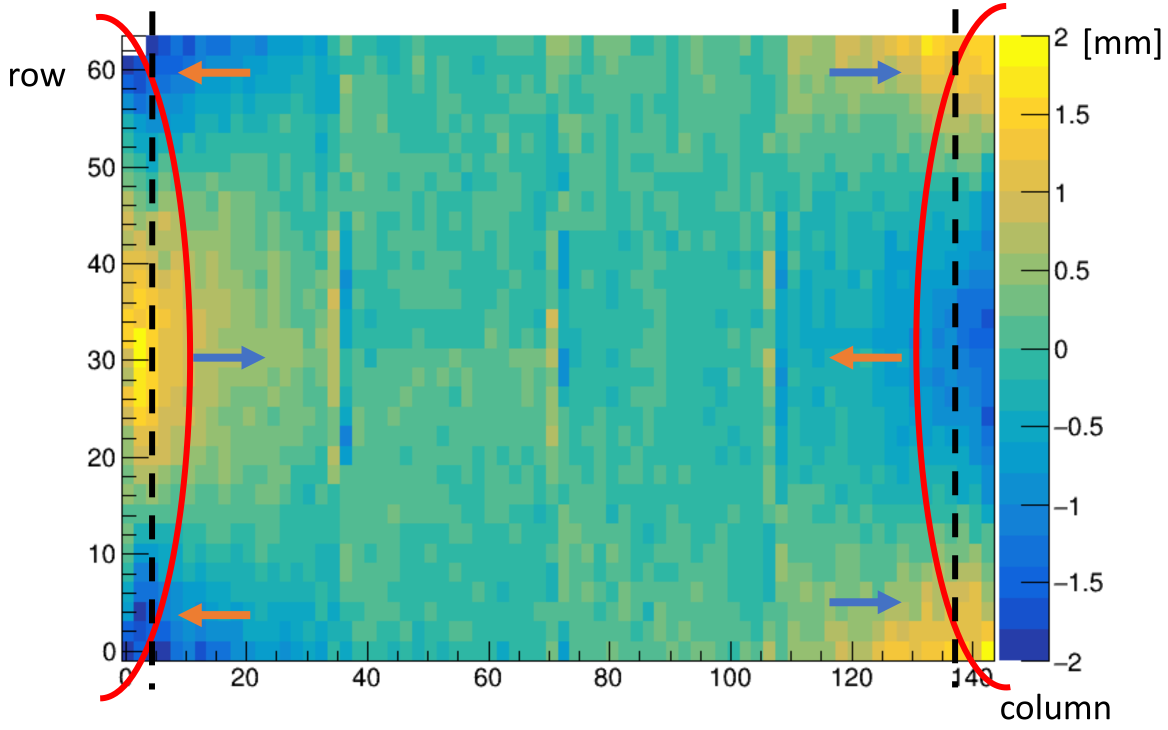

AFTER CORRECTION

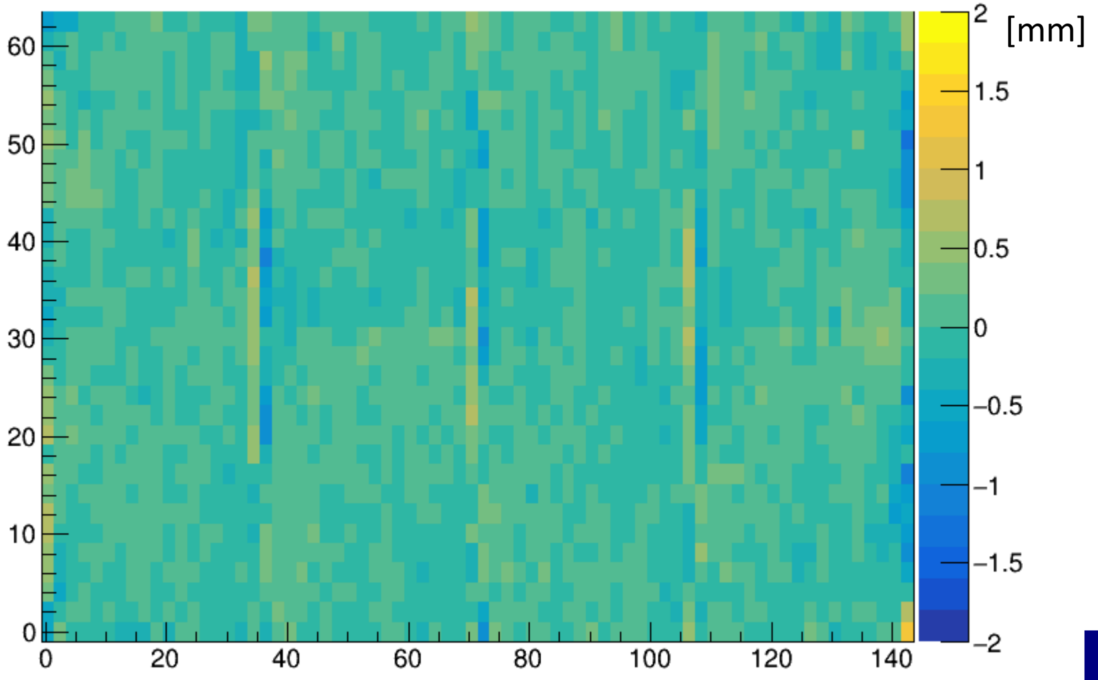

Measuring the Electric field with FC0 refurbished

With the recovery of FC0, it will be possible to directly probe the Electric field with a LASER source as a complimentary source of tracks with respect to cosmics

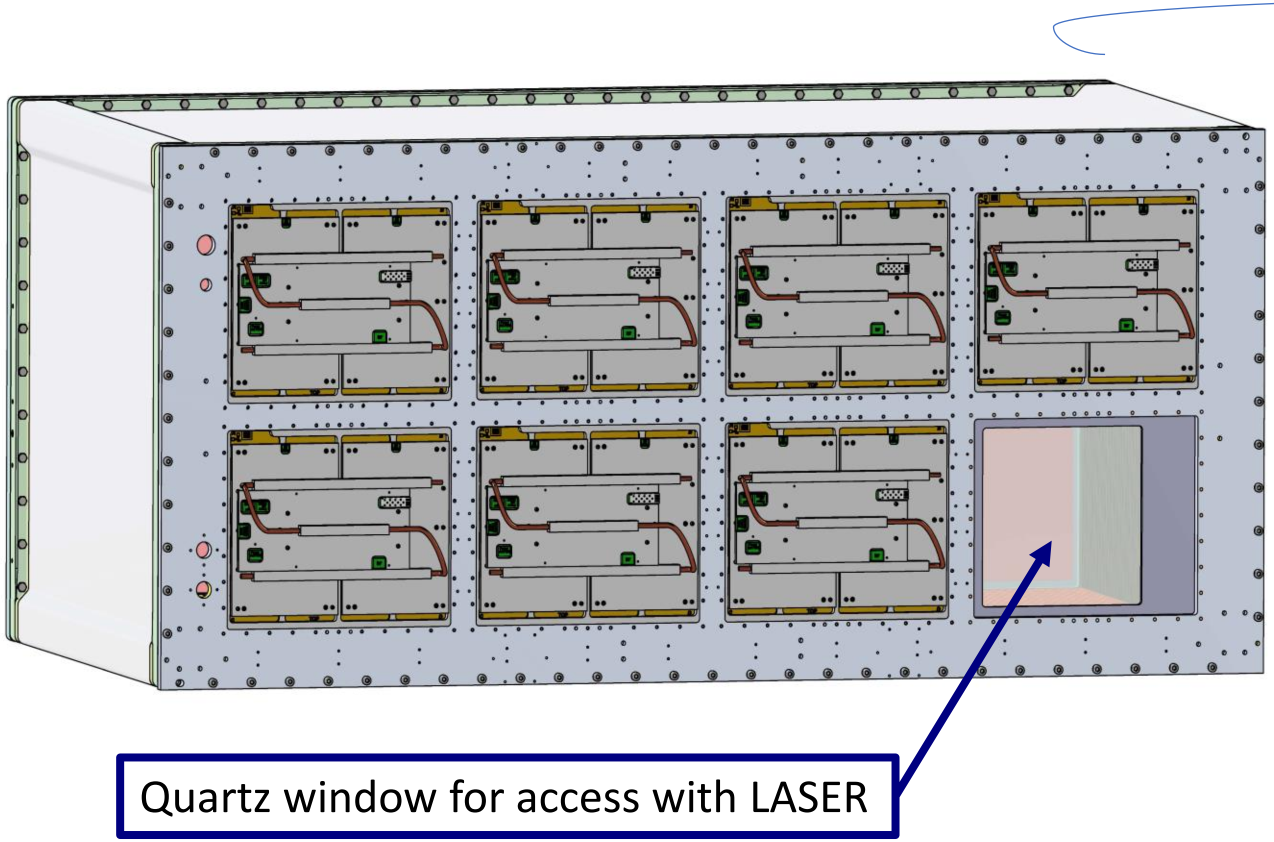

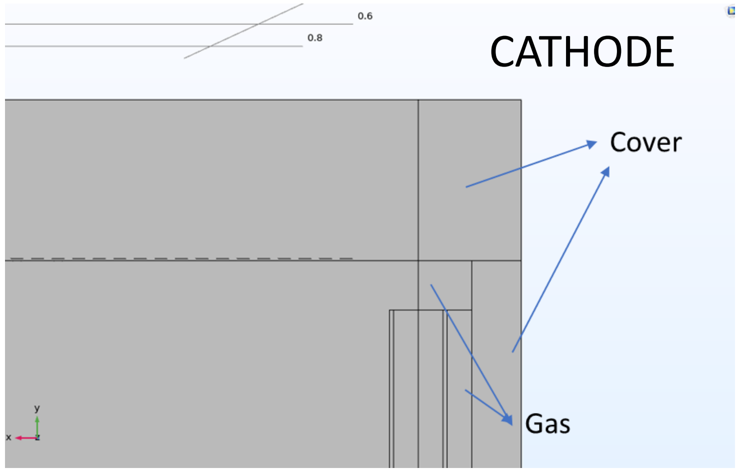

We need to take in consideration the fact that there is **only one** Field Cage:
No symmetry!

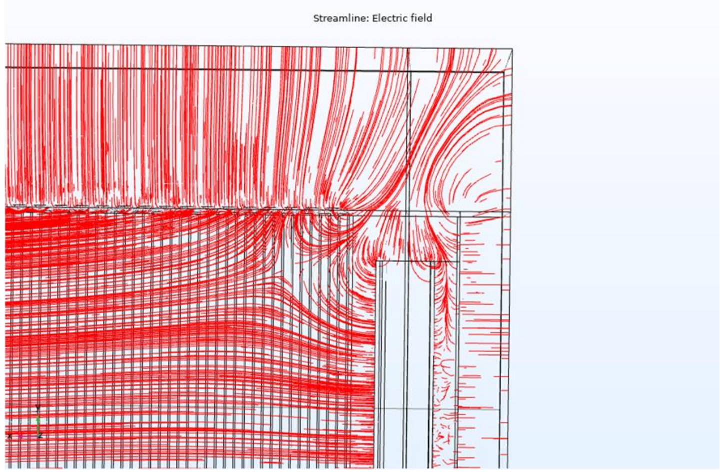

1. Introduction to Neutrino Physics

2. T2K Experiment

3. High-Angle Time Projection Chamber

4. Field Cage production and characterization

5. Study on Field Cage 0 insulation issue

6. Study on Electric field of Field Cages

7. **Track Reconstruction algorithm with Machine Learning**

Resistive MicroMegas Sensors (ERAMs)

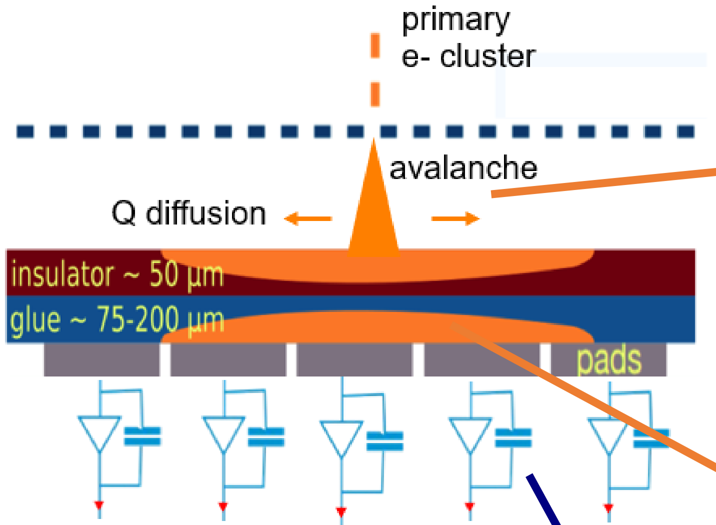

1

ERAM response characterization was performed at CERN on a test bench with a 55-Fe source

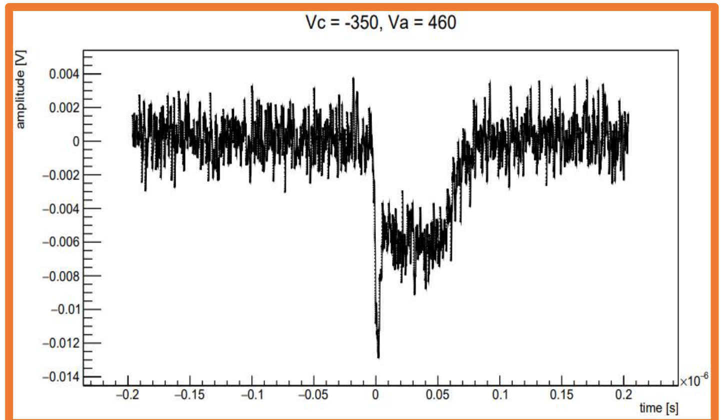

2

Signal has same time scale as shaping time O(100 ns)

2D diffusion equation

$$\rho(r,t) = \frac{RC}{4\pi t}\exp\left(-\frac{r^2 RC}{4t}\right)$$

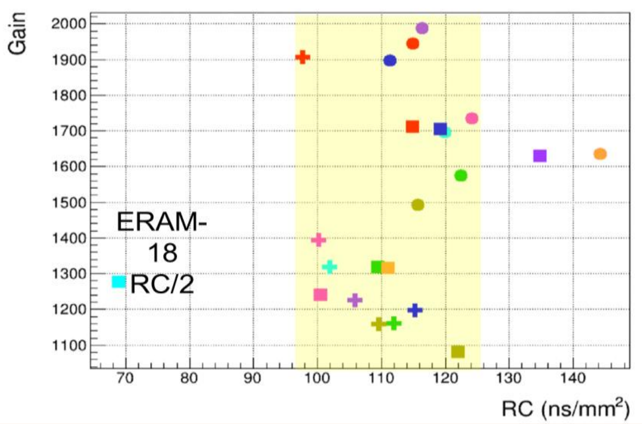

4

FEE response function

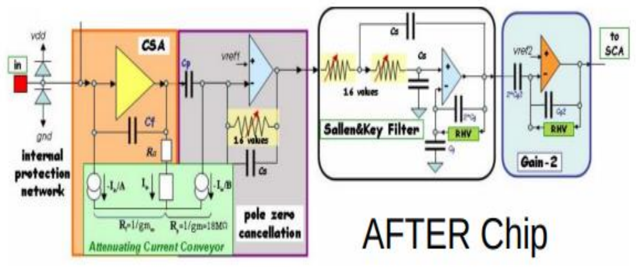

3

Electrical model of the sensor

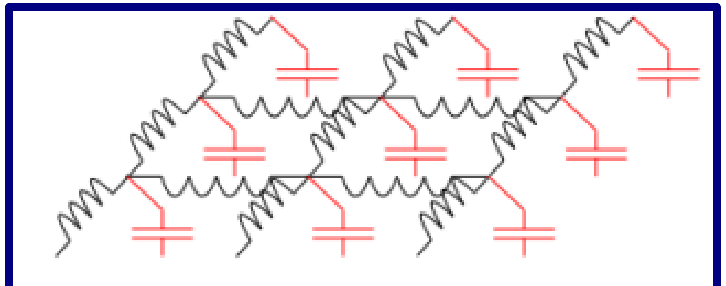

Spatial reconstruction with clustering method

Amplitude and shape of the waveform depends on *"how far"* the track has passed from the pad

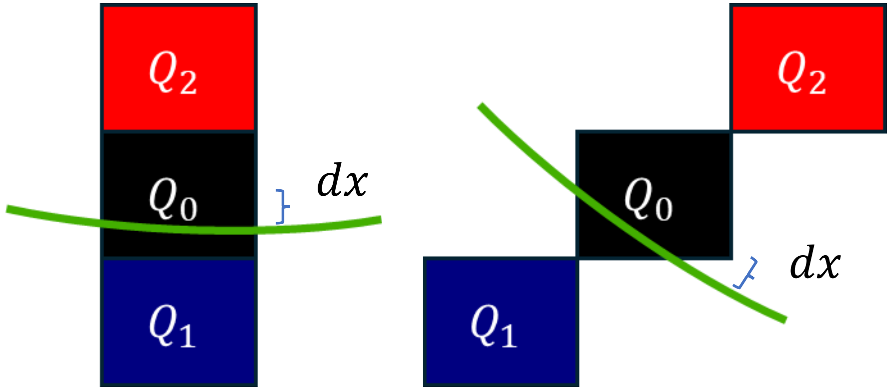

Leading pad: signal is induced from avalanches

Secondary pads: signal is induced by charge moving on the DLC

$$dx = \alpha_{10} \ln^3\left(\frac{Q_1}{Q_0}\right) + \beta_{10} \ln\left(\frac{Q_1}{Q_0}\right)$$

$$dx = \alpha_{21} \ln^3\left(\frac{Q_2}{Q_1}\right) + \beta_{21} \ln\left(\frac{Q_2}{Q_1}\right)$$

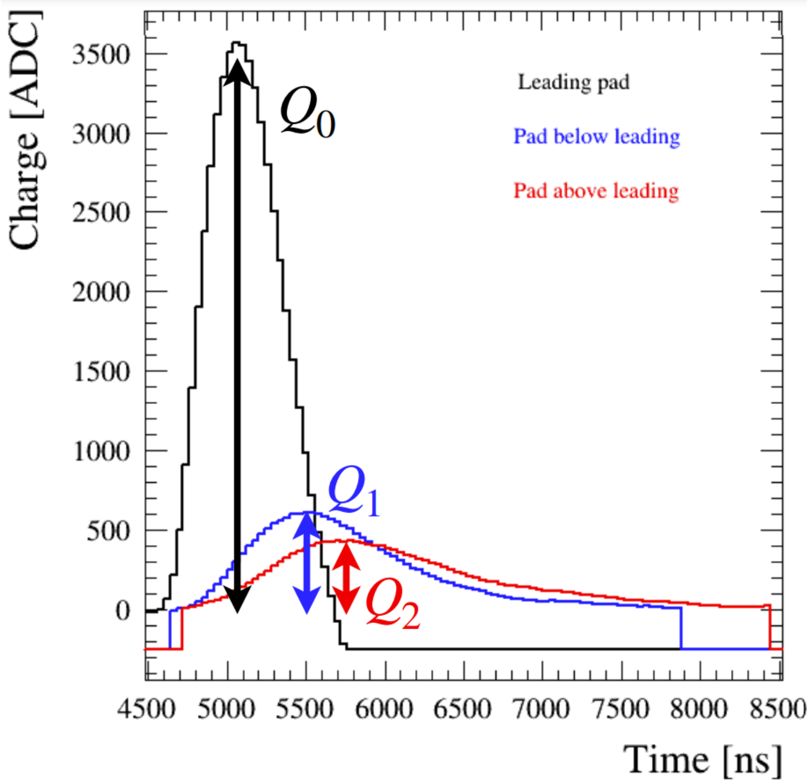

Each set of point in the 3D space is then fitted to a helix

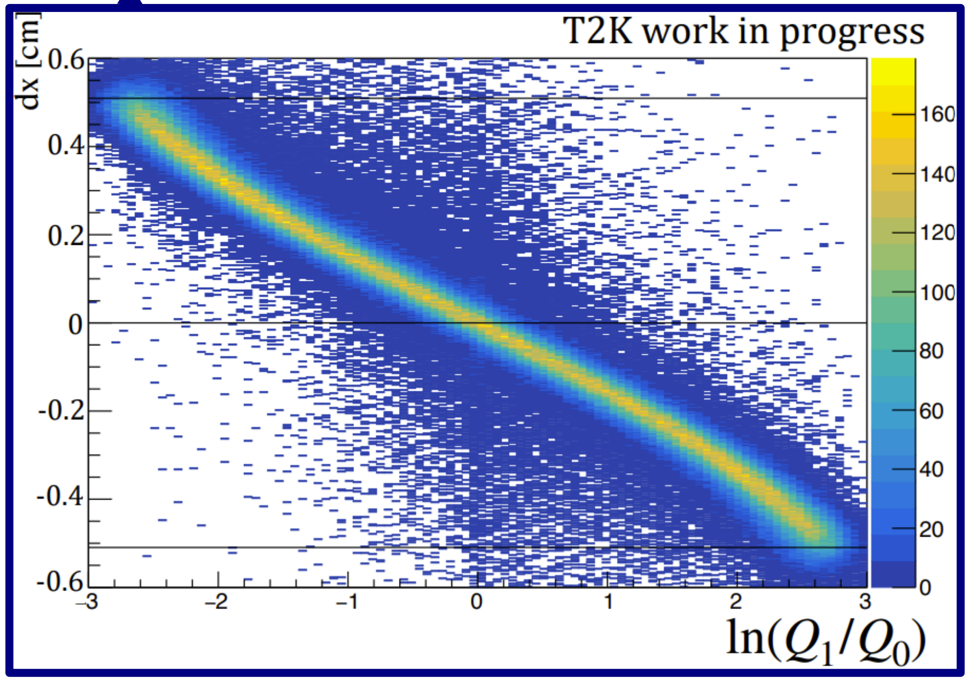

Reconstruction with Machine Learning technique

Track reconstruction in HA-TPC is performed by using a **user defined empirical relation** between:

1. Track position in a cluster
2. Amplitude of the waveform

A new reconstruction method was developed with three main ideas:

1. Expand the information extracted from the waveform
2. Reduce the clustering dependance on the track orientation
3. Introduce an empirical relation for track reconstruction not given by the user

For these purposes, a ML algorithm based on regression was chosen

Square Method Clustering

The idea is to avoid the dependence of clustering to the angle of tracks on anode plane

Different cluster shapes

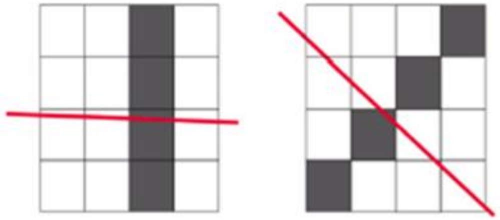

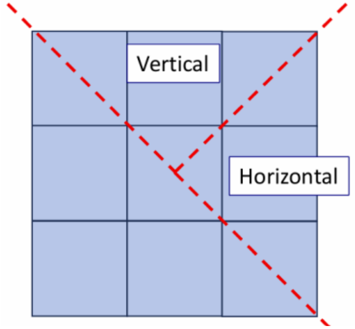

Single “square” cluster shape made by **3x3 pads**

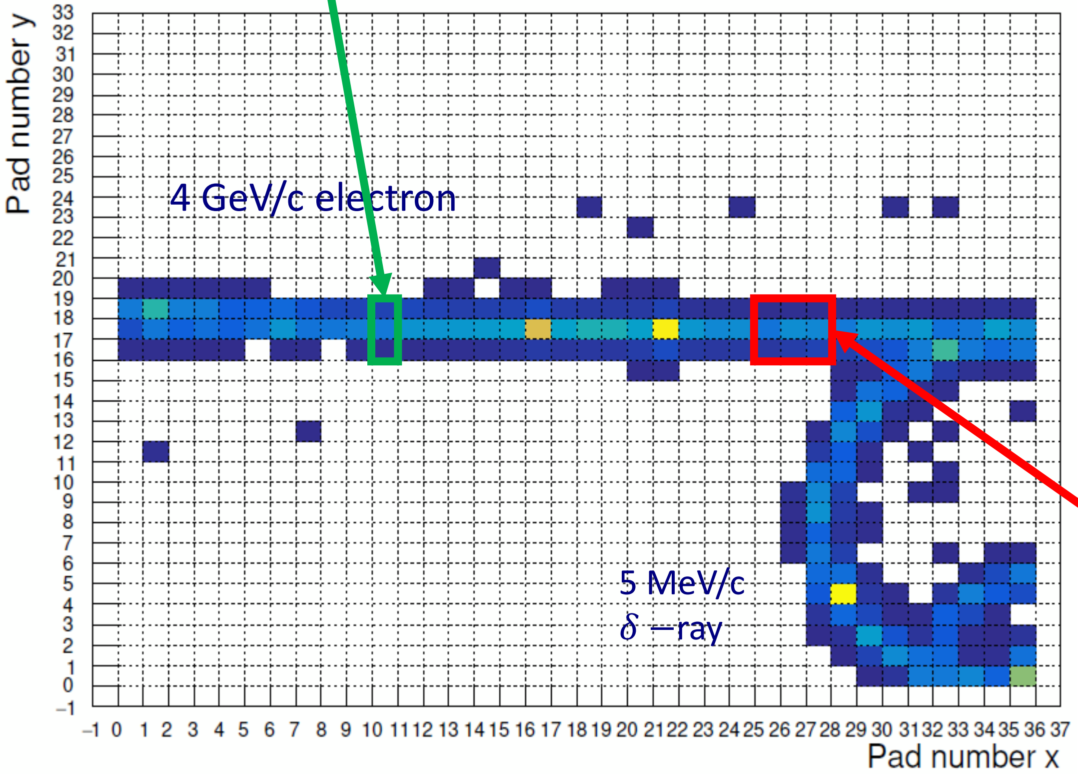

Clusters are divided into two classes of Orientation:

- **Horizontal**
- **Vertical**

Since pads are not perfect squares

Squares are created by scanning the pad grid moving **by 1 column or row,** so each pad appears may appear more than once

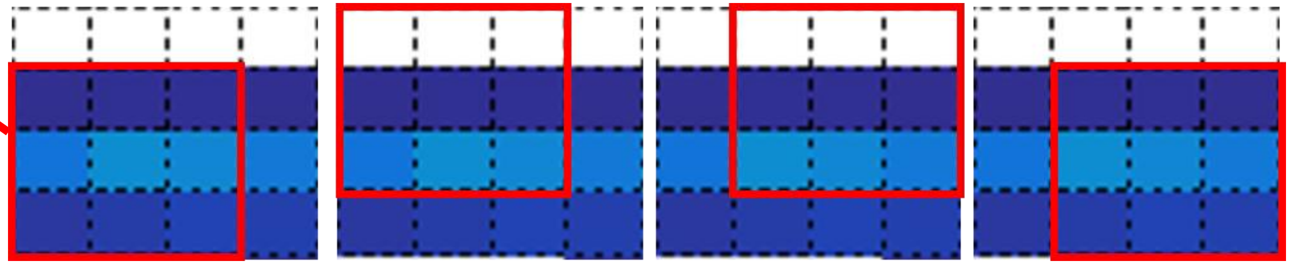

For each pad, its **maximum amplitude** and **FWHM** are estimated

$$\{(Q^i_{max}, 1/\sigma^i)\}_{i=1,\ldots,9} \longrightarrow (q, m)$$

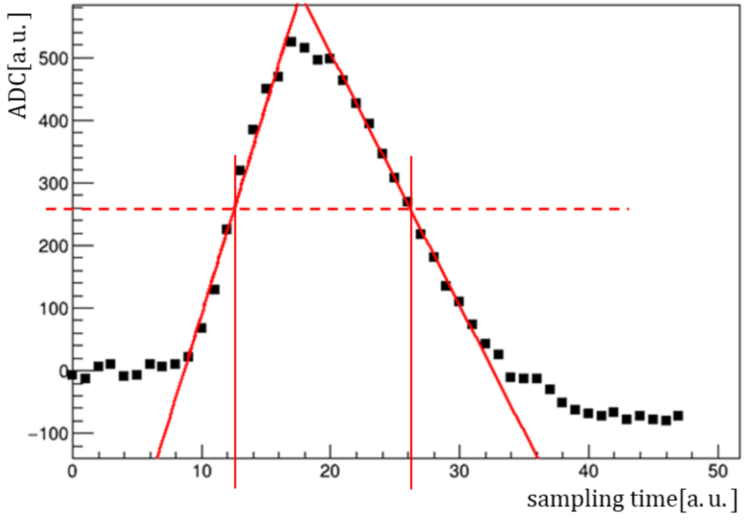

For each square, 9 couples of variables are extracted and can be used for finding the parameters of the curve passing into the square

Example of clusters and true information for a simulated event

2	5	8
1	4	7
0	3	6

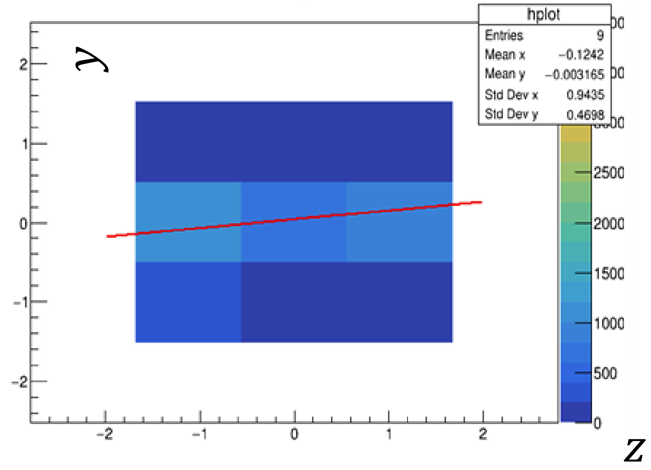

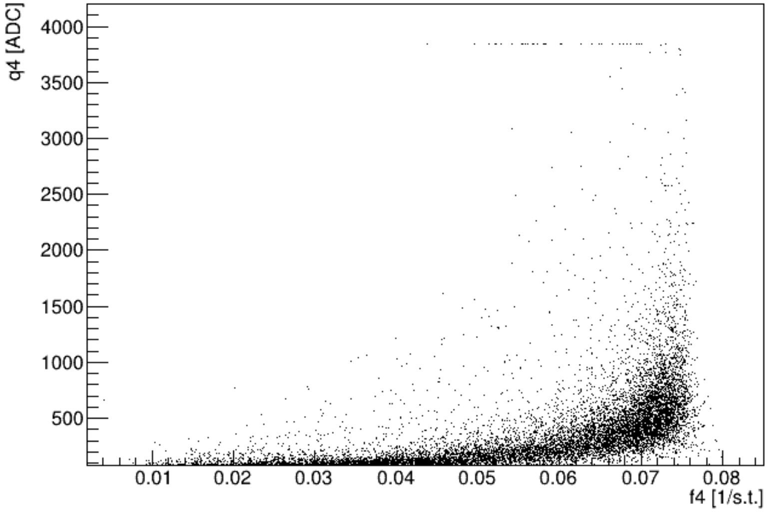

The training is performed on a **2D uniform distribution** in (q_{true}, m_{true})

Reconstruction with Machine Learning technique

The Multi Layer Perceptron is a neural network where neurons are organized in layers which are connected only with the previous and next one

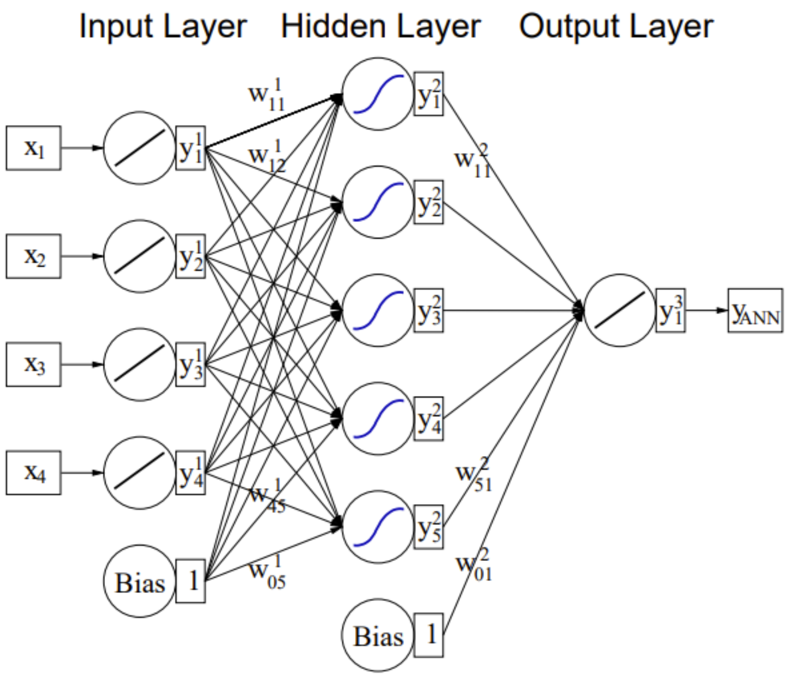

The problem belongs to the ***regression*** category in which a set of inputs is used to predict a set of outputs in a continuous domain

Neurons are entities that produce a non-linear scalar response to a given set of inputs

Neurons response function can be considered as composition of a

- ***neuron activation function***
- ***synapse function***

The training is performed by minimizing a ***loss function on training data***

$$E(x) = \sum_{a}^{N} (y_{true}^{a} - y_{NN}^{a})^2$$

The studies reported in the thesis have been performed with TMVA package for CERN ROOT

Training Characterization

Residuals for test dataset for training on horizontal clusters

Pads nomenclature:

2	5	8
1	4	7
0	3	6

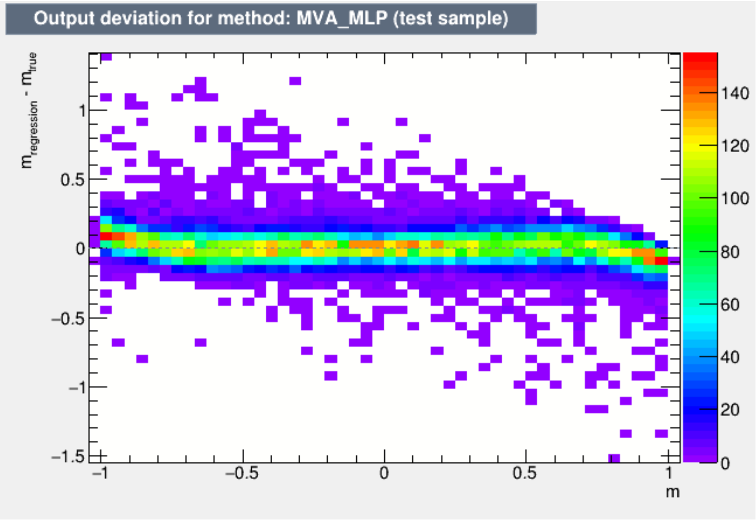

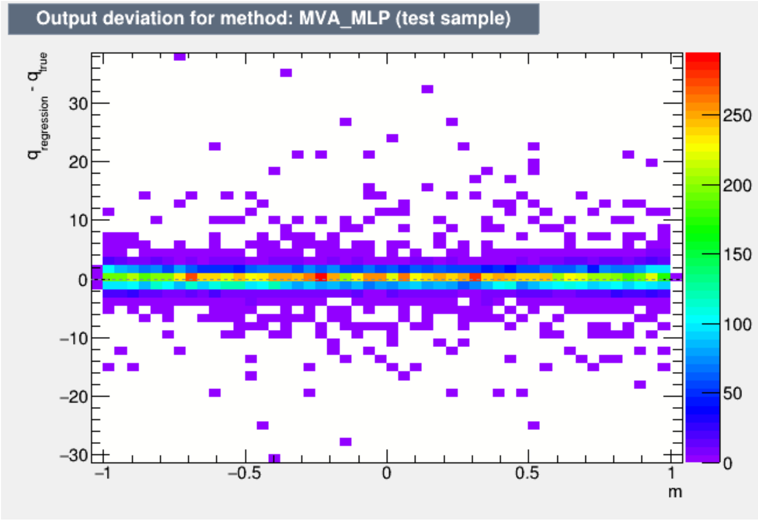

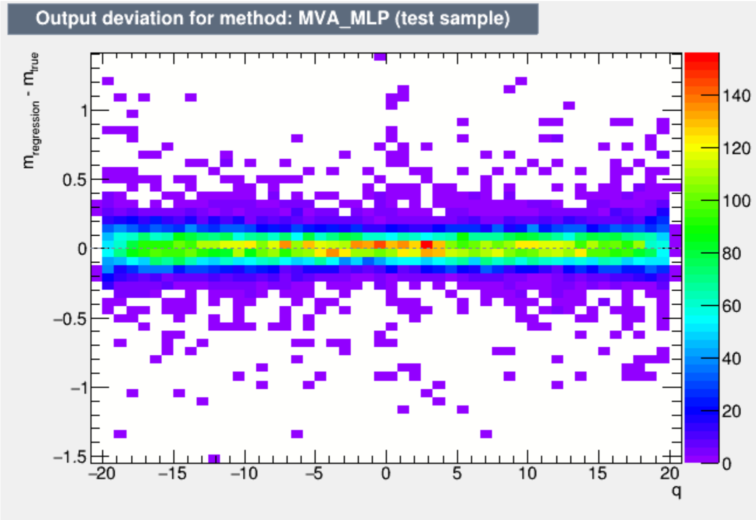

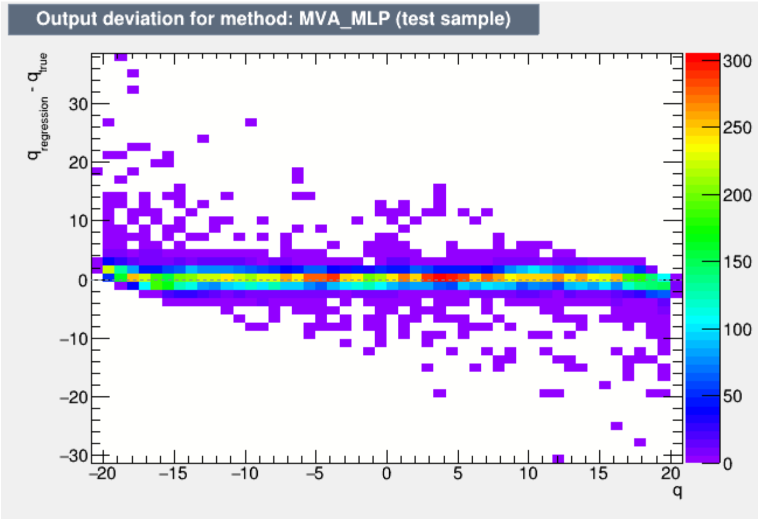

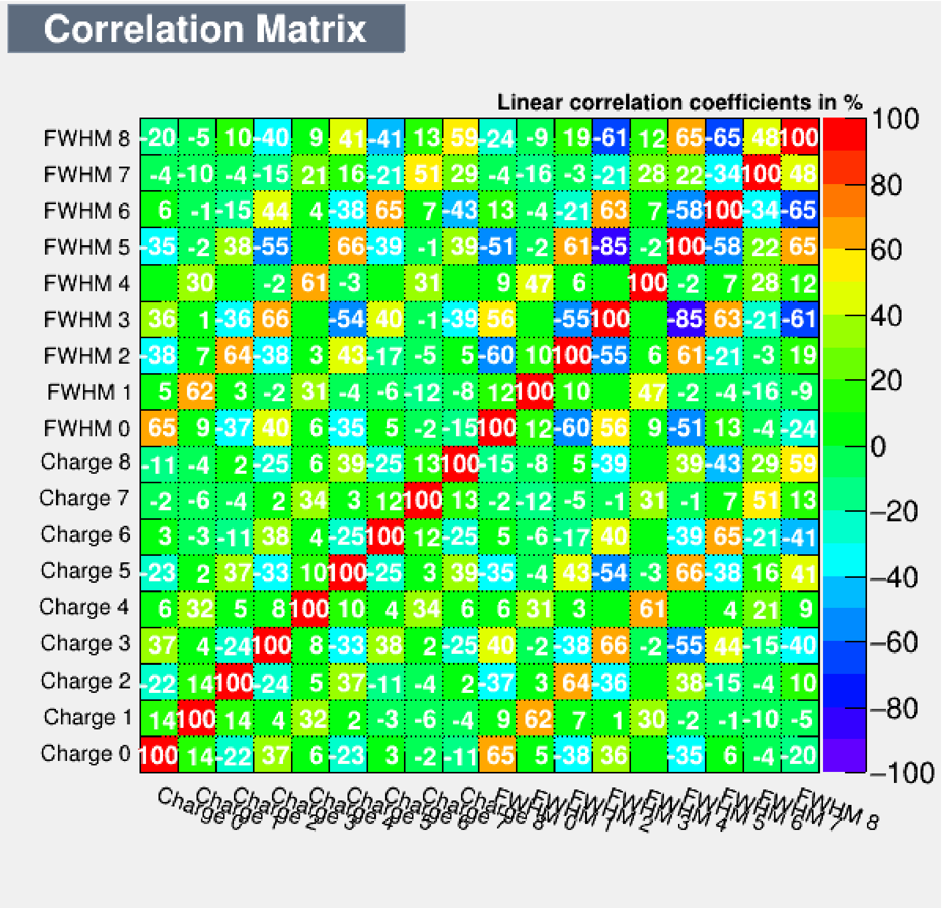

Local Hit Estimation

The idea is to estimate the closest point of the track passing near a *"leading pad",* in order to have triplets:

$$\{(t_i, y_i, z_i)_{i=1,\dots,n}\}$$

For n *leading pads*

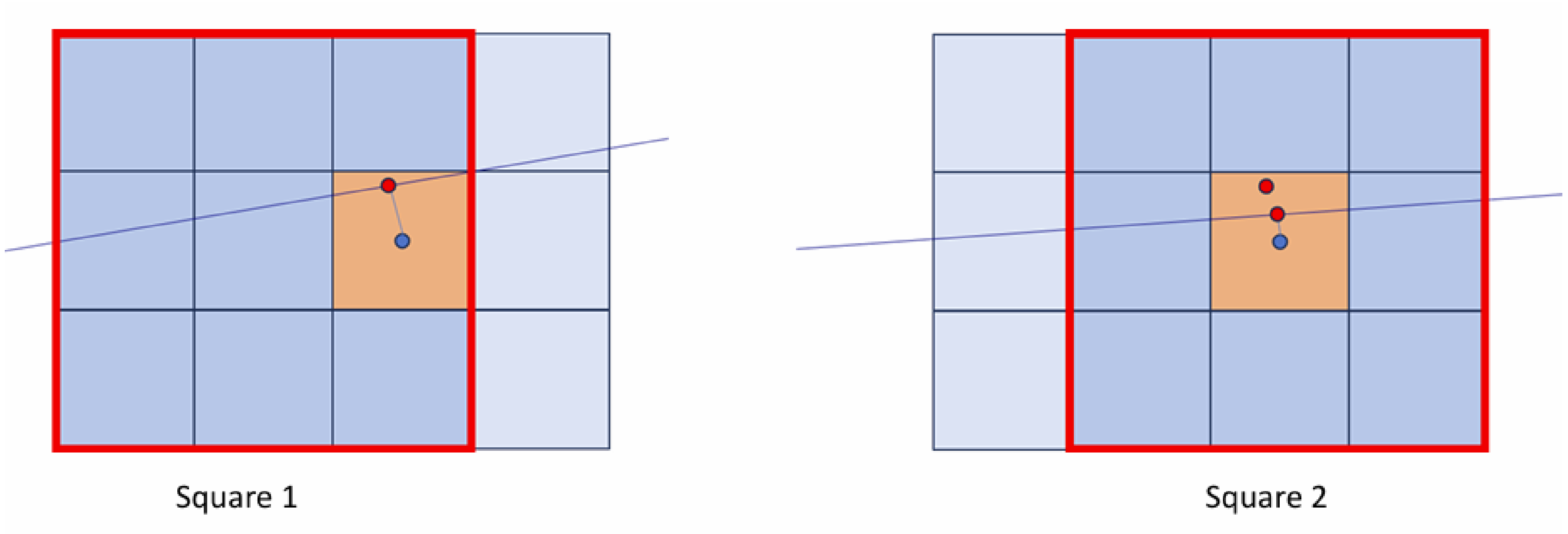

A **leading pad** usually appears in more squares, so it is possible to get an estimation of the ***closest point*** for each square

Local Hit Estimation

All the ***closest points*** are then used to find the final ***"average closest point"***

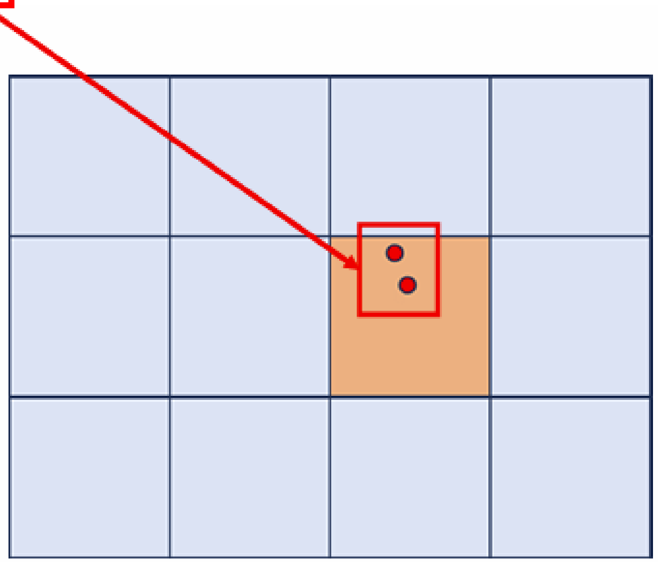

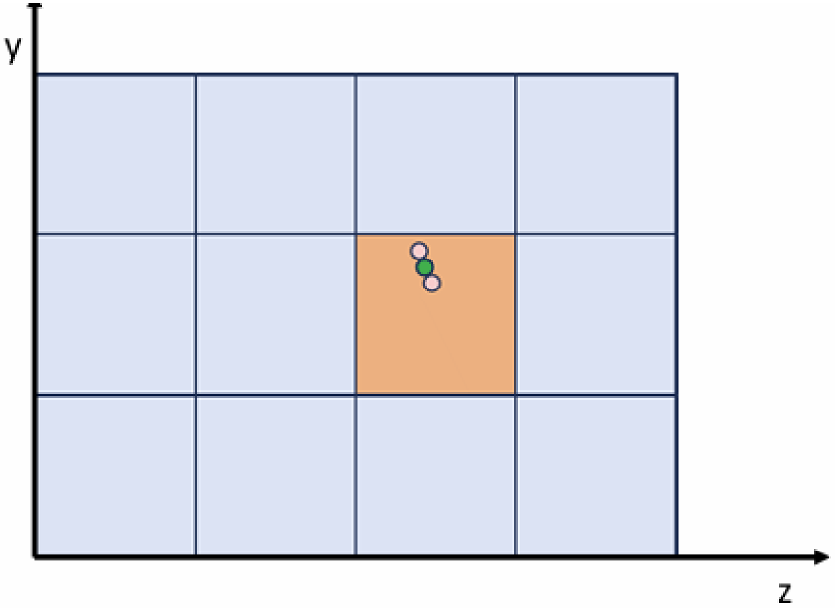

$$\bar{z} = \frac{1}{N}\sum_j z_j$$

$$\bar{y} = \frac{1}{N}\sum_j y_j$$

A certain **leading pad** j may appear in up to k=9 square clusters

As timing information, the t_{max} of the leading pad is considered

Then, the arc fitting is performed as the standard method

Results on Spatial Resolution

The goal in introducing a square cluster was to obtain a more homogeneous performance across all inclinations on ERAMs plane

Results show a **more stable** variance, but there is a **bias** in the residuals depending on the angle of the track

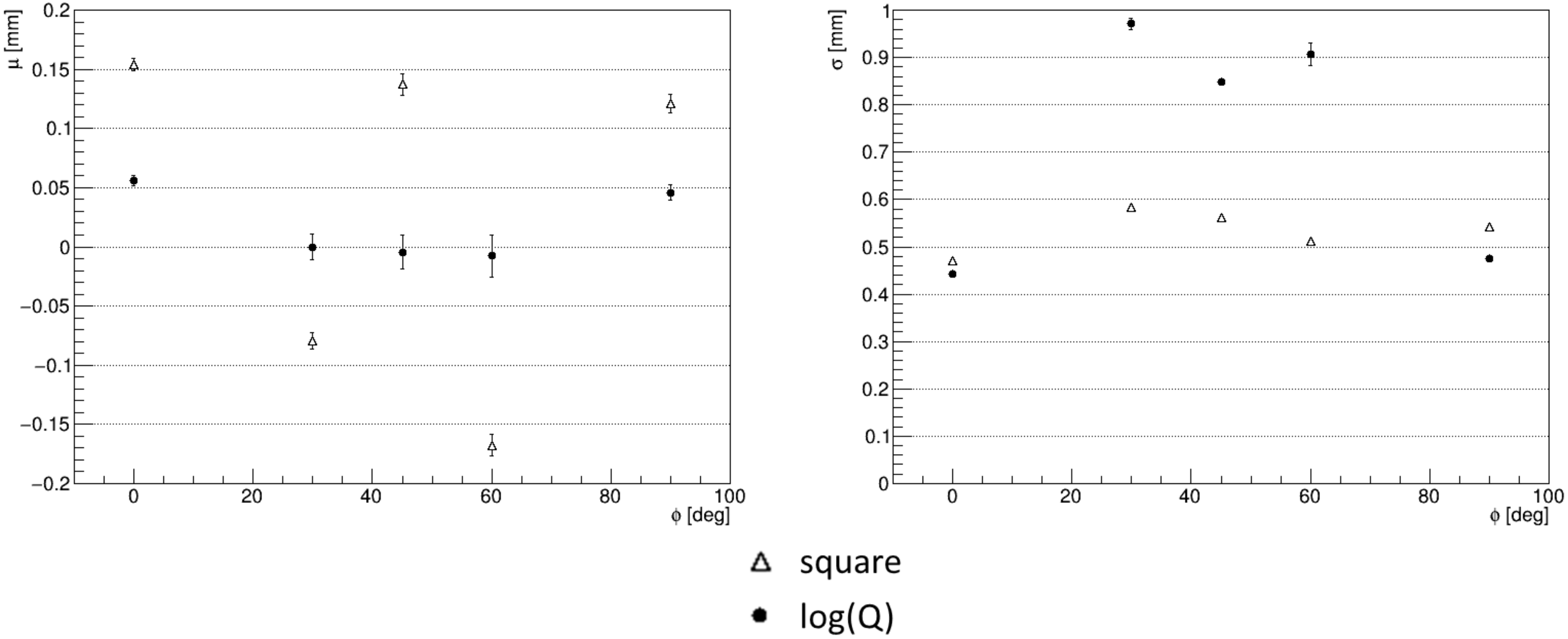

Since square clusters share pads, the Glückstern equation that relates spatial resolution holds only for *log(Q) method*

$$\frac{\sigma_{p_T}}{p_T} = \sigma_{yz}\frac{p_T}{qBL^2}\sqrt{\frac{720}{N_p+4}}$$

Results on Momentum estimation

The *log(Q)* method performs better in particular for shorter tracks ($\phi = 90°$) probably due to the influence of reconstruction biases

△ square

● log(Q)

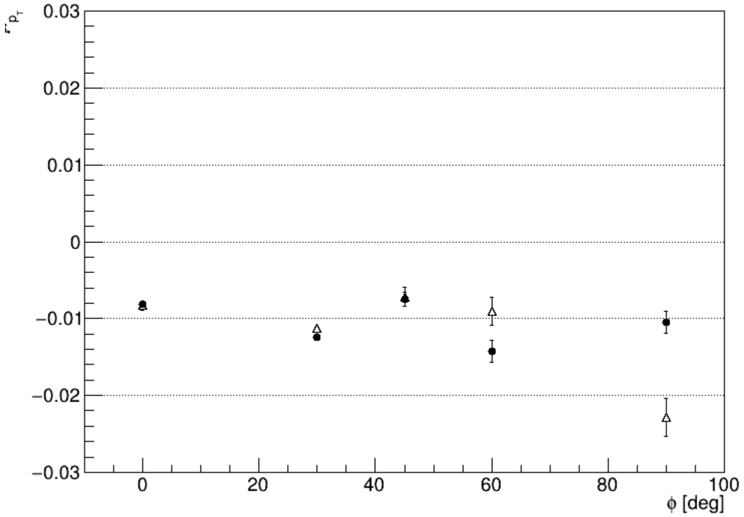

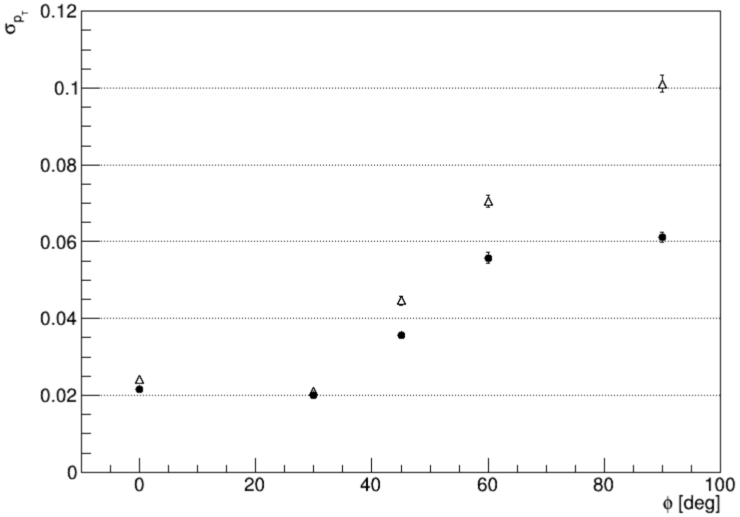

$p_{true} < 1000\ \mathrm{MeV/c}$

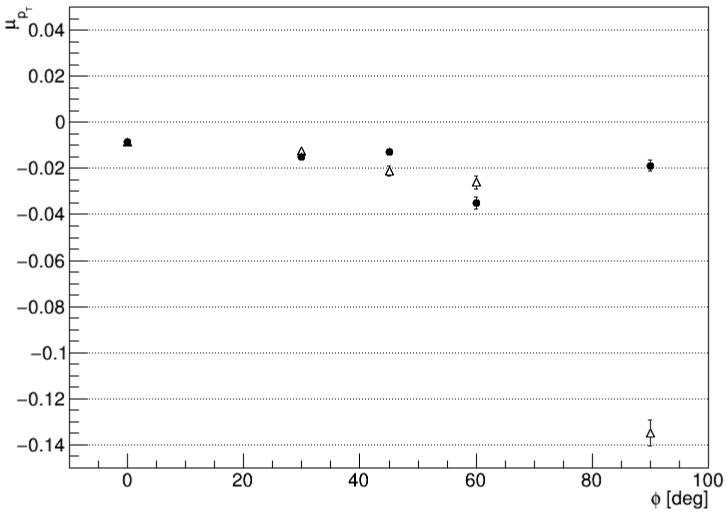

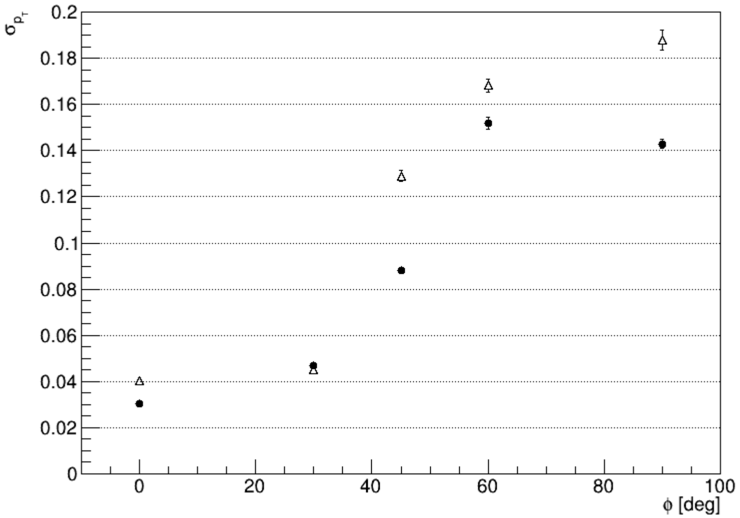

$1000\ \mathrm{MeV/c} < p_{true} < 3000\ \mathrm{MeV/c}$

HA-TPC performances with Neutrino Data

- **Spatial Resolution**

Residuals r are computed starting from the global fit

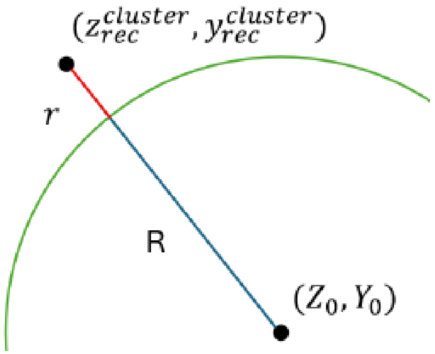

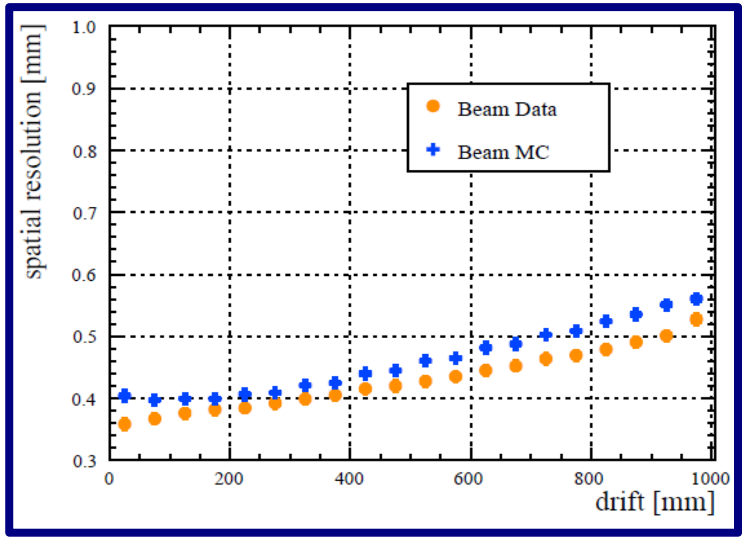

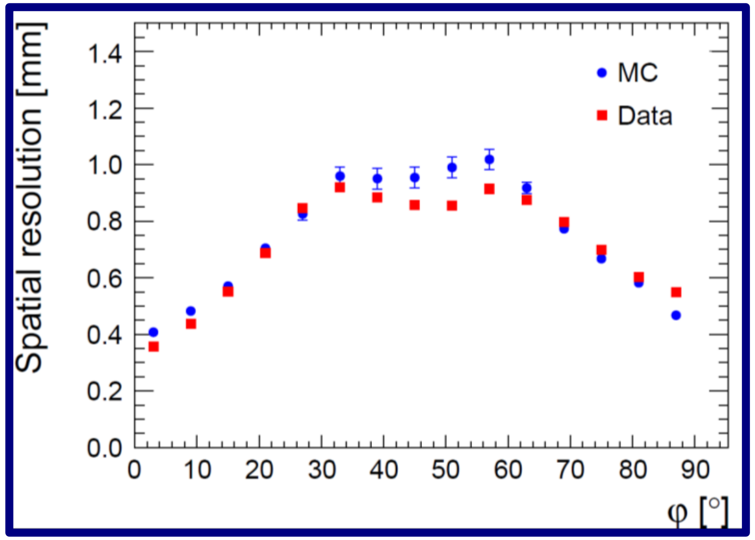

The σ of Gaussian distribution which fits the residuals is reported

T2K Preliminary

- **Energy Loss Resolution**

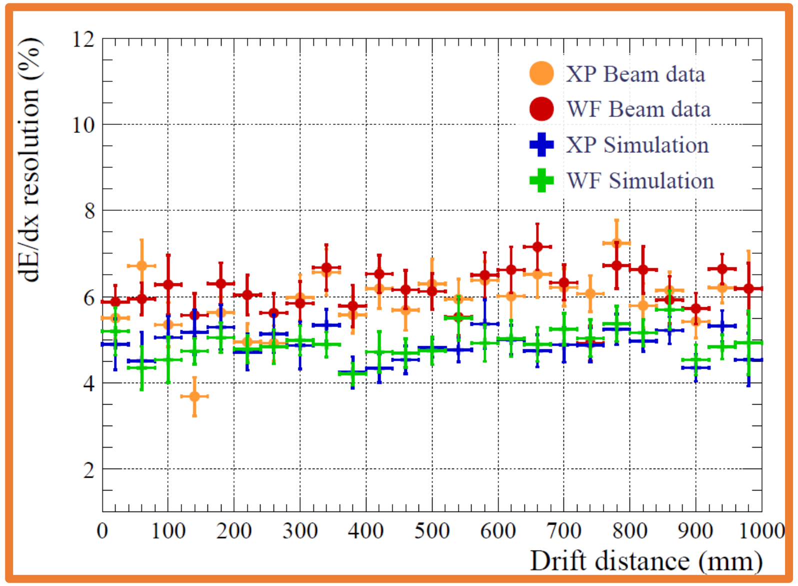

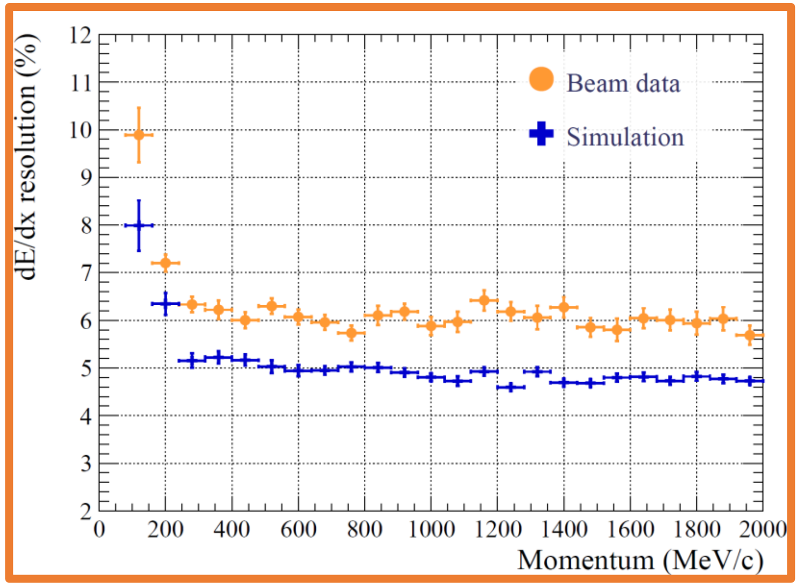

Conclusions

During my Ph.D., I had the unique opportunity to closely follow all stages of the HA-TPC construction, with a particular emphasis on the Field Cages, beginning from the prototype phase

The work described in the thesis focus on:

1. Production
2. Electrical and Mechanical Characterization
3. Study of Electric field performance

of the field cages of the new High Angle TPC of T2K Experiment

In addition, an innovative

4. Track reconstruction algorithm

for HA-TPC has been developed, with promising results that require additional detailed studies

Thanks for your attention!

Energy Loss (dE/dx) estimation

The energy loss estimation uses the overall information of each cluster j by defining the *waveform sum:*

$$WF_{sum}^{j}(t) = \sum_{i=0}^{n} WF_{i}^{j}(t)$$

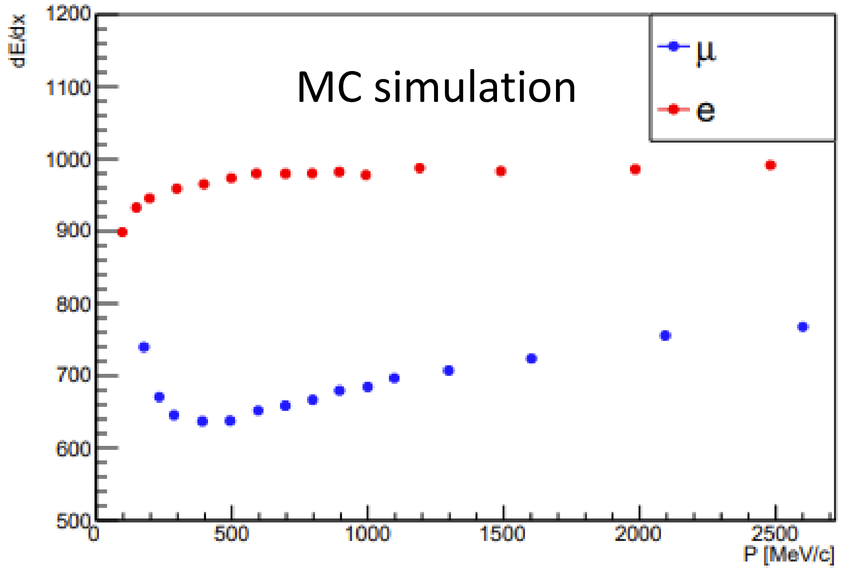

Then a **truncated mean is performed** for the 70% less energetic clusters ($\alpha = 0.7$)

$$C_T = \frac{1}{\alpha N} \sum_{j}^{\alpha N} WF_{sum}^{j}$$

The expected energy loss for a given charged particle is given by equation

$$C_E = \frac{p_0}{\beta^{p_3}} p_1 - \beta^{p_3} - \ln\left[p_2 + \frac{1}{(\beta\gamma)^{p_4}}\right]$$

A relation between the expected values under the hypothesis of particle *i* and the measured values is defined:

$$\delta_E(i) = \frac{C_T - C_E(i)}{\sigma_E(i)}$$

hypotheses: e, μ, π, K, p

MC simulation

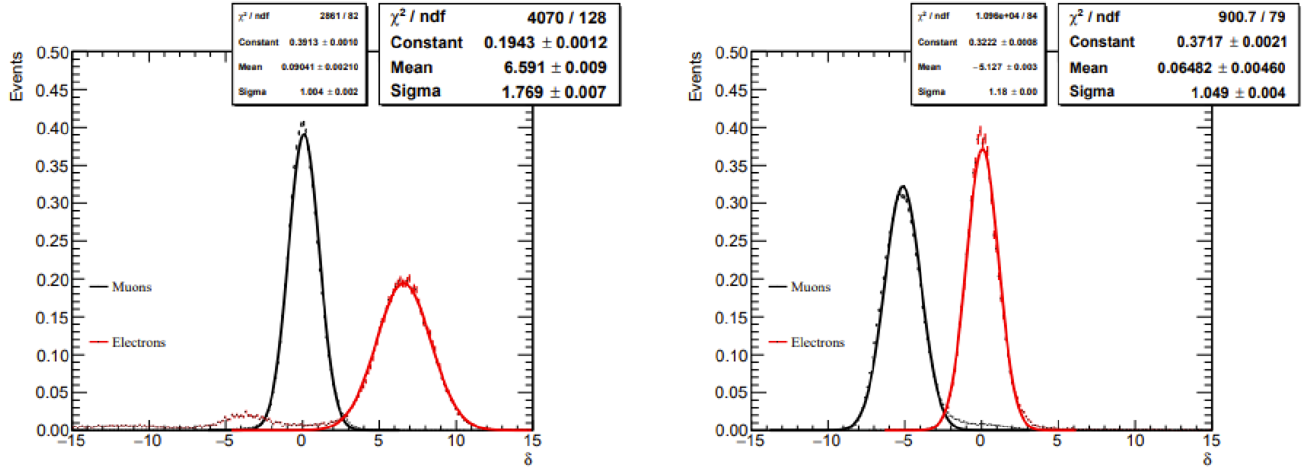

Modelization of single resistor measurements

Considering the assumption of additional paths on Twaron, the equivalent circuit is given by:

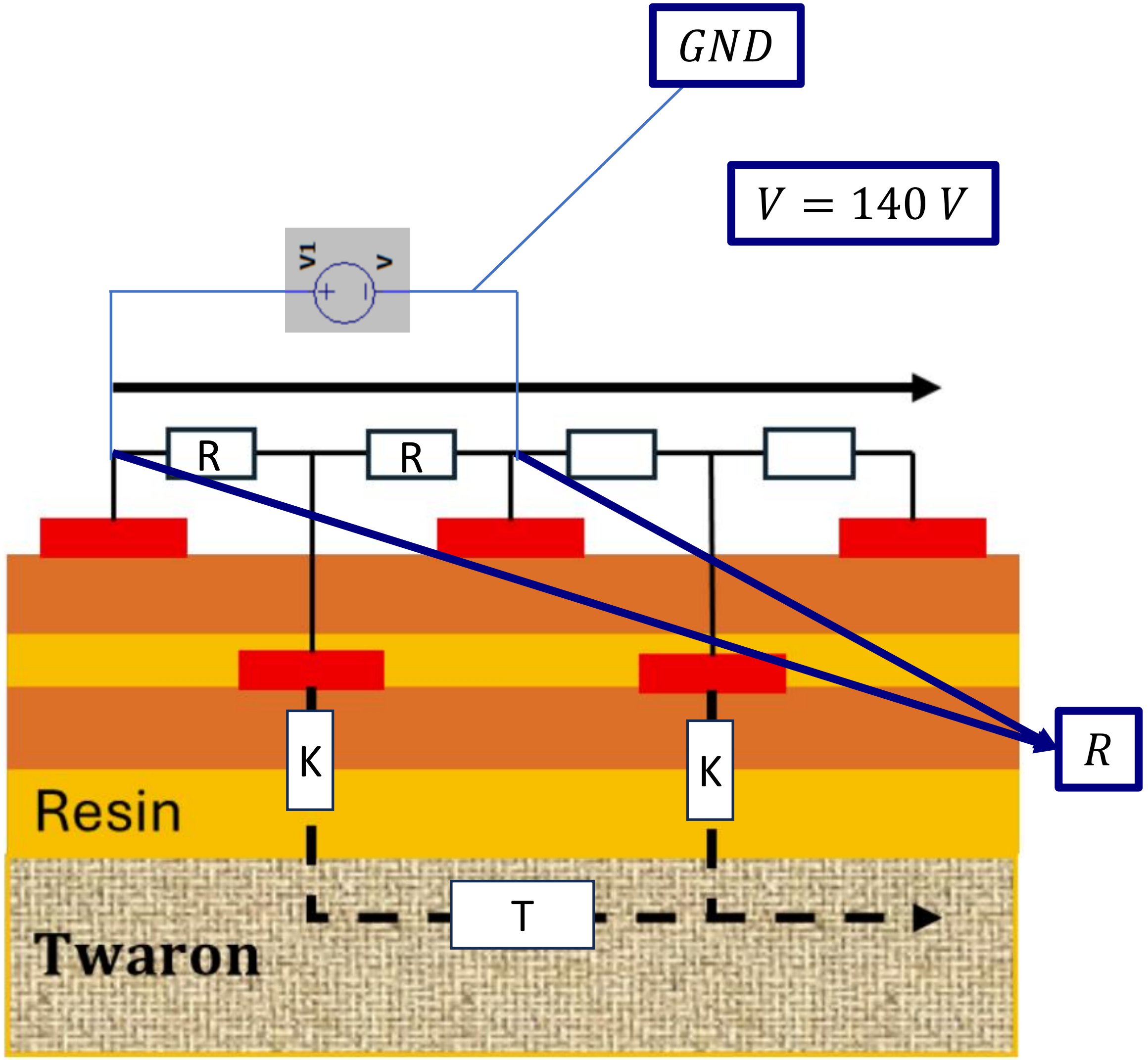

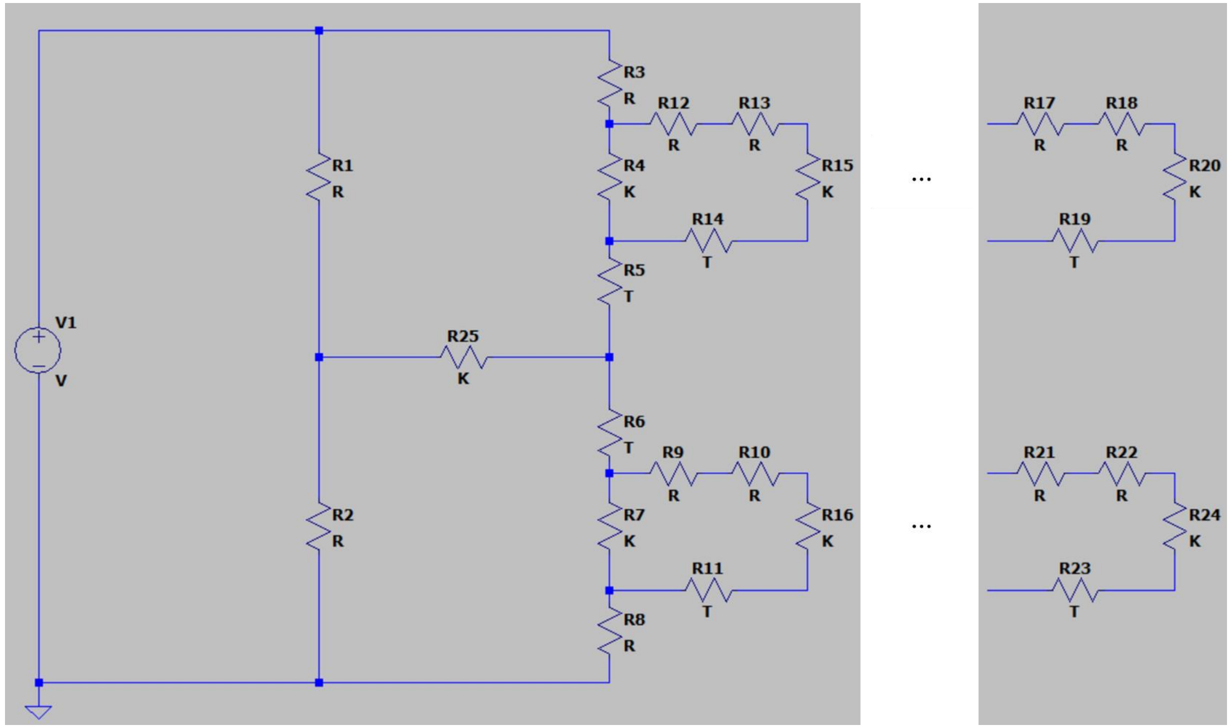

In which the additional loops are due to current flowing through nearby mirror strips

Goal: Find K and T

Modelization of single resistor measurements

Inclusion of additional loops might modify the expected value for K and T

From model:

$$\frac{R_{eff}}{2R} = \frac{1 + \frac{K_{eff}}{R} + \frac{T}{R}}{2 + \frac{K_{eff}}{R} + \frac{T}{R}}$$

The model allows to estimate locally the values of (K_i, T_i).
However, presents a **degeneracy**:

- **N measurements**, but **2N variables**

To reduce the degrees of freedom, it is possible to consider **that K and T might vary locally, but their ratio is always constant:**

$$T_i = \lambda K_i, \qquad i = 1, \ldots, N$$

- Variables reduced to N+1: (K_i, λ)

λ can be estimated by data!

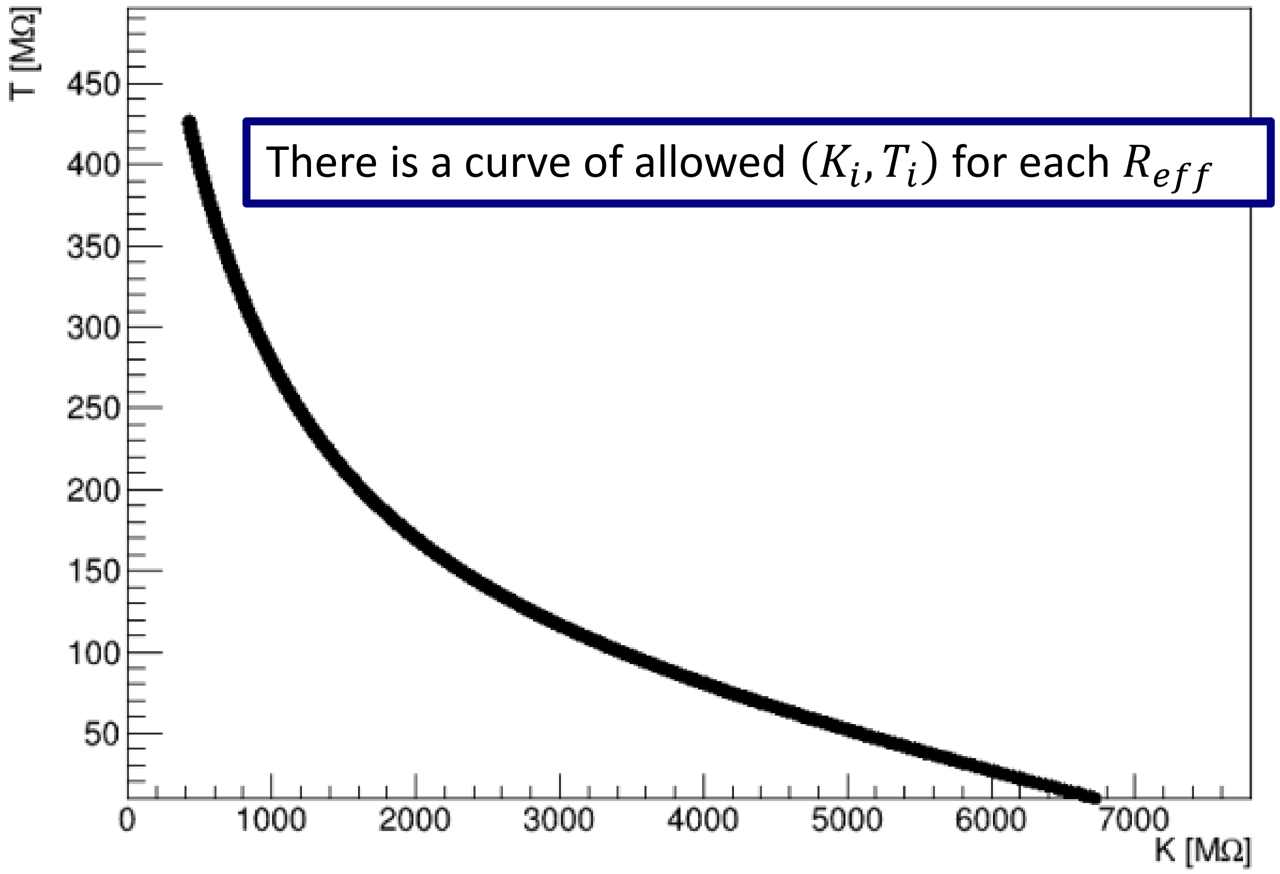

There is a curve of allowed (K_i, T_i) for each R_{eff}

HA-TPC performances at Test Beams

- **Spatial Resolution**

Residuals r are computed starting from the global fit

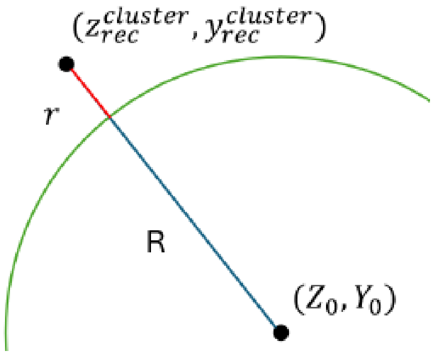

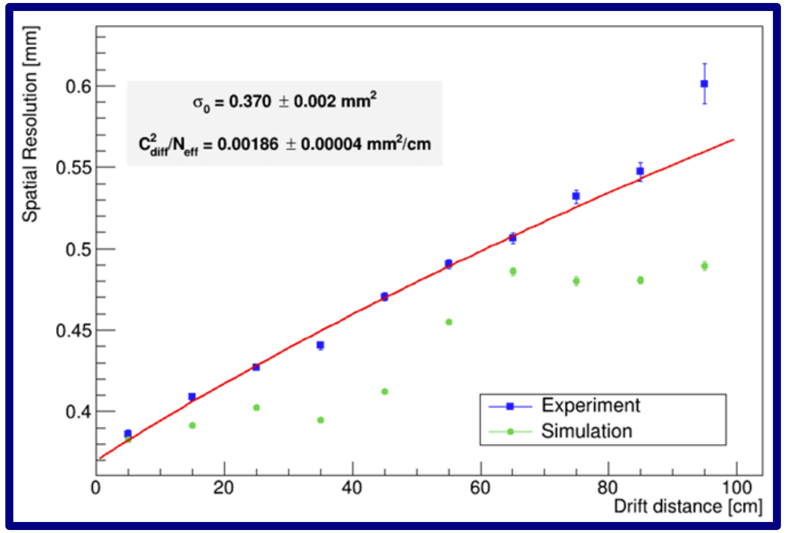

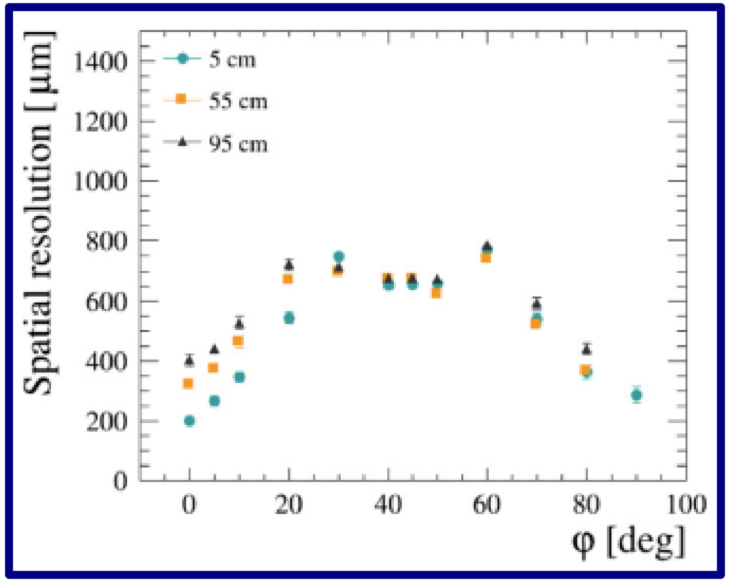

The σ of Gaussian distribution which fits the residuals is reported

- **Energy Loss Resolution**